Exploratory Approach of Developing Biomarkers for Linking Sub-Lethal Neonicotinoids Exposure and Health Risks

EXPLORATORY APPROACH OF DEVELOPING BIOMARKERS FOR LINKING SUB-LETHAL NEONICOTINOIDS EXPOSURE AND HEALTH RISKS

CHI-HSUAN CHANG

A Dissertation Submitted to the Faculty of

The Harvard T.H. Chan School of Public Health

in Partial Fulfillment of the Requirements

for the Degree of *Doctor of Science*

in the Department of Environmental Health

Harvard University

Boston, Massachusetts.

May 2018

Dissertation Advisor: Dr. Chensheng Alex Lu Chi-Hsuan Chang

EXPLORATORY APPROACH OF DEVELOPING BIOMARKERS FOR LINKING SUB-LETHAL NEONICOTINOIDS EXPOSURE AND HEALTH RISKS

ABSTRACT

Since the development of neonicotinoids, their usage has been growing dramatically in pest control while limited studies focused on their impact on human exposure. With a concern of the systemic property of neonicotinoids and their cumulative high frequency of usage, this dissertation thesis aimed to focus on the following three aspects: (1) human exposure assessment, (2) a novel biomarker, and (3) the associated metabolic pathways of cumulative neonicotinoids exposure at sub-lethal levels.

In Chapter 1, we estimated the average daily intake distributions of neonicotinoids residues in fruit and vegetable consumptions in the U.S. population using residues data from the US Congress Cafeteria study and USDA Pesticide Data Program, and consumption data from the NHANES surveys. We integrated residues of six neonicotinoids into imidacloprid-equivalent exposure (IMI_{RPF}) based on their relative toxicity compared to imidacloprid. We found the average daily intake distributions were generally below the regulatory standard, chronic reference dose (cRfD) while we discussed on limitations regarding the comprehensive inclusion of dietary exposure categories, the precision of analytical methods used, and the potential revision of the stringency of current regulatory levels based on novel biomarkers.

In Chapter 2, we identified increasing relative mitochondrial DNA copy number (RmtDNAcn) as a potential biomarker to reflect sub-lethal neonicotinoids exposure in a honeybee

model. Even without large enough samples to declare statistically significant associations, we found higher levels of RmtDNAcn in later-brood generations within a colony and in bees fed with neonicotinoids. Additionally, we found that neonicotinoids exposure and increasing RmtDNAcn were related to faster onset of bee disappearance and occurrence of hives' mortality over the winter.

In Chapter 3, we explored energy metabolism related pathways that could help explain the influence of cumulative sub-lethal neonicotinoids treatments and increasing RmtDNAcn levels in honeybees. Overall, we detected statistically significant abundance changes in metabolites due to biological aging that are aligned with findings of previous literature. We also found perturbation of metabolites in the TCA cycle and glutathione metabolisms associated with neonicotinoids treatments and change in RmtDNAcn levels. Future biological research on neonicotinoids should focus on these metabolites to validate our findings.

TABLE OF CONTENTS

LIST OF FIGURES WITH CAPTIONS

Figure 10. (A) Heatmap of average log2 fold change (FC) of abundance between later-brood generations (F2 or F4) vs. baseline generation (F0) for metabolites with significant abundance changes. **(B)** Volcano plots showing the log2 fold change of abundance in later-brood generations (F2 or F4) versus F0 for 57 metabolites given no change in RmtDNAcn ratio.

Figure 11. (A) Heatmap of average log2 fold change (FC) of abundance associated with every 2-fold increase in RmtDNAcn ratio between later-brood generations (F2 or F4) vs. baseline generation (F0) for metabolites with significant abundance changes. **(B)** Volcano plots showing effect of RmtDNAcn ratio on metabolite abundance ratio (Ctrl vs. NULL; highlighted with blue box) and neonicotinoids-attributed (IMI vs. Ctrl and CLO vs. Ctrl; highlighted with yellow box) change in log2 fold change of abundance associated with increasing RmtDNAcn ratio in later-brood generations (F2 or F4) versus F0 for 57 metabolites.

SUPPLEMENTARY FIGURES:

Figure S1. Log2(RmtDNAcn) levels for all samples by sugar and pesticide treatments. Outliers were circled and excluded from all analyses.

Figure S2. Heatmap of log2 transformed abundance ratios of later-brood generation (F2 and F4) vs. baseline generation (F0) for the 57 selected metabolites.

Figure S3. Heatmap of Difference in log2 fold change of abundance between later-brood generation (F2 and F4) vs. baseline generation (F0) for the 57 selected metabolites.

LIST OF TABLES WITH CAPTIONS

SUPPLEMENTARY TABLES:

ACKNOWLEDGEMENTS

Completing this dissertation would have been impossible without the support and love I was fortunate to receive from my mentors, family and friends. 謝謝。

First and foremost, I would like to express my deepest thank to my advisor, Dr. Chensheng Alex Lu, for his supports and encouragements throughout the accomplishment of this work. Dr. Lu has become a lifelong mentor to me not only in academics but also as a friend in my life to share and discuss thoughts from time to time. I would also like to thank my committee members, Dr. Bernardo Lemos and Dr. David MacIntosh for all the insightful guidance and discussions they have provided that help to shape this work. It is my great pleasure to work with all of them during my years at Harvard.

I would like to thank Taiwan and The Top University Strategic Alliance of Taiwan (TUSA) for sponsoring my doctoral studies. I wouldn't possibly be here without the financial supports of my country. I would also like to thank my advisors (Dr. Kuen-Yuh Wu and Dr. Chang-Chuan Chan) and professors that have taught me during my years at National Taiwan University, who encouraged me in achieving my dream of pursuing my doctoral degree.

Lastly, I would like to dedicate this work to my dearest family and friends. I thank my parents (Shao-Ching and Chiou-Ying), my grandparents (Ching-Wen and Shih-Chun), and my little brother (Chi-Cheng) for the life and love they have given me in the past 27 years of my life. I thank all of my dearest friends for their love and accompany that support me getting through the obstacles I encountered. And, I thank my boyfriend, Yichen, for the years we have gone through together at Harvard.

Chi-Hsuan Chang

Boston, Massachusetts

INTRODUCTION

Neonicotinoid (neonic), as a group of systemic insecticides, have become the most commonly used insecticides globally since late 1990's with growing usage expected. With their systemic property, neonics could be translocated to all parts of a plant once applied, regardless of the application methods.[1,2, 3] In addition, the application of neonics in the seed treatment technology has also led to the large-scale and rapid increase uses in field crops.[4] These resulted in neonics residues distributed within whole plants from insect damage while the easily applied application also brought abundant residues to the environment, and high frequency and cumulation of exposure to non-target insects and human, which triggered my interest in exploring exposure, novel biomarker, and intermediate outcomes of neonicotinoids exposure in both public and environmental health settings.

In Chapter 1, we started by exploring the exposure and risk associated with neonics dietary intakes in human. Although neonics are generally considered less toxic in humans, increasing attention of neonics in human exposure and potential adverse health effects was brought after observation of acute and chronic toxicity cases in epidemiological studies. With this in mind, we demonstrated a model simulation methodology to estimate the integrated daily dietary intakes of six neonics in fruits and vegetables consumed by the U.S. population using residue data collected from US Congress Cafeteria study (USCC) and USDA, and food consumption data from NHANES 2011 – 2012. We utilized the relative potency factor approach to integrate six neonics into a single metric with respect to the relative toxicity of those neonics, and then compare the estimated total neonic dietary exposure distributions with the current chronic reference dose (cRfD) for the reference neonic imidacloprid.

Along with the demonstration of human exposure levels in Chapter 1, we also reviewed the mode of action of neonics, which is known as their agonism on the nicotinic acetylcholine receptors (nAChRs). Although nAChR of invertebrates generally had with higher affinity to neonicotinoids than mammalian nAChR,[1, 2, 5] we were not satisfied with the argument that neonics are not toxic in humans without consideration of other plausible toxicological mechanisms. As neonics have also been shown to associate with the occurrence of colony collapse disorder (CCD), refers to the phenomenon of massive disappearance of honeybees during winter.[6] Until now, the cause of CCD remains unclear while has been linked to factors including pesticide use, habitat loss, and parasites, etc. [1, 7, 8] Beyond all possible factors, one main hypothesis of neonics exposure's association with CCD lied in the lack of sufficient ATP generation for bees' high energy-demanding activities and thermoregulation during the winter due to neonics exposure,[9-11] in which study has shown that imidacloprid could inhibit respiration, influence electron transit chain (ETC) and reduce the generation of ATP dose-dependently in both thorax and head.[9] We therefore suspected that mitochondrial dysfunction could be a potential mechanism to explain more unknown about neonics not only in honeybee, but also in human exposure. These triggered us to further investigate the mechanisms of mitochondrial dysfunction using new biomarker (in Chapter 2) and in a more comprehensive metabolic pathway analyses (in Chapter 3).

In Chapter 2, we proposed relative mitochondrial DNA copy number (RmtDNAcn) as a novel biomarker to detect mitochondrial dysfunction at an earlier stage with the knowledge of its association with mtDNA damage[12]. We evaluated whether chronic sub-lethal exposure to neonics could lead to increase in RmtDNAcn in an adult honeybee experiment. With longitudinal collected samples from hives with (imidacloprid and clothianidin) and without neonics administration, we were able to study the levels of RmtDNAcn across subsequently brood generations and whether

or not these levels were influenced by sub-lethal cumulative neonics treatments. We further analyzed the association of RmtDNAcn levels with onset risk of bee disappearance and mortality risk over the winter as downstream outcome measurements of mitochondrial dysfunction. These analyses enabled us to explore whether the RmtDNAcn increased in later brood generations due to queen's aging and neonics treatments, and whether the onset of bee disappearance and mortality in neonics-treated hives occurred earlier.

In Chapter 3, we conducted metabolomics analyses with a selection of pathways associated with energy metabolism as the major pathway neonicotinoids influence on with the hypothesis for CCD stated above. We evaluated the change of metabolite abundance across the subsequently brood generations from the same queens collected in Chapter 2. We linked the changes of metabolite abundance with the aging of queens, chronic sub-lethal neonicotinoids exposure, and the increase in RmtDNAcn associated with both aging and treatment effects. We specifically focused on pathways closely related to the energy metabolism and identified them using KEGG PATHWAY Database. At the end of this chapter, we'd give hypothetical metabolic mechanisms as explanation of our findings in changing metabolite abundance among later-brood generations and different treatment groups.

CHAPTER 1

Population-based Daily Dietary Intake of Neonicotinoid Insecticides through Fruit and Vegetable Consumption in the U.S.

Chi-Hsuan Chang[1],

David MacIntosh[1],

Bernardo Lemos[1],

Quan Zhang [1,2],

Chensheng Lu[1, †]

[1]Department of Environmental Health, Harvard T.H. Chan School of Public Health, Boston, Massachusetts

[2]College of Environment, Zhejiang University of Technology, Hangzhou, Zhejiang, China

Abstract

Neonicotinoids have become the most commonly used insecticides in agriculture globally in the past 20 years. However, very limited data related to human dietary intake of neonicotinoids is available. In this chapter, we aggregated the individual neonicotinoid intakes using the relative potency factor approach into a single metric (IMI_{RPF}) representing the dietary intakes of total neonicotinoids in relate to imidacloprid for each food item. We then estimated population-based average daily intake (ADI) of neonicotinoids through fruit and vegetable consumption in the U.S. using residue data collected from US Congress Cafeteria study (USCC) and USDA, and food consumption data from NHANES 2011 – 2012. Among USCC study analyzed samples, squash (427.2 ng/g), tomatoes (132.5 ng/g) and peppers (88.3 ng/g) had the highest average IMI_{RPF}. Among the 15% of USDA/PDP samples that were detectable of at least one neonicotinoid, spinach had the highest average IMI_{RPF} (569.2 ng/g), followed by baby food-peas (482.5 ng/g) and cherries (401.8 ng/g). Although the estimated ADIs using both residue datasets were below the current chronic reference dose (cRfD) for imidacloprid, we need to use more precise analytical methods to analyze more neonicotinoid residues in more diverse foods in order to facilitate the future dietary exposure and risk assessments of neonicotinoids.

Introduction

Neonicotinoid (neonic) is a group of systemic insecticides that includes acetamiprid, clothianidin, dinotefuran, imidacloprid, nitenpyram, thiacloprid and thiamethoxam. The nature of their systemic property leads to universal translocation of neonics to tissues of the applied plants regardless of the application methods.[1] As a result, neonics protect the whole plant from insect damage by distributing the active ingredients to all tissues of the plant, including the edible components.

Neonics have gradually become the most commonly used insecticides around the world since their introduction in the late 1990's. They accounted for approximately 24% and 27% of the global insecticide market in 2008 and 2010, respectively, with continuous growth in their use expected.[2, 3] The invention and adoption of neonics in the 1990s were due to insects' resistance to the dominant classes of pesticides of carbamates, organophosphates, and pyrethroids used at that time.[1, 13] In addition, the application of neonics in the seed treatment technology has led to the large-scale and rapid increase uses in field crops (e.g., soybeans and maize).[4] Two neonic compounds are in particularly wide use; imidacloprid and thiamethoxam, which are registered for use on 140 and 115 crops worldwide and accounted for about 41.5% and 23.8% of the neonic sales in 2009, respectively.[3]

Previous and current research on neonics mainly focuses on their toxicological effects on invertebrates. The known mode of action of neonics, which is similar to nicotine, is to function as agonists on the nicotinic acetylcholine receptors (nAChRs).[1, 2, 5] Although insect nAChR has a cationic subunit that can interact with the nitro- or cyano-end of neonics with higher affinity, mammalian nAChR does not.[1, 2, 5] With this perspective in

mind, neonics are generally considered less toxic in humans and thus very few studies have focused on human exposure to neonics and the potential adverse health effects.[14]

In this chapter, we demonstrated a model simulation methodology that allows for the estimation of daily dietary intakes of total neonic in fruits and vegetables that are consumed by the U.S. population as they are important crops of neonics residues for human dietary exposure.[3] We utilized the relative potency factor approach[15, 16] to integrate six neonics into a single metric with respect to the relative toxicity of those neonics, and then compare the estimated total neonic dietary exposure distributions with the current chronic reference dose (cRfD) for the reference neonic imidacloprid. **Figure 1** details the approach taken for this chapter.

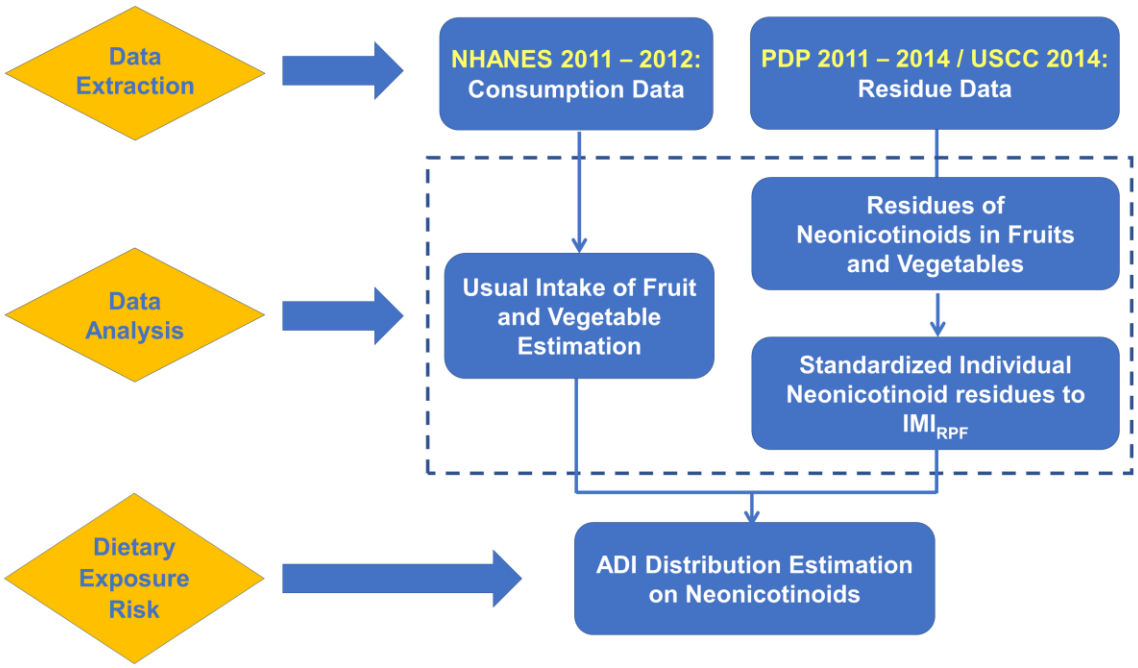

Figure 1. Schematic Display of the Research Design.

Materials and Methods

Neonics Residues in Foods. We obtained residue data for six neonics from two sources; the U.S. Congress Cafeteria (USCC) study[17] and data published by the U.S. Department of Agriculture (USDA), Pesticide Data Program (PDP).[18-21] We supplemented residue data from the USCC study to expand the types of fruit and vegetable items that are reported by the USDA/PDP in order to better reflect potential exposures to neonics in foods consumed by participants of NHANES.

For the USCC residue data, a total of 64 samples including seven fruits (apple, cantaloupe, cranberry, grapes, honeydew, melon and strawberry) and seven vegetables (broccoli, cilantro, corn, cucumber, lettuce, pepper, spinach, and tomato) were analyzed for seven neonics (acetamiprid, clothianidin, dinotefuran, imidacloprid, nitenpyram, thiacloprid and thiamethoxam) and flonicamid in 2014.[17] Flonicamid and nitenpyram were excluded from the RPF calculation due to the uncertain classification as a neonic and the lack of residue/cRfD data, respectively. For the USDA/PDP dataset, we extracted six neonics (no nitenpyram) from a total of 39,159 samples including 22 fruits and 29 vegetables (**Table 1**). USDA/PDP was initiated in early 1990s to measure pesticide residues in foods and to support U.S. Environmental Protection Agency (EPA)'s review of the maximum residue limits or tolerances for dietary exposure assessment. Fruit and vegetable samples were collected at volunteered terminal markets and large chain store distribution centers (approximately 2,400 sites granted access and provided information in 2011 to 2014). PDP's operation procedures were developed to ensure that the samples are randomly selected from the national food distribution system to reflect what is typically available to the consumers while also with an emphasis on foods consumed by infants and

children. The same commodities were cycled through PDP approximately every five years.[18-21]

Residue analysis. The limits of detection (LODs) for individual neonic analyzed by the USCC study and USDA/PDP were listed in **Table 1**. All non-detectable (ND) residue concentrations were substituted with one half of the LOD for model simulation purpose.[22] We used the relative potency factor (RPF) approach[15, 16] to integrate six neonics in a vegetable or fruit sample into a single measurement of imidacloprid$_{RPF}$ (IMI$_{RPF}$)[23] by using the respective chronic reference dose (cRfD), as shown in **Table 1**. As we adopted cRfD as the comparison metric of relative toxicity of neonics, this approach was also equivalent to the integration of comparing the margin of each neonic exposure to the corresponding cRfD. We chose imidacloprid as the reference neonic because it is the most widely used and studied neonic among all for risk communication purpose. Specifically, we used the following equation to calculate IMI$_{RPF}$ (the imidacloprid-equivalent total neonic) for each fruit or vegetable sample:

$$IMI_{RPF} = \sum_k RPF_k \times neonic_k \text{ (ng/g)} \quad \textbf{(Equation 1)}$$

where k represents the specific neonics.

***Dietary Consumption Data*.** We used fruit and vegetable consumption data collected by the Centers for Disease Control and Prevention (CDC), National Health and Nutrition Examination Survey (NHANES) 2011-2012, which was the latest publicly available dataset online when we conducted this chapter in 2016. NHANES is designed to examine the health and nutritional status of the U.S. population excluding those residing in nursing homes, members of armed force, institutionalized persons, or U.S. nationals living abroad.

In total, NHANES 2011-2012 obtained dietary recall information from 8,519 individuals, 7,605 of whom completed both days of the two 24-hr dietary recall surveys. We included those 7,605 participants in our usual intake (UI) analyses based on the NHANES sampling weights and the scope of data analyses.

Long-term Usual Consumption of Fruits and Vegetables. In order to select nationally representative participants, NHANES uses a multistage probability sampling design in which each participant in the NHANES is weighted differently according to the sampling process as well as the questionnaires or biological examination provided. NHANES assigns a sample weight to each participant which represents the number of people in the population represented by such participant in NHANES, reflecting the unequal probability of selection, non-response adjustment, or adjustment to independent population controls. These weights were calculated from the base weight adjusting for non-response and post-stratification adjusting to the 2000 U.S. Census population totals. We used WTDR2D for analyses on both Day 1 and Day 2 dietary data. This two-day weight was constructed for the 7,605 participants by taking the Day 1 weights (WTDRD1) and further adjusting for (a) the additional non-response for the second recall and (b) for the proportion of weekend-weekday combinations of Day 1 and Day 2 recalls.

We used SAS® 9.4 in the application of the validated National Cancer Institute (NCI) method[24, 25] to estimate the long-term usual intake (UI), which is defined as the long-term average daily consumption (g/day) in the NCI method. In addition, consumption data is usually right-skewed rather than symmetric since values can never be negative. Therefore, we log-transformed the two 24-hr recalls approximating a normal distribution in order to estimate long-term usual consumption of fruit and vegetables by using the NCI

method[24, 25], including both the probability of consuming a specific food item and the amount (gram) of such consumption in a day. In brief, NCI method fits the following two-part model with random mixed-effects for each vegetable/fruit item:

$$\text{logit}(p_{ij}) = \beta_0 + u_i \qquad \textbf{(Equation 2)}$$

$$\log(\text{amount}_{ij}) = \beta_0^* + u_i^* + e_{ij}^* \qquad e_{ij}^* \sim N(0, \sigma_{e^*}^2) \qquad \textbf{(Equation 3)}$$

$$UI_f\ (\text{g/day}) = p_f \times \text{amount}_f \qquad f \text{ for individual food item} \qquad \textbf{(Equation 4)}$$

β_0 and β_0^* are the global intercepts for probability and amount models, respectively. u_i and u_i^* are the person-specific random effects and e_{ij}^* is the within-person variations in the two 24-hr recalls under the two-part model. Both models are fit using the NCI-established SAS macro, MIXTRAN, which outputs the parameter estimates for both the probability and the amount models. The DISTRIB macro used the results from the MIXTRAN macro to estimate the usual food intakes to calculate percentiles and cut points of the usual intake distribution. We used R statistical software (3.2.4) for all other analyses.

Average Daily Intake (ADI) Estimation of Imidacloprid-equivalent Total Neonic (*IMI_{RPF}*). To capture how the residue levels of each food item, as well as how the dietary consumption would contribute to the overall ADI distribution, we performed the following steps:

1. ***Residue:*** We randomly sampled 1000 IMI_{RPF} with replacement from both USCC and PDP residue datasets to estimate the corresponding 5th, mean, and 95th percentile of the residues for each food item.

2. ***Consumption:*** To improve the precision of the estimated UI distributions, we used the DISTRIB macro to simulate 100 pseudo-persons' UI of each food item for the 7,605 NHANES participants with different simulated person-specific effects.
3. ***ADI estimation:*** We combined the residue and consumption datasets by each food item for every NHANES participants. We then calculated the cumulative distribution of IMI_{RPF} estimated ADI, using the following equation, based upon the individual participant's weights (WTDR2D) under different residue levels (5^{th}, 95^{th} percentile and mean).

$$\text{ADI (ng/kg/day)} = \sum_f IMI_{RPF\_f} \text{ (ng/g)} \times UI_f \text{ (g/day)} \times \text{Exposure Duration (year)} / \text{BW (kg)} \times \text{Average Lifetime (year)}$$

(Equation 5)

Specifically, f is an individual fruit or vegetable item, UI_f is the long-term usual intake of the specific food item f, and BW is each participant's body weight (if missing, we used the average body weight of the participants who have the same characteristics, household income levels, gender, age groups, race and ethnicity, and adult education attainment as the body weight of such participant). The exposure duration is approximately the same as the average lifetime since the interest of exposure is for daily dietary consumption.

Sensitivity Analysis. We conducted sensitivity analyses on commonly sampled fruit and vegetable items in order to determine the magnitude of uncertainty of results originated from:

1. The management of ND data: We have considered different methods to manage the ND data in which some were similar to method used by MacIntosh et al. (1996).[22] Rather than the original treatment (replacing ND with one-half of the LOD), we

also replaced all ND values with 0, or random variables sampled from a uniform distribution ranging from 0 to the given LOD of the respective analytical method.

2. The inclusion of samples without repeated residue measurements. For instance, squash in the USCC study was not included in the data analysis due to the lack of repeated samples to capture its distribution.

Results and Discussion

Table 1 shows the calculated RPFs for neonics using the relative toxicity of individual neonics to that of imidacloprid. For the 64 vegetable and fruit samples that the USCC study analyzed, the overall frequency of detection for at least one neonic (not including nitenpyram) was 91%. Thiamethoxam was the most frequently detected neonic (61%), followed by imidacloprid (58%), clothianidin (36%), acetamiprid (33%), dinotefuran (27%), and thiacloprid (6%). Among all analyzed food items, tomatoes contained the highest average level of clothianidin (9.1 ng/g), dinotefuran (18.9 ng/g), and imidacloprid (8.3 ng/g). Apples contained the highest average level of acetamiprid (19.1 ng/g); squash contained the highest level of thiamethoxam (43.1 ng/g); and, peppers contained the highest level of thiacloprid (0.2 ng/g). Overall, squash (with only one sample) had the highest average of IMI_{RPF} (427.2 ng/g), followed by tomatoes (132.5 ng/g), peppers (88.30 ng/g), and honeydews (54.9ng/g).

For the 36,167 fruit and vegetable samples that we extracted from USDA/PDP 2011 to 2014 datasets, the overall detection rate of at least one neonic was 15%, substantially lower than that of the USCC study. Cherries were most frequently detected with neonics (94%), followed by apples (59%), strawberries (47%), and peppers (47%). Imidacloprid was the most frequently detected neonic (7%) among those fruits and vegetables, followed by acetamiprid (5%), thiamethoxam (3%), dinotefuran (1%), and clothianidin (1%). Thiacloprid was the least frequently detected among the six neonics in both residue datasets. Hot peppers contained the highest average level of acetamiprid (40.3 ng/g) and dinotefuran (41.4 ng/g); onions contained the highest average level of clothianidin (23.3 ng/g) and thiamethoxam (20.4 ng/g); and cherries contained the highest average level of imidacloprid

(32.1 ng/g) and thiacloprid (12.2 ng/g). Overall, spinach had the highest average IMI_{RPF} (569.2 ng/g), followed by baby food - peas (482.5 ng/g), cherries (401.8 ng/g), baby food - carrots (378.2 ng/g), and hot peppers (362.6 ng/g).

Table 2 shows the summary estimates of long-term UI (g/day) using NHANES consumption 2011-2012 data. For the USCC dataset, we included seven out of 12 vegetables and all 6 fruits in the final analysis but excluded squash because of the lack of multiple residue measurements and edamame due to no consumption as reported by the NHANES participants in the two 24-hr recalls. We also excluded cilantro, kale, and zucchini as the result of a SAS macro warning of unstable estimation because of rare consumption (less than 10 participants had two 24-hr recall consumption). For the USDA/PDP dataset, we included 22 out of 29 vegetable commodities and 17 out of 22 fruit commodities in the final analysis. We excluded cherry tomatoes, infant formula (soy-based), and soybean grain from all analyses because no NHANES participants consumed those items in the two 24-hr recalls. Beets (canned), mushrooms, papaya, peaches (baby food) and raspberries (fresh and frozen) were also excluded by the NCI method due to less than 10 participants reported consumptions of those items. Because of the right skewness of the usual intake (UI) distribution, we reported both mean and median of UIs for comparisons. Tomatoes (11.9 & 7.1 g/day) and lettuce (10.8 & 7.9 g/day) had the highest mean and median UI of vegetables, respectively, whereas orange juice (35.3 & 9.7 g/day) and bananas (18.6 & 8.2 g/day) had the highest mean and median UI among all fruits, respectively.

Table 1. Relative potency factors (RPF) for neonicotinoids based on relative chronic reference doses (cRfD).

Neonicotinoid	NOAEL[a] (mg/kg/d)	Study and observation endpoints	Species	cRfD[b] (mg/kg/d)	RPF[c]	LOD[d] (ng/g)		Ref[g]
						PDP	USCC	
Acetamiprid (U.S. EPA 2012)	7.1	Chronic/Oncogenicity: Decreased body weight and body weight gains in females and hepatocellular vacuolation in males.	Rat	0.071	0.8	1 – 160	0.03	26
Clothianidin (U.S. EPA 2005)	9.8	2-Generation reproduction: Reduction in mean body weight gain; delayed sexual maturation; decreased absolute thymus weights in the first filial generation (F_1) pups. Increase in stillbirths in both generations	Rat	0.0098[e]	5.8	1.5 – 90	0.03 – 0.15	27
Dinotefuran (U.S. EPA 2005)	20[f]	Chronic: Decreased thymus weight in males	Dog	0.02[e]	2.9	3 –100	0.03 – 0.15	28
Imidacloprid (U.S. EPA 2005)	5.7	Chronic/Oncogenicity: Increased incidence of mineralized particles in thyroid colloid in males.	Rat	0.057	1.0	1 – 56	0.03 – 0.15	29
Thiacloprid (U.S. EPA 2003)	1.2	Chronic: Hepatic hypertrophy and cytoplasmic change and thyroid hypertrophy and retinal degeneration.	Rat	0.004[e]	14.2	1 – 10	0.03	30
Thiamethoxam (U.S. EPA 2000)	0.6	2-Generation reproduction: Increased incidence and severity of tubular atrophy in testes of F_1 generation males.	Rat	0.006	9.5	1 - 80	0.03	31

[a]NOAEL, no observed adverse effect level.
[b]cRfD, U.S. EPA derived chronic reference dose.
[c]RPF, relative potency factor calculated based on cRfD of each neonic normalized by the cRfD of imidacloprid.
[d]LOD, limit of detection.
[e]**Clothianidin:** Additional 10x for the absence of developmental immunotoxicity study; **Dinotefuran:** Additional 10x for the extrapolation from LOAEL to NOAEL; **Thiacloprid:** Additional 3x as safety factor (SF) for the lack of morphometric assessments for the low- and mid-dose group animals in the developmental neurotoxicity study.
[f]LOAEL, lowest observed adverse effect level.
[g]Reference.

Table 2. Estimated long-term usual intake (UI) from NHANES 2011-2012.

	Food Items	Long-term Usual Intake (g/day)			
		Mean	**5th**	**Median**	**95th**
Vegetables	Avocado	1.79	0.69	1.67	3.32
	Green Beans[a]	5.36	0.60	3.36	16.79
	Broccoli	4.85	0.28	2.36	17.63
	Cabbage	1.88	0.20	1.36	5.31
	Carrot	4.44	0.10	1.63	18.30
	Cauliflower	1.17	0.35	1.02	2.50
	Celery	1.04	0.09	0.64	3.31
	Corn[b]	5.28	2.30	5.03	9.13
	Cucumber	3.49	4.45E-02	0.91	15.05
	Hot pepper	0.06	0.04	0.06	0.09
	Lettuce	10.84	1.31	7.34	32.14
	Onion	2.31	0.15	1.23	8.13
	Snap Peas	1.88	1.82	1.88	1.93
	Bell Pepper	2.10	0.09	0.91	7.97
	Spinach[a]	2.31	2.02E-02	0.49	10.10
	Squash[c]	2.06	1.01	1.95	3.49
	Tomato	11.93	0.73	7.12	39.47
Fruits	Apples	19.83	0.31	7.12	85.34
	Apple juice	12.64	0.01	0.94	70.11
	Apple sauce[d]	1.50	0.31	1.32	3.31
	Banana	18.63	0.39	8.23	73.27
	Blueberries[e]	1.91	<0.01	0.14	9.50
	Cantaloupe	3.86	0.44	2.42	11.99
	Cherries[f]	1.70	1.65	1.70	1.75
	Cranberries	0.46	0.04	0.25	1.52
	Grape juice	3.49	1.14	2.96	7.63
	Grapes	4.74	0.13	1.78	19.83
	Honeydew melon	0.74	0.25	0.63	1.58
	Nectarine	1.93	1.40	1.92	2.49
	Orange juice	35.28	0.25	9.69	162.85
	Peach	4.79	2.33E-02	0.8	22.3
	Pear[d]	4.60E-02	1.26E-08	1.51E-05	1.81E-02
	Plum	0.70	0.26	0.61	1.45
	Strawberries	3.86	0.06	1.09	17.17
	Tangerine	1.36	0.60	1.24	2.55
	Watermelon	9.12	8.73	9.12	9.53

[a]Including canned and frozen; [b]Sweet corns, including fresh and frozen; [c]Including summer and winter squash; [d]Baby food; [e]Including cultivated and frozen; [f]Including frozen.

Table 3 shows the descriptive statistics of the estimated average daily intake (ADI) of imidacloprid-equivalent total neonic or $IMI_{RPF,}$ under the assumption that the mean imidacloprid-equivalent total neonic was used as the total neonic residue level in fruits and vegetables that were consumed. For items collected from the USCC study, tomatoes contributed the most to the ADI of $IMI_{RPF,}$ among vegetables at the 5th percentile (1.33 ng/kg/day), median (14.4 ng/kg/day), and the 95th percentile (108 ng/kg/day). Apples contributed the most to the ADI of IMI_{RPF} among fruits at median (2.03 ng/kg/day) and the 95th percentile (28.6 ng/kg/day), whereas honeydews contributed the most of ADI at the 5th percentile (0.12 ng/kg/day). For USDA/PDP dataset, squash, tomatoes, and spinach contributed the most to the ADI of IMI_{RPF} among vegetables at the 5th percentile (2.69 ng/kg/day), median (7.28 ng/kg/day), and at the 95th percentile (106 ng/kg/day), respectively. Cherries (5.91 ng/kg/day) and banana (26.5 and 286 ng/kg/day) contributed the most to the ADI of IMI_{RPF} among fruits at the 5th, and median and 95th percentile. **Figure 2** shows the estimated overall ADI distributions of IMI_{RPF} via fruits and vegetables consumption using the USCC, USDA/PDP, and both datasets on the same scale of IMI_{RPF} (x-axis), and its relationship to the cRfD of imidacloprid. With the USCC residue data, the distributions of fruit ADI were higher than that of vegetable ADI. Whereas with the USDA/PDP residue data, the distributions of fruit ADI were lower than that of vegetable ADI. In general, we found that the estimations of ADI of IMI_{RPF} using either residue dataset were several orders of magnitude lower than the cRfD of imidacloprid ($57x10^3$ ng/kg/d).

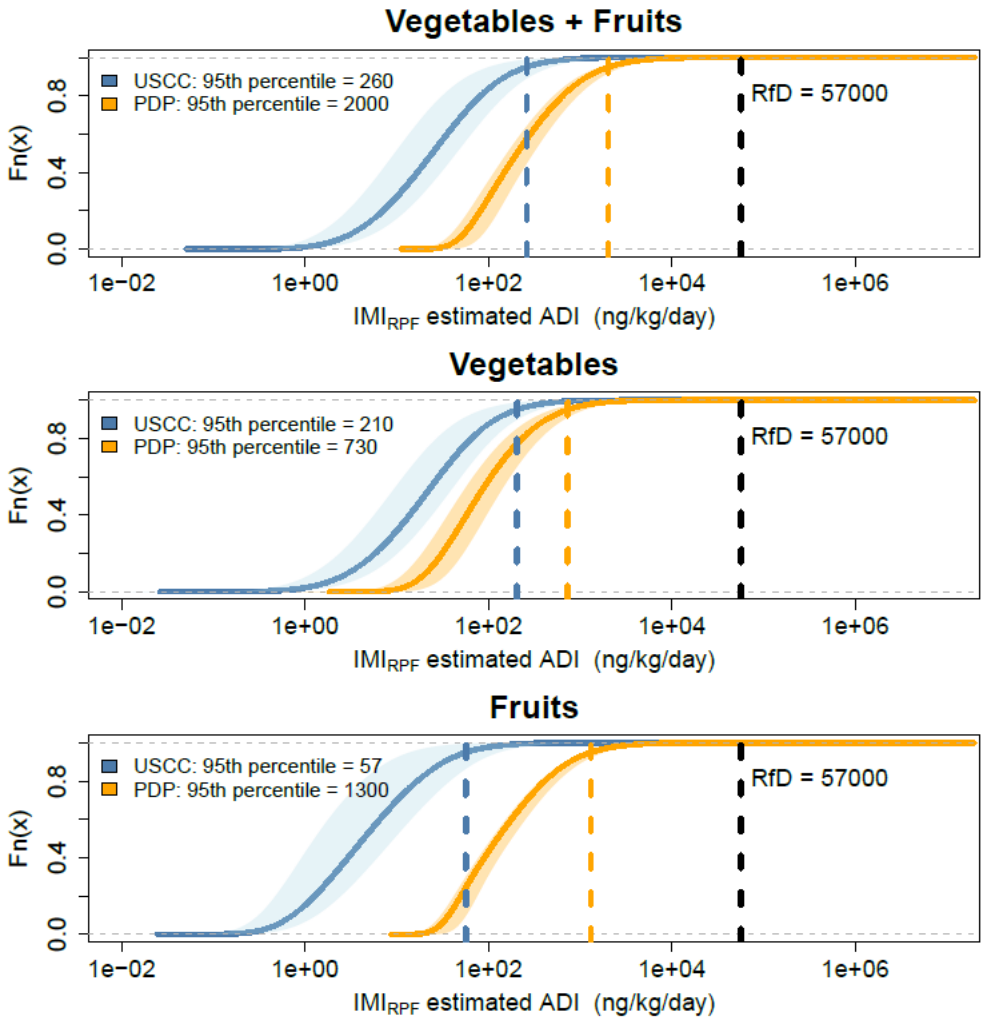

Figure 2. Average Daily Intake (ADI) Distribution of Neonicotinoid Dietary Exposure through Fruit and Vegetable Consumption from USCC and PDP 2011-2014 Datasets. The blue shaded area showed the difference of cumulative density of IMIRPF estimated ADI originated from distribution of neonicotinoid residues in USCC (5th to 95th percentile of residue levels; blue lines were for mean residue levels). The orange shaded area showed the difference of cumulative density of IMIRPF estimated ADI originated from distribution of neonicotinoid residues in PDP 2011-2014 (5th to 95th percentile of residue levels; orange lines were for mean residue levels). The labeled 95th percentiles showed the 95th percentile IMIRPF estimated ADI when mean residue levels were consumed.

Table 3. Estimated Average Daily Intake (ADI) of Total Neonics by Vegetable and Fruit Consumption Using the Mean IMIRPF as the Total Neonic Residue.

		ADI (ng/kg/day)			
	USCC Food Items	**Mean**	**5th**	**Median**	**95th**
Vegetables **(N=7)**	Broccoli	0.34	0.01	0.13	1.25
	Corn	0.01	<0.01	<0.01	0.02
	Cucumber	0.67	0.01	0.14	2.70
	Lettuce	0.36	0.03	0.19	1.20
	Pepper	3.70	0.11	1.24	14.00
	Spinach	1.45	0.01	0.24	5.90
	Tomato	31.50	1.33	14.40	108.00
Fruits **(N=6)**	Apple	7.17	0.08	2.03	28.60
	Cantaloupe	1.23	0.09	0.59	4.18
	Cranberries	0.12	0.03	0.08	0.35
	Grapes	0.10	<0.01	0.03	0.42
	Honeydew	0.57	0.12	0.36	1.72
	Strawberries	1.27	0.01	0.28	5.28
	PDP/USDA Food Items	**Mean**	**5th**	**Median**	**95th**
Vegetables **(N=16)**	Avocado	2.12	0.51	1.42	6.38
	Green Beans[a]	11.19	0.84	5.36	38.14
	Broccoli	15.80	0.62	5.95	58.60
	Cabbage	2.95	0.22	1.60	9.57
	Carrot	6.43	0.11	1.84	25.50
	Cauliflower	1.20	0.23	0.76	3.60
	Celery	1.53	0.09	0.72	5.30
	Corn[b]	7.63	2.01	5.16	23.02
	Hot Pepper	0.46	0.18	0.32	1.40
	Lettuce	12.50	1.02	6.42	41.40
	Onion	16.50	0.72	6.80	59.60
	Peas	2.00	0.86	1.37	6.16
	Pepper	11.80	0.35	3.96	44.80
	Spinach[a]	26.20	0.16	4.36	106.00
	Squash[c]	9.30	2.69	6.27	28.02
	Tomato	15.90	0.67	7.28	54.70
Fruits **(N=16)**	Apple Juice	15.10	0.01	0.88	72.10
	Apple	31.60	0.35	8.85	126.00
	Applesauce[d]	4.83	0.66	3.09	14.70
	Banana	77.30	1.14	26.50	286.00
	Blueberries[e]	5.07	<0.01	0.29	22.13
	Cantaloupe	14.10	1.08	6.75	48.00
	Cherries[f]	13.70	5.91	9.38	42.20

(Continued)	Grape Juice	4.05	0.82	2.53	12.20
	Nectarine	10.40	4.04	7.17	31.80
	Orange Juice	35.50	0.18	7.63	149.00
	Peach	16.50	0.06	2.12	70.10
	Pear[d]	0.05	<0.01	<0.01	0.02
	Plum	0.68	0.15	0.44	2.03
	Strawberries	7.01	0.07	1.55	29.20
	Tangerine	4.69	1.23	3.08	14.00
	Watermelon	11.60	5.02	7.99	35.90

[a]Including canned and frozen; [b]Sweet corns, including fresh and frozen; [c]Including summer and winter squash; [d]Baby food; [e]Including cultivated and frozen; [f]Including frozen.
(Common commodities collected in both residue datasets were colored in shade.)

Figure 3 shows the results from the sensitivity analyses for the estimations of ADI distributions by including fruits and vegetables (including broccoli, corn, lettuce, pepper, spinach, tomatoes, apple, cantaloupe, and strawberries) that were collected by the USCC study and USDA/PDP 2011 – 2014. We summarized the ADI estimates with respect to different uncertainty scenarios and across different residue levels in **Table 4**. It appears that the results of ADI estimation using USCC residues were generally more stable than those using USDA/PDP residues. The estimated ADIs using the USCC study data were also relatively robust in terms of having similar means at different residue levels regardless of how those ND were managed, except for the inclusion of a single squash residue data. However, estimations of ADI based on USDA/PDP residues were much more fluctuated across different ND management strategies. In the case that we replaced ND samples with zeros (Strategy #3 in **Table 4**), the USDA/PDP estimated ADIs were actually lower than those estimated by the USCC residue data when individuals consumed fruits and vegetables containing the 5^{th} percentile and mean of IMI_{RPF}.

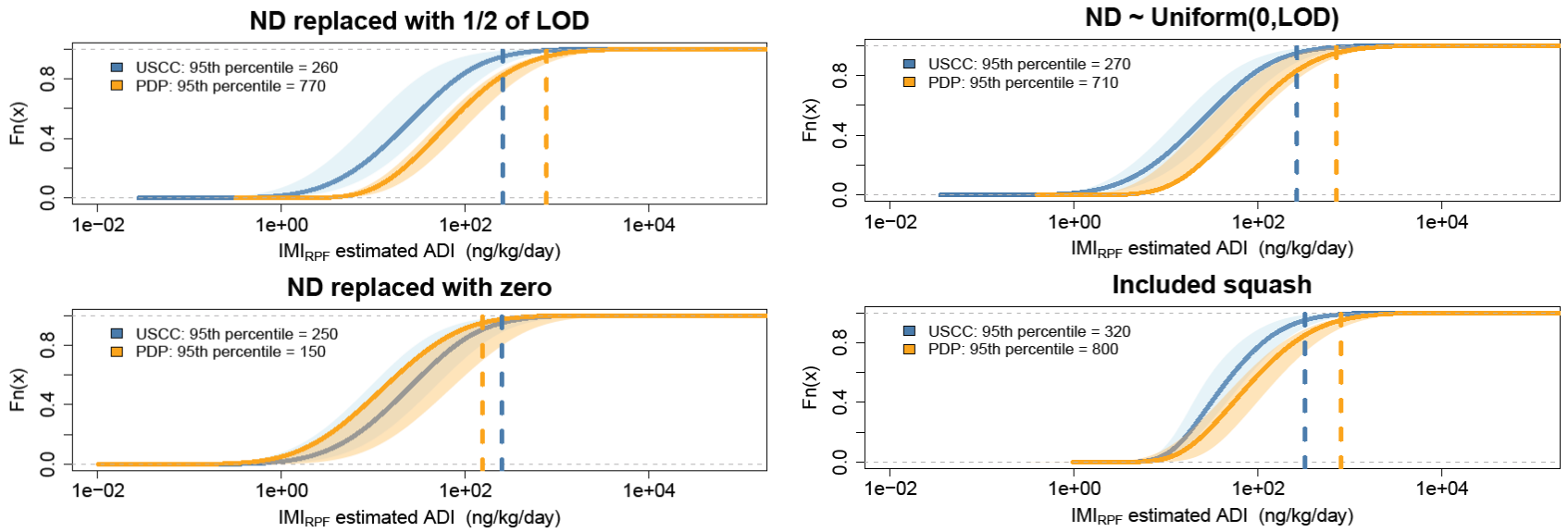

Figure 3. Sensitivity analysis of both USCC and PDP 2011 - 2014 residue datasets. Only common vegetables and fruits (broccoli, corn, lettuce, pepper, spinach, tomatoes, apple, cantaloupe, and strawberries) in both datasets were included for comparison. The blue shaded area showed the difference of cumulative density of IMI_{RPF} estimated ADI originated from distribution of neonicotinoids residues in USCC (5^{th} to 95^{th} percentile of residue levels; blue lines were fore mean residue levels). The orange shaded area showed the difference of cumulative density of IMI_{RPF} estimated ADI originated from distribution of neonicotinoid residues in PDP 2011-2014 (5^{th} to 95^{th} percentile of residue levels; orange lines were for mean residue levels). The labeled 95^{th} percentiles showed the 95^{th} percentile IMI_{RPF} estimated ADI when mean residue levels were consumed.

We conducted additional sensitivity analyses by including squash as an uncertainty factor because of the concern of a single large measurement of 427.2 ng/g of IMI_{RPF}, a value to which the ADI distributions could be significantly affected. We found large variations among squash's $IMI_{RPF,}$ calculation in which the 5^{th} and 95^{th} percentiles of IMI_{RPF} were 10 and 448.8 ng/g, respectively, using the USDA/PDP dataset. Therefore, we have adopted the most conservative approach treating IMI_{RPF} of USCC squash as a fixed value (427.2 ng/g) for all residue percentiles. We found that squash could be influential in terms of the relative percentage increase in the USCC ADI distributions involving mean IMI_{RPF} residues. Compared to the original settings (Strategy #1 in **Table 4**), significant differences of ADI distributions ($p<0.0001$) at all three residue levels were observed. The estimated mean ADI with respect to consumption of mean IMI_{RPF} increased from 66 to 91 ng/kg/day (38% increase) in the USCC dataset. However, no significant differences among the USDA/PDP dataset were observed, in which the mean ADI with respect to consumption of mean IMI_{RPF} increased from 202 to 215 ng/kg/day (7% increase).

Table 4. Results from the Sensitivity Analysis on the Estimated Average Daily Intake (ADI in ng/kg/day) of Imidacloprid-Equivalent Total Neonics.

Residue Dataset	Uncertainty Scenarios/ ND Management Strategy[b]	Estimated Mean ADI (p-value)[a]		
		5th IMI_{RPF}	Mean IMI_{RPF}	95th IMI_{RPF}
USCC	1	26	66	122
	2	30* ($1.1x10^{-4}$)	69	124
	3	25	65	121 (0.78)
	4	50* (<0.0001)	91* (<0.0001)	147* (<0.0001)
USDA/PDP	1	163	202	338
	2	80* (<0.0001)	189	259* (<0.0001)
	3	0* (<0.0001)	40* (<0.0001)	217* (<0.0001)
	4	165	215	372* ($1.38x10^{-2}$)

[a]Mean of the estimated ADI used the 5th, mean, or 95th percentile residue levels of every common commodities included in the sensitivity analysis. P-values were for Welch's t-tests comparing between strategies with Strategy #1. Bonferroni correction for the significance levels was used for multiple testing (p-values < $1.67x10^{-2}$), statistically significant differences were marked with *. [b]ND Management Strategies: 1. NDs replaced with ½ of LODs; 2. NDs replaced with a random variable from Uniform (0, LOD); 3. NDs replaced with zero; Main analyses were conducted based on the shaded strategy; 4. Analyses included neonic residues from the single squash sample. Strategies 1-3 excluded neonic residues from the single squash sample.

To our best knowledge, this is the first study aiming to estimate the daily intake of total neonic from fruit and vegetable consumption based on the U.S. population. We found the estimated average daily intake (ADI) of imidacloprid-equivalent total neonic using residue data from the USCC study were lower than those using USDA/PDP dataset. One of the reasons to explain such disparity is that fruits and vegetables served in the US Congressional cafeterias were provided by a food service company that advertises sustainable food practices and source organically grown agriculture.[17] Whereas food commodities collected by USDA/PDP are intended to supply general supermarkets and grocery stores across the country and therefore may be more representative of typical U.S. consumption. Notably though, the estimated ADIs of IMI_{RPF} using either USCC,

USDA/PDP, or the combined dataset were significantly lower than the existing cRfD of imidacloprid.

Intuitively, this outcome would be interpreted as the daily total neonic intake via fruit and vegetable consumption at the U.S. population level is unlikely to pose an appreciable risk of adverse health effects over a lifetime. However, we are aware that the uncertainties embedded in the analysis may alter such conclusion in the event that one of the following circumstances was existed. First of all, if more neonic residue data for fruits and vegetables collected from more diverse sources were available, the distributions of ADI of total neonic intake are likely to shift to the right from those estimated values as shown in **Figure 2**. This scenario seems plausible given the fact that both USCC and USDA/PDP residue datasets only covered a small portion of fruits and vegetables that were consumed by NHANES participants. Even with the expansion of the sampling years to include NHANES 2013 and 2014 for USDA/PDP analysis, the results presented here were still not sufficient for implication on the total fruit and vegetable consumption. Furthermore, we did not take into account other possible dietary sources, such as the consumption of other crops and drinking water which might also be contaminated with neonics.

Secondly, had more precise analytical methods with substantially lower LODs for neonics been used by the USDA/PDP, it is likely that many ND samples as reported by USDA/PDP would have become detectable with concentrations higher than the one-half of the LODs that we assigned for the purpose of model simulation. This would have direct impact on the upward estimation of ADI distributions for total neonic. As we compared the uncertainties originated from the selection of LODs in the sensitivity analysis, it is evident that the USCC dataset gave more stable ADI estimates regardless of how the ND samples were managed, but this is not the case for the USDA/PDP dataset. One plausible explanation is that USCC study utilized the analytical method

with LODs that are two to three orders of magnitude lower than those used by the USDA/PDP for the same neonic (**Table 1**). That led to 91% of detection for the USCC samples were detectable with at least one of the six neonics whereas only approximately 15% of USDA/PDP samples were above the LODs, and therefore we have to arbitrarily assign the values of one-half of their respective LOD for simulation. We are also aware that USDA/PDP datasets aimed for risk monitoring and management and therefore higher LODs close to the regulatory level were used. However, due to the lack of more comprehensive and precise datasets that could be used to generalize the risk assessment for the U.S. population, USDA/PDP dataset that contained lots of ND data was chosen for dietary risk assessment and comparison with the USCC dataset.

Lastly, in the future event when cRfD were to be revised lower based on the growing evidence of toxicological effects of neonics in mammals, the issue of the sensitivity of analytical methods used to analyze neonics in fruits and vegetables would become critically important. For instance, the current cRfDs of neonics were established based on observed endpoints listed in **Table 1**, which have very little or no relevance to the known toxicological mechanism of neonics that is functioned as the nAChR agonists. Even though neonics are known to be less selectively bound to mammalian nAChR, it is possible that the inhibition of nAChR would occur at lower levels of neonic exposure than those observed endpoints. Under the current cRfDs for neonics, the issue of ND data resulting from the elevated LODs might not be a matter for concern because the estimated ADIs are significantly lower than those cRfDs. However, if results from the future studies prove the hypothesis that the inhibition of nAChR or other neurological adverse outcomes could take place at lower NOAELs as shown in **Table 1**, the revision of cRfDs for neonics to lower levels would be necessary in order to better reflect biologically plausible endpoints and subsequently to better protect public health. Under this circumstance, a sensitive analytical method

would be essential to quantify neonic residues in foods at levels that are allowed to compute ADI with great confidence in order to compare to the cRfDs.

In this chapter, we demonstrated a methodology aiming to simulate human dietary intakes of total neonic by linking residue data with fruit and vegetable consumption patterns. There are two innovate approaches that we used in order to facilitate the estimation of the average dietary intake (ADI) of total neonic. We adopted the validated NCI method[24] for estimating the distribution of long-term ADI of food items among the population using the NHANES two 24-hr dietary recalls. It is generally agreed that when using these short-term recall measurements to estimate UI, 24-hr recall intake is an unbiased estimate of the long-term UI,[32] and by repeating the measurements of recalls from an individual, the within-person variations should be canceled out. However, we should also note that NCI method assumed no misclassification of respondent's food intake even though this ideal scenario would most likely to be violated giving the nature of using recall data. Although the 24-hr dietary recalls could capture more comprehensive and detailed information about all food consumption by the respondents in the past 24 hours, the memory dependent interview leading to potential recall bias (e.g. bad estimation of consumed food portion, bias reporting of food types based on knowledge of nutritional values) and interviewers' bias (whether they were well-trained to conduct the interview) should not be neglected[33, 34].

We applied RPF approach to integrate individual neonics found in a fruit or vegetable sample into a single matrix that is corresponding to the imidacloprid-equivalent total neonic, or IMI_{RPF}. RPF has been used for integrating a mixture of chemicals that share the same toxicological mode of action, such as PAHs[15] or dioxins[16], and has recently been applied in assessing neonics in pollen collected from honeybees based on relative lowest-observed-adverse-effect-level (LOAEL).[23] By integrating all neonics into an imidacloprid-equivalent total neonic, the IMI_{RPF}

reported for each food item is no longer a simple summation of individual neonic residues, but encoded with the cumulative toxicity of all six neonics via fruits and vegetable consumption.

We calculated RPFs based on the comparison of individual neonic's cRfD with imidacloprid's cRfD. We used relative cRfD rather than the relative no-observed-adverse-effect-level (NOAEL) or LOAEL because cRfD is independent from species used in the toxicological studies and therefore is more suitable for the application in integrating human exposure to total neonic. Since U.S. EPA uses cRfD in their regulatory framework for assessing daily exposure to human population without an appreciable risk of adverse non-cancer health effects over a lifetime,[35-37] using cRfD in the RPF calculation shall minimize the uncertainties arising from interspecies, intraspecies, sub-chronic to chronic experiments, and incomplete to complete database.

We acknowledge that the methodology and the residue and consumption databases that we utilized for estimating the ADIs of total neonic comes with several limitations. First of all, although the USDA/PDP residue dataset offers more fruit and vegetable samples, a large portion of those samples were either ND that leads to very low frequency of detection of any neonic. As we replaced ND samples with one-half of their respective LODs in the main analyses, it occurred quite often that the average IMI_{RPF} for less frequently detected items remain positive and sometimes even higher levels than more frequently detected items. This problem would have been prevented had more sensitive analytical methods with lower LODs been used for USDA/PDP samples. Per our own research experience, we have developed an analytical method with LODs that are two-three orders of magnitude lower than those used by the labs contracted with USDA/PDP without any technical difficulties or cost issues.[38] In order to improve the robustness of the ADI simulation

for total neonic, it is necessary to lower the LODs, or reduce the percentage of ND samples so the ADI estimates would not be affected by how the ND data is managed.

The second limitation has to do with the use of NHANES consumption information in which two 24-hr dietary recalls from the same participants were collected within 3-10 days. Although the collection of dietary recalls in consecutive days could be reflective of random daily consumption, by no mean that it reflects the seasonal or annual consumption patterns both qualitatively and quantitatively. Besides, we didn't adjust for other participants' characteristics (such as race, gender, or ages) in the analyses. As we stratified all participants by consumption items, further adjustment for other covariates would lead to non-identifiability of the covariates' effects in certain food items, especially in the analyses of food items that are less likely to be consumed. However, since we are interested in an inference for the general population, the variabilities within population were still reflected by the body weight, in which were presented in the ADI cumulative distribution.

CHAPTER 2

Increase Mitochondrial DNA Copy Number in Honeybees (*Apis mellifera*) Resulting from Sub-Lethal Neonicotinoids Exposure

Chi-Hsuan Chang[1],

Bernardo Lemos[1],

David MacIntosh[1],

Chensheng Lu[1, †]

[1]Department of Environmental Health, Harvard T.H. Chan School of Public Health, Boston, Massachusetts

Abstract

Neonicotinoids, a group of widely used systemic insecticides, have been shown as one of the risk factors to honeybee colony collapse disorder (CCD). Although the exact biological mechanisms of CCD have yet to be made clear, we postulated that mitochondrial DNA damage in honeybees leading to mitochondrial dysfunction and malfunctioned thermoregulation of bees is a plausible biological mechanism. In this chapter, we aimed to demonstrate using relative mitochondrial DNA copy number (RmtDNAcn) as an early biomarker of chronic sub-lethal neonicotinoid effects in honeybees. We analyzed three generations of adult worker bees collected from sub-lethal imidacloprid-, clothianidin-treated and control hives before, during, and after treatments. We found a significantly higher ($p<0.001$) mean RmtDNAcn among bees reared from later brood generations by the same queens. In addition, positive but not significant association between RmtDNAcn among later brood generations and neonicotinoid treatments was observed. These results gave support to the hypothesis of the causation of sub-lethal neonicotinoid exposure and increase in mitochondrial DNAcn in two perspectives. Firstly, increase in RmtDNAcn could be inheritable in honeybees regardless of neonicotinoid treatments. Secondly, sub-lethal neonicotinoid exposure could result to additional increase in RmtDNAcn caused by normal aging in bees. Future research should focus on verifying inheritable mtDNAcn due to chronic sub-lethal neonicotinoid exposure and its subsequent mitochondrial damage in bees in order to elucidate the potential toxicity of sub-lethal neonicotinoid exposure.

Introduction

Although the cause of the massive decline in global honeybee (*Apis mellifera*) population remains unclear or controversial, the phenomenon of massive disappearing of honeybee in winter, known as colony collapse disorder (CCD), has been linked to pesticide/insecticides use, habitat loss, parasites, or other factors.[1, 7, 8] Neonicotinoids (neonics) are systemic insecticides that are most widely used worldwide with considerable increasing usage nowadays.[1, 3] Neonics have been shown to associate with impairing reproductive and behavioral abilities in honeybees at sub-lethal levels[39], including decreasing brood size[40-42], affecting foraging activities[8, 40-43] and syrup consumption, and implication in the occurrence of CCD.[6]

Neonics' effects on mitochondrial bioenergetics and dysfunctions among honeybees and bumblebees (*Bombus terrestris*) renders the biological plausibility linking sub-lethal neonics exposure to the reduction in ATP generation. Because the lack of sufficient ATP would adversely influence high energy-demanding activities in bees, it could be a possible mechanism leading to CCD.[9-11] Study has shown that imidacloprid could inhibit respiration, influence electron transit chain (ETC) and reduce the generation of ATP dose-dependently in both thorax and head.[9] Bumblebees exposed to 1 nM of imidacloprid for 2 days and 10 nM of clothianidin in acute manner (minutes) were found to express rapid nicotinic acetylcholine receptor (nAChR)-dependent mitochondrial depolarization.[10] In order to eliminate colony heat loss and minimize energy expenditure in winter, bees are shivering and crowding tightly together by forming a cluster inside the hive.[11] Being the thermal homeostasis maintaining mechanism, shivering thoracic flight muscle is highly energy demanding.[11] Therefore, considering the thermoregulation mechanism in bees and the appearance of CCD in winter season in which massive numbers of adult bees suddenly

disappear from their hive,[44] the hypothesis of mitochondrial dysfunction being a plausible cause of colony death bears significant scientific merit for further investigation.

In this chapter, we hypothesized that chronic sub-lethal exposure to neonics could lead to increase in relative mitochondrial DNA copy number (RmtDNAcn) in adult honeybees. As increasing RmtDNAcn has been shown to relate to mtDNA damage[12] and knowing the mechanism of mitochondrial heteroplasmy[45-47], we proposed using RmtDNAcn as a novel biomarker to detect mitochondrial dysfunction at an earlier stage under the sub-lethal exposure conditions that are more environmentally relevant. We evaluated the hypothesis that (i) later brood generations from the neonics-treated hives would have higher level of RmtDNAcn than the control hives; (ii) whether or not RmtDNAcn could be inherited from queen to worker bees raising from later brood generations; (iii) whether neonics-treated hives have a higher onset risk of bee disappearance and mortality risk over the winter; and (iv) whether the higher onset risk of bee disappearance and mortality risk, as downstream outcome measurements of mitochondrial dysfunction, were associated with increased level of RmtDNAcn ratio.

Materials and Methods

Neonics Administration in adult foraging honeybees. We collected adult worker bees at the entrance of their hive after returning from the foraging activity in a split-plot designed field study in 2012.[48] We set up those experimental hives at three independent sites (at least 12 km away from one another) with six honeybee hives per site (N = 18). At each site, colonies were either fed with sucrose- (table sugar; N = 3) or high-fructose corn syrup-fed (HFCS; N = 3) group. Colonies within each sugar group (N=3) were administered with either imidacloprid (IMI), clothianidin (CLO), or no pesticide (control) weekly. We administered 258 µg of IMI (1-((6chloro-3-pyridinyl) methyl)-N-nitro-2-imidazolidinimine) or CLO ((1-(2-Chloro-5-thiazolylmethyl)-3-methyl-2-nitroguanidine) dissolved in 0.5 gallon of either sucrose or HFCS to the colonies each week for 13 consecutively weeks, or equivalent to 37 µg/colony/day for 91 consecutively days. The dosing regime started on July 2nd and ended on September 17th, 2012. With an estimation of 50,000 bees per colony during the active foraging season, the administered dose was approximately equivalent to 0.74 ng/bee/day for both IMI- and CLO-treated hives. All 18 colonies in the study were healthy and alive before, during, and after the 13-week neonics administration.

We collected adult worker bees from each hive on July 2nd (F0), August 20th (F2), and October 15th (F4) 2012 by intercepting them at the entrance of the hive when they returned from foraging. Those adult bees were subsequent generations from the same queen at different "ages", and also represented as pre-treatment (F0), during-treatment (F2), and post-treatment (F4) groups. As normal spring and summer worker bees generally have an average lifespan of 25 – 35 days[49, 50] and they start foraging when they are approximately 21 days old[51], worker bees collected monthly represented different generations brooded by the same queen. Upon capturing, we

transferred bees to a 50-mL centrifuge tube immediately, placed the tubes in a cooler with dry ice during transportation, and stored in a -80^{o}C freezer in the lab until analysis.

Mitochondrial DNA copy number (mtDNAcn) Measurement. We quantified mtDNAcn in the thoracic muscle (middle) section of an adult foraging honeybee. We dissected bees immediately after removing them from the -80^{o}C freezer and then extracted the total gDNA using the DNeasy Blood & Tissue Kit (Qiagen). We first homogenized individual thoracic samples with 180 µL of ATL buffer using a disposable pestle, and then added 20 µL of proteinase K to the homogenized samples and vortexed thoroughly. The mixture was incubated at 56 °C overnight on a shaking water-bath. To obtain RNA free gDNA, we added 4 uL of 100mg/ml of RNase A (Qiagen) to the sample and then incubated the mixture at room temperature for 2 minutes followed by vortexing for 15 seconds. We then added the following buffers in the order of 200 µL of AL and 200 µL of ethanol (100%) to the sample. The final mixture was applied into the DNeasy Mini spin column. After washing the column with AW1 and AW2 buffer, the total gDNA was obtained by eluting the DNeasy Mini spin column with 200 µL of AE.

We used the QuantiTect SYBR Green PCR Kit (Qiagen) for the q-PCR analysis (Applied Biosystem StepOne Plus Real-time PCR). We selected Cyt *b* gene (11004bp-12155bp) and *18s rRNA* to represent mtDNA and the nuclear gene, respectively. The thermal cycling conditions for *cyt b* and *18s rRNA* PCR are as follows; initial 15 minutes at 95 °C to activate the HotStarTaq DNA Polymerase and 40 cycles comprised of 15 seconds denaturation at 95 °C, 30 seconds anneal at 58 °C, and 30 seconds extension at 72 °C. Each run is completed by melting curve analysis to confirm the amplification specificity and the absence of primer dimers.

We normalized mtDNA copy number (mtDNAcn) by the copy number of a selected nuclear DNA (nDNAcn) as the internal reference gene to ΔCt using equation (6):

$$\Delta Ct = Ct_{(Cyt.\ b)} - Ct_{(18s\ rRNA)}$$

(Equation 6)

where Ct is the threshold cycle number at the determined level of log-based fluorescence and therefore inverse proportional to the log-based initial copy number of the target gene. Cyt *b* and *18s rRNA* were used to measure the Ct for mtDNA and nDNA, respectively. The primers used for Cyt b and*18s rRNA* genes for q-PCR were: *Cyt b* F-5'AGC AGC TGC ATT TAT AGG ATA TG 3'; *Cyt b* R-5' AGA TTA GTA ATA ACT GTT GCA CCT C 3'; *18s rRNA* F- 5'GTG GGC CGA TAC GTT TAC TT 3'; *18s rRNA* R-5' CCG AGG TCC TAT TCC ATT ATT CC 3'.

To ensure similar amplification efficiencies for the designated primers of Cyt *b* and *18s rRNA*, we calculated the amplification efficiencies for those primers by running five serial dilutions of DNA samples on q-PCR using equation (7) and (8):

$$Ct = \alpha - \beta \log_{10}[X_0]$$

(Equation 7)

$$E = 10^{-1/\beta} - 1$$

(Equation 8)

where X_0 is the initial DNA concentrations of targeted genes, and E is the amplification efficiency.

Well-being Measurements of Honeybee Hives. We kept track of the well-being of experimental hives by measuring the brood counts and numbers of frames containing adult bees during and after neonics administration using the methods described previously.[6] Brood counts were recorded bi-weekly from June 29th, 2012 (before treatment administration started) to September 24th, 2012 (one week after the completion of neonics administration), and the numbers of frames containing adult bees in each hive were then tracked from October 27th, 2012 to April 4th, 2013. We then used both measurements served as the outcomes linking to the changes in RmtDNAcn.

Data analysis. We used R software (3.4.1) to perform all statistical analyses. We used the comparative Ct ($2^{-\Delta\Delta Ct}$) method to calculate the relative mtDNAcn (RmtDNAcn) ratio[45, 52, 53]. Because of the auto-correlation among those three bees collected at the same time from the same hive, they were considered replicate samples. Therefore, we measured RmtDNAcn ratio (which is $2^{-\Delta\Delta Ct}$) at the hive level (N = 18) using regression in the following steps:

1. ***Quality control.*** We conducted quality control analyses of ΔCt within treatment-sugar groups (6 groups). Since we only have triplicates per generation per hive, it is rather difficult to identify outliers. We therefore computed the average ΔCt among the hives per treatment-sugar group per generation (F0, F2, F4), and then excluded outliers (or samples) not within the range of IQ3 ± 1.5 x (IQ3 − IQ1) where IQ3 is the upper quartile and IQ1 is the lower quartile.
2. ***Statistical modeling.*** Since the objective of this chapter was to identify the association between sub-lethal neonicotinoid treatments and change in RmtDNAcn, as well as treatments' ultimate adverse effects on honeybee health, we conducted the following statistical analyses:

   2.1. Association between RmtDNAcn ratios and neonicotinoid treatments over time. We used equation (9) as an application of the $2^{-\Delta\Delta Ct}$ approach to calculate RmtDNAcn ratios between treatment groups across generations of honeybees in individual hives:

$$-\Delta Ct_{hive} * \log(2) = a_0 + a_{hive} + b * J + \sum c_k I[Treatment_{k,\,hive}] + \sum d_k J * I[Treatment_{k,hive}] \quad \textbf{(Equation 9)}$$

   where a_{hive} represents random hive effect; J = 2 and 4, corresponding to F2 and F4 (linear assumption on normal aging effects), respectively; k = 1 and 2, corresponding to IMI and CLO treatments, respectively;

   2^b represents the RmtDNAcn ratio of F2 vs. F0 or F4 vs. F2 generation among control groups treatment effects;

2^{ck} represents the RmtDNAcn ratio of $treatment_k$ as compared to the control group; and 2^{dk} represents the additional generational effects due to $treatment_k$ (that didn't exist in the control group).

2.2. Association between onset of bee disappearance and neonicotinoid treatments. We tracked the numbers of frame (2 sides per bee frame) that contained bees weekly over the winter and spring next year (from October 27th to April 4th) in order to confirm the timing of onset of bee disappearance. To incorporate the information of time that we observed for the onset of bee disappearance and to determine whether both **(a)** neonicotinoid exposure and **(b)** its contribution to the higher RmtDNAcn ratios would pose significant risk of bee disappearance, we adopted the mixed effect Cox proportional hazard model shown in equation (10) to calculate the average onset risk of bee disappearance over the winter associated with treatments and RmtDNAcn levels. We used RmtDNAcn ratio of F4 versus F0 as it was the last measurement of RmtDNAcn before we started collecting the bee disappearance data within the same hive.

$$h(t_{fs}) = h_0(t_{fs}) \exp[a_{fs,\,hive} + \sum a_k I[Treatment_{k,\,fs}] + b_0 \, Log2(RmtDNAcn\ Ratio_{fs})]$$

$$a_{fs,\,hive} \sim N(0, \sigma_{hive}^2) \qquad \textbf{(Equation 10)}$$

where t_{fs} represents the duration of time that one side of any given frame remained the presence of bees (or no onset of bee disappearance); $h(t_{fs})$ represents the onset risk of bee disappearance from a side of frames in a hive at t_{fs}, adjusting for treatments and RmtDNAcn ratio; $h_0(t_{fs})$ is the baseline hazard at $t_{fs,}$ known as the onset risk of bee disappearance in a side of bee frames of a control hive when RmtDNAcn ratio was 1 at F4; $a_{fs,\,hive}$ refers to the random intercept that

influence the onset risk of bee disappearance from a side of frames, which is assumed to follow a normal distribution with a variance of σ_{hive}^2.

Similarly, $Exp[a_k]$ and $exp[b_0]$ show the hazard ratios of the onset of bee disappearance in a side of frames in a hive due to neonicotinoid treatments and with every 2 times increase in RmtDNAcn ratio, adjusting for other covariates. Under the assumption of Cox PH model, hazard ratios were independent of time.

2.3. Association between hive survival over the winter and neonicotinoid treatments. Similar to 2.2., we used the Cox PH model in equation (11) to calculate the average mortality risk of bee hives over the winter that were associated with treatments and RmtDNAcn levels:

$$h(t_{hive}) = h_0(t_{hive}) \exp[\sum a_k I[Treatment_{k,\,hive}] + b_0 \, Log2(RmtDNAcn\ Ratio_{hive})]$$

(Equation 11)

where t_{hive} represents the survival time of a hive; $h(t_{hive})$ represents the mortality risk at t_{hive} given treatment (k = 1 and 2, corresponding to IMI and CLO treatments, respectively) and the last measurement of RmtDNAcn ratio; $h_0(t_{hive})$ is the baseline hazard at $t_{hive,}$ known as the mortality risk of control hives with RmtDNAcn ratio equal to 1 at F4; $Exp[a_k]$ and $exp[b_0]$ represent the hazard ratios due to neonicotinoid treatments and with the increase in RmtDNAcn ratio, adjusting for other covariates.

Power analysis. To evaluate the experimental goal of identifying the neonics-induced generation effects we also conducted a power analysis. We simulated the data to determine the number of total hives (n) needed to achieve certain power (%) of detecting the estimated magnitude difference of generation effects between the IMI/CLO treatments and the control (the four interaction terms) using equation (9). We run 5000 simulations and power was defined as the probability of these

simulations (for the effect sizes of each interaction term) in detecting a statistically significant effect of each interaction term at our model estimated level using equation (9).

Results and Discussion

To ensure the quality of experimental data, we implemented several quality control steps. Results from the five serial dilutions of DNA samples on q-PCR showed that the amplification efficiencies (E) of the designated primers for 18srRNA and cyt b genes were about the same (-3.41 and -3.37). The measurements for Ct of 18s rRNA and cyt b gene were within 18 – 24 and 15 – 23 with the coefficient of variations (CV) across samples of 6.9% and 9.6%, respectively. Those results showed stable Ct measurements. Overall, there was one missing measurement (control sample at F0) out of the 162 samples (18 hives x triplicates/hive x 3 generations). We excluded measurements for eight samples because they were either outliers (n = 7) or missing (n = 1) among their corresponding treatment-sugar groups (**Figure S1**). At the end, a total of 154 bee samples across 18 hives were included in the following analyses.

Table 5. Relative mitochondrial DNA copy numbers (RmtDNAcn[a]) in the thoracic muscle of honeybees collected before (F0), during (F2), and post-administration (F4) of no neonicotinoids (control), imidacloprid (IMI), or clothianidin (CLO) in sucrose, or high-fructose corn syrup (HFCS).

Treatment[a]	Sampling Generation	Hives (N_{Hives})	Bees (N_{Bees})	Mean (95% CI)		
				Sucrose	**HFCS**	**Sucrose & HFCS**
Control	F0[b]	3/3	16	0.18 (0.10, 0.36)	0.17 (0.08, 0.36)	0.18 (0.11, 0.28)
	F2[b]	3/3	17	0.47 (0.30, 0.74)	0.35 (0.20, 0.62)	0.41 (0.19, 0.86)
	F4[b]	3/3	18	1.18 (0.61, 2.29)	0.73 (0.34, 1.53)	0.93 (0.58, 1.49)
IMI	F0[b]	3/3	16	0.23 (0.12, 0.44)	0.17 (0.08, 0.36)	0.20 (0.12, 0.32)
	F2[b]	3/3	18	0.70 (0.44, 1.10)	0.55 (0.31, 0.97)	0.62 (0.44, 0.87)
	F4[b]	3/3	18	2.14 (1.11, 4.12)	1.80 (0.85, 3.80)	1.96 (1.22, 3.15)
CLO	F0[b]	3/3	15	0.18 (0.10, 0.35)	0.20 (0.09, 0.41)	0.19 (0.12, 0.30)
	F2[b]	3/3	18	0.53 (0.34, 0.83)	0.46 (0.27, 0.82)	0.50 (0.35, 0.70)
	F4[b]	3/3	18	1.53 (0.79, 2.95)	1.10 (0.52, 2.32)	1.30 (0.81, 2.08)

[a]RmtDNAcn is defined as the relative mitochondrial DNA copy numbers with respect to the nuclear DNA copy number ($2^{-\Delta Ct}$, where $\Delta Ct = Ct_{(Cyt\ b)} - Ct_{(18s\ rRNA)}$).
[b]F0, F2, and F4 generations of bees were collected on 7/2/2012, 8/20/2012, and 10/17/2012, respectively.

Table 5 summarizes the RmtDNAcn in the thoracic muscle of honeybees with respect to different neonic treatment groups and generations (F0, F2, and F4). To better understanding whether RmtDNAcn were different between hives fed with different sugar syrups, we presented the mean and the 95% CI of RmtDNAcn across treatments and generations among hives fed with sucrose-based syrup, HFCS-based syrup, and with both sucrose- and HFCS-based syrup. We found that at each sampling generation, hives fed with HFCS had slightly lower average of RmtDNAcn than those fed with sucrose, although the differences were not significantly different (**Tables S2** and **S4**). Therefore, we combined both sugar groups when presenting patterns across treatments and generations for all statistical analyses.

Table 6. Relative mitochondrial DNA copy numbers (RmtDNAcn) ratio[a] in the thoracic muscle of honeybees collected before (F0), during (F2), and post-administration (F4[b] of no neonicotinoids (control), imidacloprid (IMI), or clothianidin (CLO).

Treatment	Sampling Generation	Hives (N_{Hives})	Bees (N_{Bees})	Mean (95% CI) [c]
Control	F0[b]	6	16	1.00
	F2[b]	6	17	2.29 (1.64, 3.18)
	F4[b]	6	18	5.23 (2.70, 10.12)
IMI	F0[b]	6	16	1.11 (0.57, 2.16)
	F2[b]	6	18	3.50 (1.87, 6.55)
	F4[b]	6	18	11.06 (5.06, 24.15)
CLO	F0[b]	6	15	1.07 (0.55, 2.09)
	F2[b]	6	18	2.80 (1.50, 5.23)
	F4[b]	6	18	7.31 (3.35, 15.97)

[a]RmtDNAcn ratio is defined as the relative mitochondrial DNA copy numbers with respect to the nuclear DNA copy number of specific group compared to that of the June Control group ($2^{-\Delta\Delta Ct}$, where $\Delta\Delta Ct = \Delta Ct_{(TRT,\,j)} - \Delta Ct_{(CON,\,j)}$).
[b]F0, F2 and F4 generations of bees. were collected on 7/2/2012, 8/20/2012, and 10/17/2012, respectively.

As we compared models with different assumptions on the generational effect (or normal aging) expressed as the levels of mtDNAcn, the linear generation effect model was selected for the final interpretation (Details shown in **Tables S2** and **S3**). We did not find significant difference of RmtDNAcn among all 3 treatment groups (Control: 0.18; IMI: 0.20; CLO: 0.19) prior to neonics administration, suggesting the similar baseline of mtDNA status among queens across experimental hives. However, we found significant increase ($p<0.001$) of RmtDNAcn in bees collected from later brood generations of the same colony regardless of the treatment groups (control, IMI or CLO). The ratios of RmtDNAcn in bees collected from the control group increased from 2.29 in F2 to 5.23 in F4 (**Table 6**), comparing to mtDNAcn levels in F0 ($p< 0.001$).

We also found positive associations between RmtDNAcn and neonics-treated bees, in which higher RmtDNAcn ratios among later-brood generations were seen among neonics-treated bees. **Table 6** shows the descriptive statistics of RmtDNAcn ratios of F2 and F4 in IMI and CLO treated bees as compared to that of F0 in the control group. At F2 and F4, the magnitude of increase of the mean RmtDNAcn ratios among the neonics-treated bees was clearly higher than those in the control bees. The mean RmtDNAcn ratios of F2 vs. F0 among IMI and CLO bees were 3.15 (=3.50/1.11), and 2.62 (=2.80/1.07), respectively, whereas the mean RmtDNAcn ratios of F4 vs. F0 among IMI and CLO bees were 9.96 (=11.06/1.11), and 6.83 (=7.31/1.07), respectively. IMI-treated bees showed the largest increase of RmtDNAcn ratios for F4 vs. F2 and F2 vs. F0. These trends were presented visually in **Figure 4A**, where steeper slopes for mean RmtDNAcn among neonics-treated bees were observed when subsequent brood generations were compared. In **Figure 4B**, we also showed that RmtDNAcn levels associated with neonics exposure were cumulative over time in the subsequent brood generations. We found increasing trend of mean RmtDNAcn

when excluding the normal aging effect (levels observed among neonics-treated groups divided by that of the control group, also known as RmtDNAcn ratio) as exposure time lengths increase. The incremental increases of the mean RmtDNAcn among neonics-treated bees could still be observed at the post-treatment generations (F4), indicating that the increasing levels of RmtDNAcn in adult foraging honeybees were associated with cumulative exposure of sub-lethal neonics of the queens over time. Those results clearly demonstrated that while normal aging effect on increasing RmtDNAcn levels of the queens that pass on to the later brood generations is observed, the additional increase in RmtDNAcn levels measured in F2 and F4 worker bees were likely inherited from the aging queen bees who have been exposure to IMI or CLO.

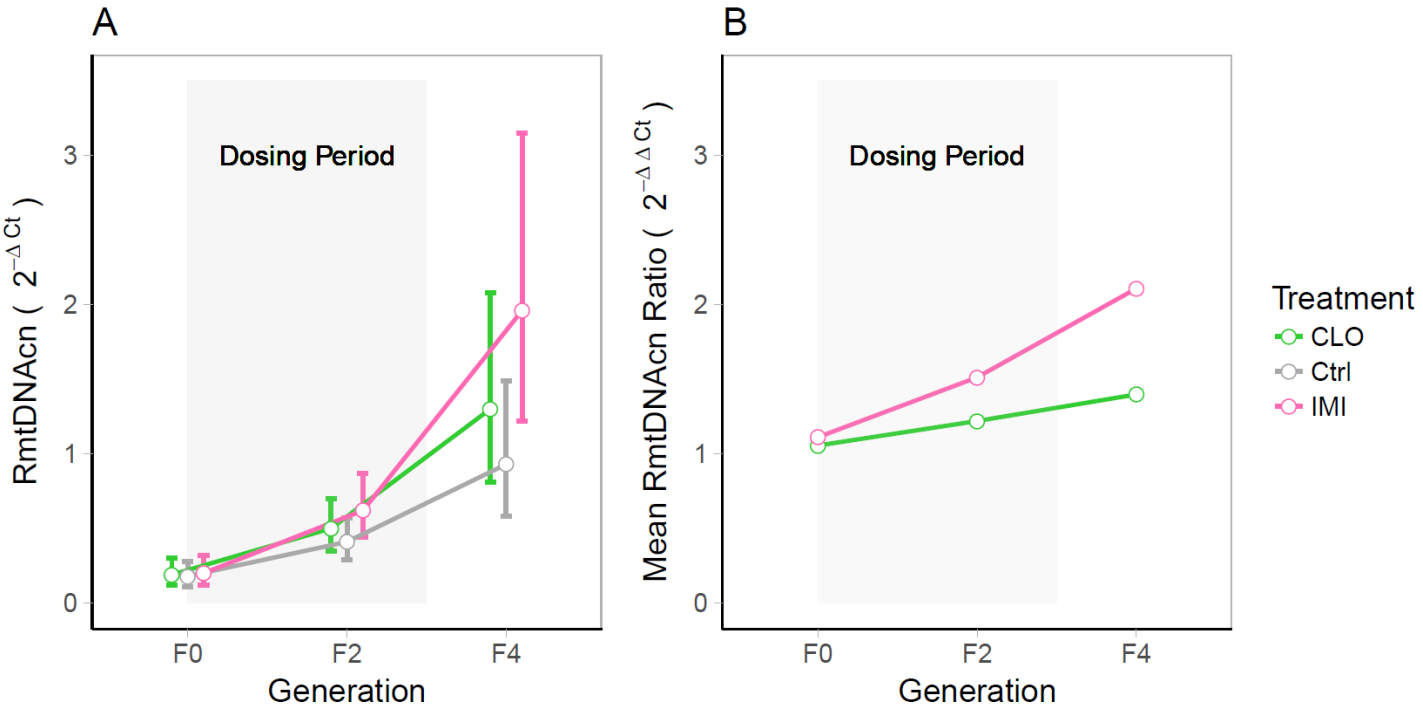

Figure 4. Increasing mtDNA copy numbers in the subsequent brood generations from the same colony (queen) with sub-lethal neonics administration.(A) Magnitude of RmtDNAcn ($2^{--\Delta Ct}$) across different brood generations (F0, F2, F4) representing pre- (F0), during- (F2), and post-administration (F4) of neonics. Gray, pink, and green points and error bars show the mean and 95% CI of the RmtDNAcn levels we observed from the control, IMI, and CLO groups. (b) Increasing mean RmtDNAcn ratios in subsequent brood generations in conjunction with sub-lethal IMI and CLO administration. Dosing Period (13 weeks in total) is shaded, which started immediately after baseline (F0) measurements on July 2nd and completed on September 17th, 2012.

Beyond finding the increasing trend of RmtDNAcn levels associated with cumulative exposure to sub-lethal levels of neonics, we also linked these findings to brood sizes during neonic administration and survival probabilities of hives over winter. **Figure 5** shows overall decreasing trends of brood counts and frames with bees per hive over the study period regardless of neonics treatments (as the mean ±SD intervals already overlapped). Although no significant difference of brood sizes was seen, we observed a clear separation of the numbers of frames remained with bees between control and neonics treated-hives since the 180th day from the beginning of neonics administration (December 29th, 2012). IMI-treated hives showed the greatest disappearance of bees from frames in hives with an average 1.42 frames that left with bees on April 4th, 2013, followed by the 2 frames of CLO-treated hives. Control hives, on average, were left with 5.83 frames of bees at the end of the study.

We noticed that hives suffered from disappearance of bees could eventually recover toward the end of winter (decreasing then again increasing numbers of frames with bees), as shown in **Figure 5**. This phenomenon was especially obvious in control hives at an earlier time during winter. For example, the average frames of bees in the control hives increased from December 16th, 2012 to January 26th, 2013 as well as from March 7th to April 4th, 2013. On the other hand, hives treated with IMI or CLO exhibited a steady decrease of the number of frames with bees.

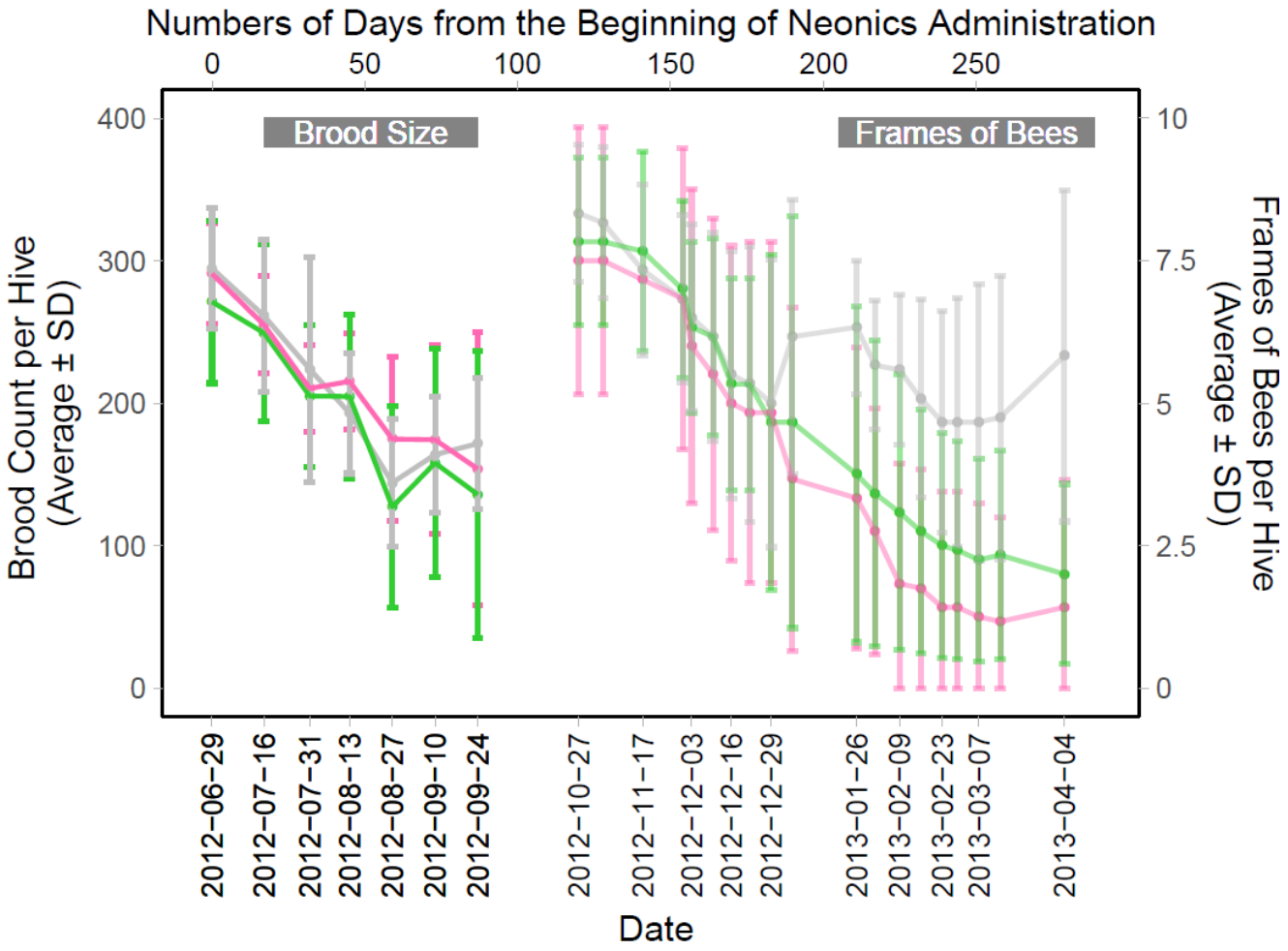

Figure 5. Records of brood size and frames of bees per hive. Error bars were referred to (±SD). Lower bounds below zero were set to zero.

In **Figure 6**, we compared the numbers of bee frame (two sides per frame) that had onset of bee disappearance at multiple time points over the winter (October 27th to April 4th, 2013) and found that IMI-treated hives had a faster onset of bee disappearance, followed by CLO-treated hives. **Figure 6** also shows the time to the death of bee hives across different treatments (Ctrl, IMI, or CLO) over the winter. Overall, we observed a higher survival probability of control hives compared to IMI- or CLO-treated hives, in which less dead control hives was observed at all time points. At the end of the field study (April 4th, 2012), 5 out of 6 control hives still alive, however,

4 and 2 out of 6 CLO and IMI hives remained survive, respectively. It is also true that not only higher mortality was associated with neonic-treated hives, but also the timing of dead hives occurred earlier among the neonic-treated hives than the control hives.

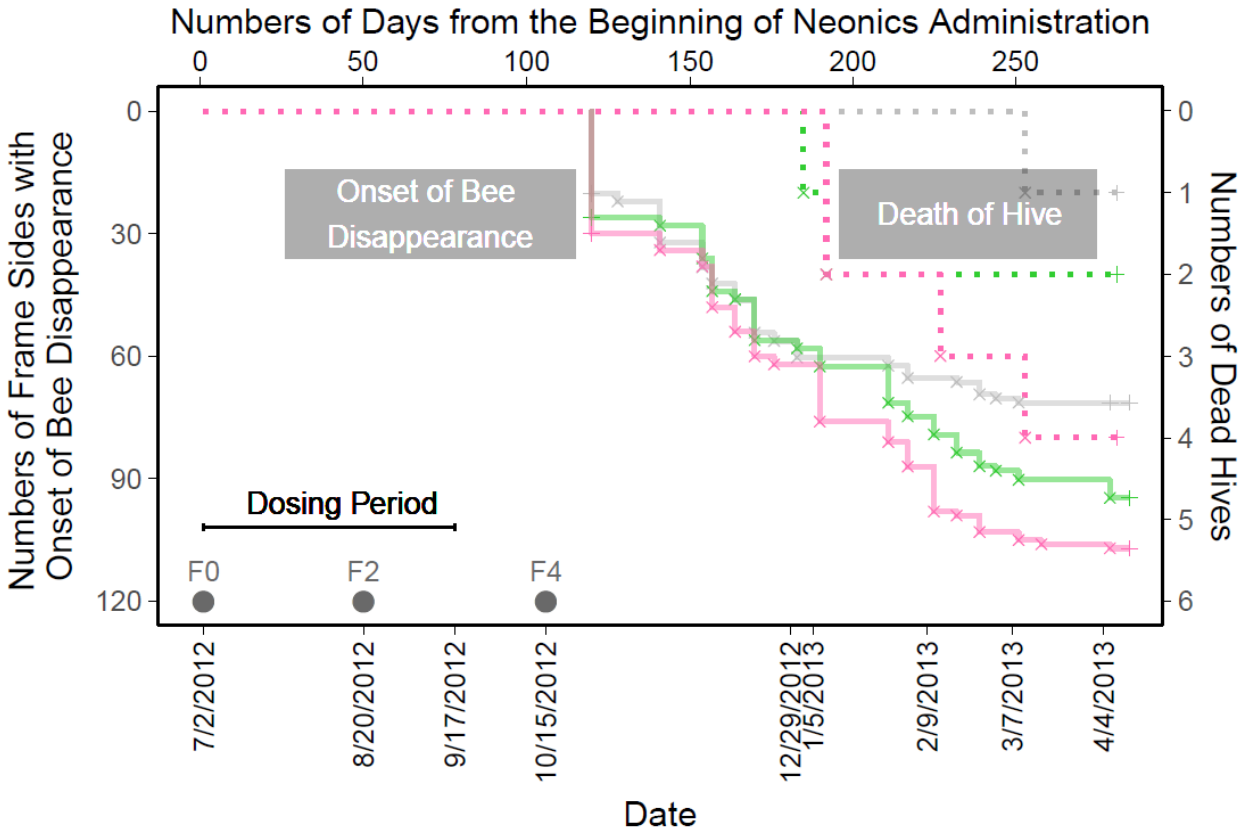

Figure 6. Chronological events of dosing period, RmtDNAcn measurements (F0, F2 and F4) observation of bee disappearance, and observation of dead hives over the winter from the beginning of neonics administration until the end of field study. Solid lines show the time of bee disappearance (measured as the first-time complete disappearance of bees from inside of bee hive) and dotted lines show the time of the occurrence of hive death. Events are shown as 'x' and censored data are shown as '+'. Gray, pink, and green represent the control, IMI, and CLO treatments, separately.

We summarized the hazard ratios of the onset risk of bee disappearance associated with neonicotinoid treatment and RmtDNAcn levels in **Table 7** and the mortality risk of a hive in **Table 8**. IMI- and CLO-treated hives posed a 2.2 and 1.6 times higher onset risk (nearly statistically significant, $p = 0.056$) of bee disappearance compared to the control hives. Adjusting for the treatment effects, we found a 1.2 times higher onset risk of bee disappearance in an any given side of a frame inside a hive with every 2-fold increase of RmtDNAcn ratio. In addition to the increase risks of the onset of bee disappearance in neonic-treated hives, we also found higher hazard ratio of mortality in both IMI- (HR = 5.3) and CLO- treated (HR = 2.6) hives, and slightly larger hazard ratios of mortality associated with increasing RmtDNAcn adjusting for the effect of treatments (HR = 1.1).

Table 7. Hazard ratios of the onset of bee disappearance (as measured of the numbers of frame sides containing adult bees) in hives over the winter across treatments and with respect to the change of every 2-fold increase in RmtDNAcn ratios[a].

Coefficient	Hazard Ratio (95% CI)	p-value
Treatment Effects:		
Ctrl	1.00	
IMI	2.15 (0.98, 4.73)	0.056[b]
CLO	1.55 (0.74, 3.27)	0.25[b]
RmtDNAcn Effects:		
RmtDNAcn Ratio	1.21 (0.80, 1.84)	0.37[b]

[a]RmtDNAcn ratio is defined as the relative mitochondrial DNA copy numbers with respect to the nuclear DNA copy number of the last sampled generation (F4) to that of the baseline generation (F0) for each hive ($2^{-\Delta\Delta Ct}$, where $\Delta\Delta Ct = \Delta Ct_{(F4,\ hive)} - \Delta Ct_{(F0,\ hive)}$).

[b]p-values were testing whether the effects were significantly ($\alpha = 0.05$) different from that of the Ctrl group; note that Ctrl: RmtDNAcn effects were testing whether significant risk exists with increasing RmtDNAcn ratio among the Ctrl group.

Table 8. Hazard ratios of dead hives over winter season across treatments and with respect to the change of every 2-fold increase in RmtDNAcn ratio[a].

Coefficient	Hazard Ratio (95% CI)	p-value
Treatment Effects:		
Ctrl	1.00	
IMI	5.29 (0.51, 55.04)	0.16[b]
CLO	2.60 (0.23, 29.10)	0.44[b]
RmtDNAcn Effects:		
RmtDNAcn Ratio	1.06 (0.45, 2.47)	0.90[b]

[a]RmtDNAcn ratio is defined as the relative mitochondrial DNA copy numbers with respect to the nuclear DNA copy number of the last sampled generation (F4) to that of the baseline generation (F0) for each hive ($2^{-\Delta\Delta Ct}$, where $\Delta\Delta Ct = \Delta Ct_{(F4,\ hive)} - \Delta Ct_{(F0,\ hive)}$).

[b]p-values were testing whether the effects were significantly ($\alpha = 0.05$) different from that of the Ctrl group; note that Ctrl: RmtDNAcn effects were testing whether significant risk exists with increasing RmtDNAcn ratio among the Ctrl group.

These findings are of crucial as studies have shown that higher level of mtDNAcn is associated with mtDNA damage, and we could support the current understanding of mechanism of sub-lethal neonic exposure by linking both upstream with neonics exposure[45-47] and downstream with hives' overall health (brood sizes, numbers of frames with bees, and hive survival). Mitochondrial DNA is known to be more vulnerable to environmental toxicants than nuclear DNA

(nDNA) with its close proximity of nucleoids to the electron transit chain (ETC) and limited repair pathway.[54] Dysfunction of ETC could lead to increasing reactive oxidative species (ROS) generation, reduction in ATP production, and changes in membrane potential.[47] Mitochondria are eukaryotic organelles for energy production through oxidative phosphorylation. In cells with higher energy demands, there is larger number of mitochondria per cell. In addition to energy needs, the state of mtDNA could also vary given different oxidative stress conditions.[12] Under normal condition, ROS generated during oxidative phosphorylation (1 - 2% of the oxygen consumption) can damage mtDNA while could be gradually repaired. With multiple copies of mitochondrial genome, the corresponding biochemical defects and tissue dysfunction are not detected until certain threshold (typically a ratio of 60% - 90% mutant to wild-type mtDNA variated by tissues and species).[47, 55, 56] In contrary, ROS generated under ROS-stressed conditions could damage mtDNA persistently, leading to dysfunction of oxidative phosphorylation.[57] This chronic oxidative stress resulted from damaged mitochondria could increase mtDNA replication and repair.[12] Therefore, increasing mtDNAcn could be the compensatory mechanism to maintain mitochondrial transcripts by increasing the number of wild-type mtDNA.[12, 58-60]

Limited repair pathways of mtDNA compared to nDNA, such as the absence of nucleotide excision repair (NER) responsible for repairing processes of several environmental genotoxicants (e.g. PAHs, mycotoxins), could indirectly result in irreparability of certain types of mtDNA damage.[47, 54, 57, 61, 62] As shown in the present study, the increasing mtDNAcn in the adult bees from later brood generations in the same hive (or queen), may have caused by the limited repair capability of mtDNA, and under the circumstance when exposure to neonics is continuous and yet at the sub-lethal levels the neonic-induced mtDNA damage is likely to be irreparable and even inheritable. One plausible explanation linking to CCD is that winter bees inherit a higher baseline

level of RmtDNAcn as they were more later brood generation by their queens, and higher baseline level of RmtDNAcn leads the insufficient energy production a hive needs to survive through winter. The observation of lower survival probabilites among neonic-treated hives over the winter could be a supportive evidence. Therefore, studies evaluating hive thermoregulation due to mitochondrial dysfunction following sub-lethal neonics exposure is in need to further evaluate this mechanism.

One major limitation of this chapter is the numbers of bees that we collected from those 18 hives were too small to achieve meaningful statistical power, even though we found positive relationship between RmtDNAcn in adult foraging honeybees and the cumulative sub-lethal exposure of neonics of their queens As the outcomes of model simulation shown in **Figure 7**, we would need to substantially increase the number of hives to 90 hives in order to achieve 80% of the statistical power for detecting the same levels of significant increase in RmtDNAcn due to IMI exposure, and even larger hive numbers for CLO-induced effects. This no doubt would add significant burden to the research personnel and the project resources due to the nature of year-long field study involving intensive and frequent data and specimen collected throughout the year. In addition, the considerably increasing variability of RmtDNAcn among bees collected from later brood generations could result from both the variations among individual adult bees, as well as different inherited levels of mtDNAcn from their queens. As the baseline levels of RmtDNAcn levels were quite similar across all experimental hives, we could exclude the possibility that the variability was originated from the baseline age of different.

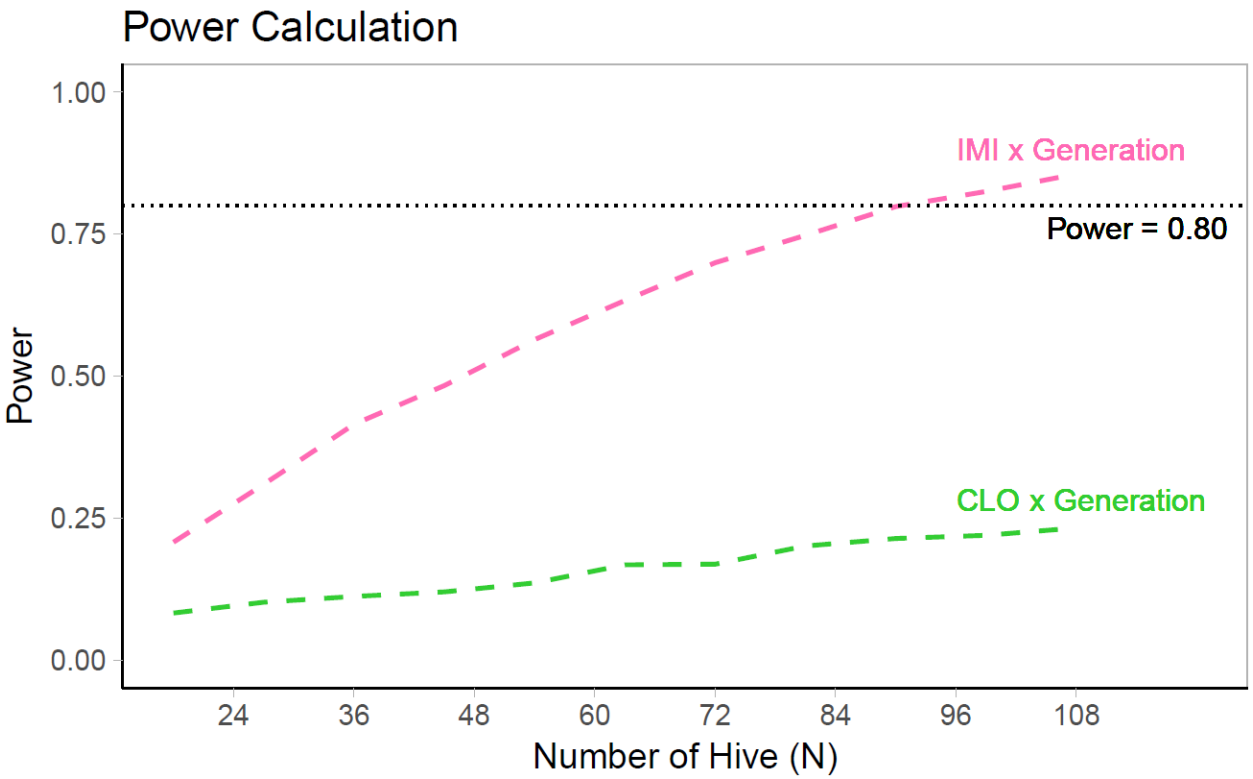

Figure 7. Power simulation for number of hives (N) needed in the field study to observe significant coefficients of individual treatment x generation interactions at the modeled level. Variances (between hive variation = 0.06, and model residual variance = 0.34) from our predicted model were used for the simulation.

Supplemental Materials

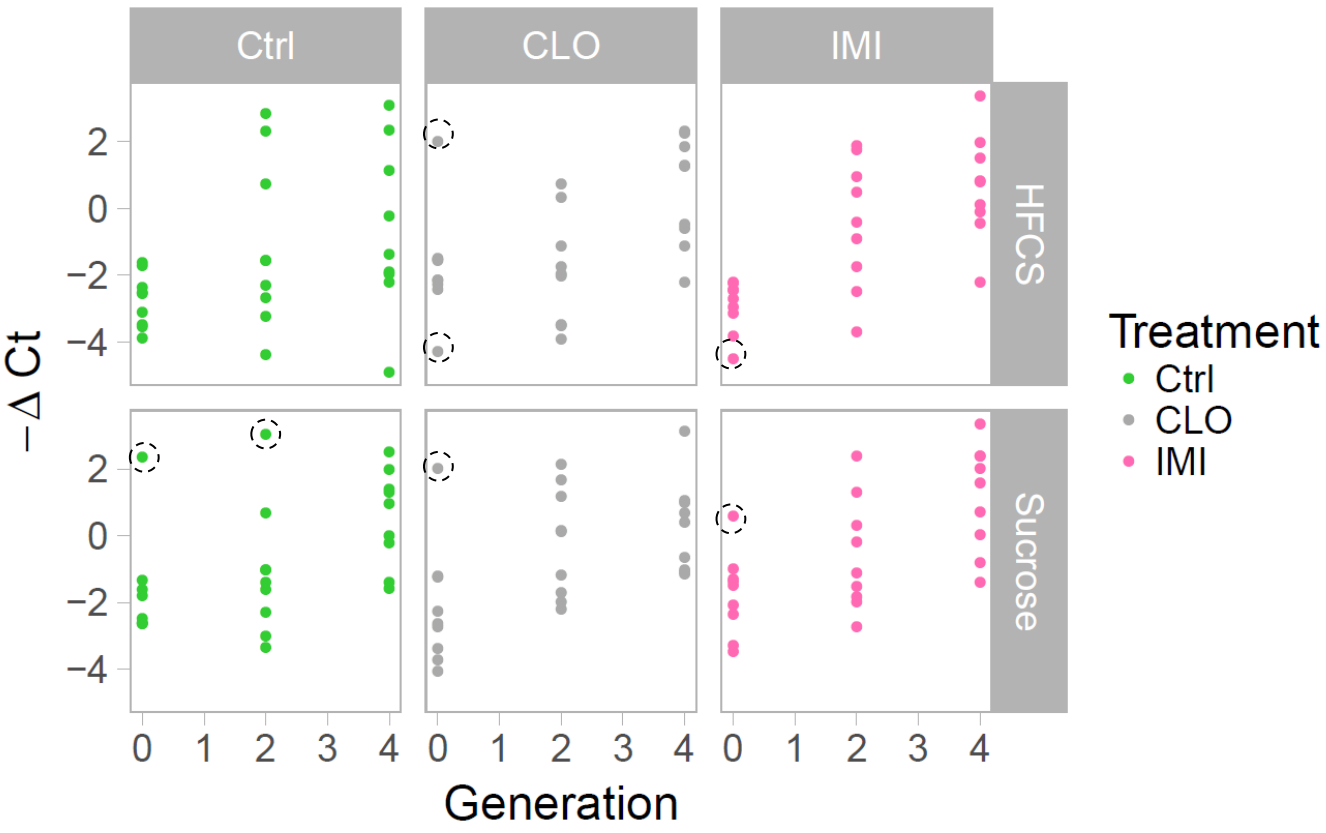

Figure S1. Log2(RmtDNAcn) levels for all samples by sugar and pesticide treatments. Outliers were circled and excluded from all analyses.

Table S1. Ct values for 18srRNA and Cytb for all hives and replicates.

HiveID	18srRNA (3 replicates)			Cytb (3 replicates)			Treatment	Hive Location	Generation	Average 18srRNA	Average Cytb
	1	2	3	1	2	3					
D3S1		18.09	19.89		19.42	21.69	Sucrose-Control	0	0	18.99	20.56
D3S3	18.37	16.37	20.39	19.41	15.69	21.40	Sucrose-Control	0	2	18.38	18.83
D3S5	16.97	16.86	20.71	16.98	18.44	19.42	Sucrose-Control	0	4	18.18	18.28
L3S1	18.82	18.80	18.78	21.31	21.45	16.41	Sucrose-Control	1	0	18.80	19.72
L3S3	21.62	20.57	19.52	18.58	23.60	20.93	Sucrose-Control	1	2	20.57	21.03
L3S5	20.72	18.69	19.41	20.95	20.08	18.46	Sucrose-Control	1	4	19.60	19.83
R3S1	20.46	19.49	19.29	22.07	22.13	21.89	Sucrose-Control	2	0	19.75	22.03
R3S3	20.73	18.95	19.77	23.03	22.30	21.40	Sucrose-Control	2	2	19.82	22.24
R3S5	21.74	20.09	20.56	19.23	18.12	19.16	Sucrose-Control	2	4	20.80	18.84
D1S1	19.78	18.46	20.30	21.85	19.96	21.66	Sucrose-IMI	0	0	19.51	21.16
D1S3	20.66	17.61	19.58	18.27	19.60	21.09	Sucrose-IMI	0	2	19.28	19.65
D1S5	20.04	18.65	20.73	20.84	16.27	20.03	Sucrose-IMI	0	4	19.81	19.05
L1S1	20.63	19.00	18.86	20.05	22.47	20.17	Sucrose-IMI	1	0	19.50	20.90
L1S3	19.90	19.14	20.09	21.02	18.85	22.82	Sucrose-IMI	1	2	19.71	20.90
L1S5	20.44	19.93	19.97	21.85	19.91	17.95	Sucrose-IMI	1	4	20.12	19.91
R1S1	21.92	19.79	20.10	22.91	23.09	22.45	Sucrose-IMI	2	0	20.60	22.82
R1S3	20.87	20.43	21.24	22.72	20.63	19.93	Sucrose-IMI	2	2	20.85	21.09
R1S5	22.23	21.65	21.90	18.87	20.08	19.52	Sucrose-IMI	2	4	21.93	19.49
D2S1	19.94	17.11	19.81	21.19	19.39	22.46	Sucrose-CLO	0	0	18.95	21.01
D2S3	18.73	17.82	23.20	20.72	19.01	21.52	Sucrose-CLO	0	2	19.92	20.41
D2S5	20.41	16.68	20.61	19.74	17.78	20.19	Sucrose-CLO	0	4	19.23	19.24
L2S1	19.30	18.31	18.34	23.04	22.40	16.32	Sucrose-CLO	1	0	18.65	20.59
L2S3	19.92	20.92	20.93	22.12	20.80	20.77	Sucrose-CLO	1	2	20.59	21.23
L2S5	19.77	20.92	18.82	20.91	21.59	17.78	Sucrose-CLO	1	4	19.84	20.09
R2S1	20.98	20.08	20.85	22.20	23.46	23.59	Sucrose-CLO	2	0	20.63	23.08
R2S3	21.88	19.23	21.17	19.74	20.93	19.99	Sucrose-CLO	2	2	20.76	20.22

(Continued)											
R2S5	21.89	21.25	19.84	18.76	20.27	20.87	Sucrose-CLO	2	4	20.99	19.97
D3H1	16.88	17.65	20.97	18.60	20.02	24.07	HFCS-Control	0	0	18.50	20.90
D3H3	16.27	18.63	20.99	17.84	15.78	23.29	HFCS-Control	0	2	18.63	18.97
D3H5	17.53	17.85	21.08	15.16	20.08	17.99	HFCS-Control	0	4	18.82	17.75
L3H1	18.71	17.99	19.34	22.24	21.89	21.90	HFCS-Control	1	0	18.68	22.01
L3H3	20.15	18.79	19.77	17.83	23.16	22.45	HFCS-Control	1	2	19.57	21.15
L3H5	18.96	21.10	19.37	20.88	19.96	19.61	HFCS-Control	1	4	19.81	20.15
R3H1	20.78	20.02	19.48	22.41	23.50	21.99	HFCS-Control	2	0	20.09	22.63
R3H3	20.79	20.17	20.13	22.35	23.42	19.41	HFCS-Control	2	2	20.36	21.72
R3H5	20.54	19.40	18.77	22.50	20.76	23.67	HFCS-Control	2	4	19.57	22.31
D1H1	17.38	17.81	19.70	19.83	20.76	21.95	HFCS-IMI	0	0	18.30	20.85
D1H3	16.94	18.50	20.16	18.69	18.01	21.08	HFCS-IMI	0	2	18.53	19.26
D1H5	16.35	18.62	21.11	15.52	17.12	19.14	HFCS-IMI	0	4	18.69	17.26
L1H1	18.97	19.23	19.94	21.39	23.05	22.14	HFCS-IMI	1	0	19.38	22.19
L1H3	20.28	20.62	21.41	22.76	24.31	19.63	HFCS-IMI	1	2	20.77	22.23
L1H5	20.61	21.70	20.51	19.81	22.14	20.60	HFCS-IMI	1	4	20.94	20.85
R1H1	19.44	19.52	18.45	22.58	22.23	22.96	HFCS-IMI	2	0	19.14	22.59
R1H3	21.08	19.06	21.38	19.20	19.46	20.44	HFCS-IMI	2	2	20.51	19.70
R1H5	21.37	19.61	20.20	18.01	21.81	20.08	HFCS-IMI	2	4	20.40	19.97
D2H1	17.46	17.25	19.37	18.95	18.80	21.52	HFCS-CLO	0	0	18.03	19.76
D2H3	16.97	17.92	19.90	18.94	19.93	21.65	HFCS-CLO	0	2	18.26	20.17
D2H5	17.84	17.98	21.91	15.57	18.44	20.61	HFCS-CLO	0	4	19.24	18.21
L2H1	20.28	19.58	19.39	21.81	17.57	21.55	HFCS-CLO	1	0	19.75	20.31
L2H3	20.69	19.30	19.78	19.93	22.82	19.43	HFCS-CLO	1	2	19.92	20.73
L2H5	20.31	19.26	21.14	17.98	19.85	19.28	HFCS-CLO	1	4	20.24	19.04
R2H1	20.19	18.75	18.96	22.47	21.17	23.27	HFCS-CLO	2	0	19.30	22.30
R2H3	21.17	19.02	19.86	22.29	22.93	23.35	HFCS-CLO	2	2	20.02	22.86
R2H5	19.97	20.91	20.22	22.19	22.05	18.97	HFCS-CLO	2	4	20.37	21.07

Shaded cells were excluded as outliers during quality control step.

Table S2. Statistical tests and analysis for final model selection.

Test	Description of the testing models[b]	LRT[a] results
Analysis of generation effects among control group (normal aging effect of queens):		
Test 1: 'Categorical generation effect' > 'Linear generation effect' (null)	**H_0:** $y \sim a_0 + a_{hive} + b * J_{hive} + \sum c_k * I[Treatment_{k, hive}] + \sum d_k * J_{hive} * I[Treatment_{k,hive}]$ **H_1:** $y \sim a_0 + a_{hive} + \sum b_j * I[Fj_{hive}] + \sum c_k * I[Treatment_{k, hive}] + \sum d_{jk} I[Fj_{hive}] * I[Treatment_{k,hive}]$	$p = 0.93$; fail to reject the null; linear generation model is sufficient
Test 2: 'Quadratic generation effect' > 'Linear generation effect' (null)	**H_0:** $y \sim a_0 + a_{hive} + b * J_{hive} + \sum c_k * I[Treatment_{k, hive}] + \sum d_k * J_{hive} * I[Treatment_{k,hive}]$ **H_1:** $y \sim a_0 + a_{hive} + b * J_{hive} + b' * J^2_{hive} + \sum c_k * I[Treatment_{k, hive}] + \sum d_k * J_{hive} * I[Treatment_{k,hive}]$	$p = 0.92$; fail to reject the null; linear generation model is sufficient
Analysis of sugar (sucrose/HFCS) effects:		
Test 3: 'Separate *sucrose/HFCS* effect' > 'Combined sucrose/HFCS effect' (null)	**H_0:** $y \sim a_0 + a_{hive} + b * J_{hive} + \sum c_k * I[Treatment_{k, hive}] + \sum d_k * J_{hive} * I[Treatment_{k,hive}]$ **H_1:** $y \sim a_0 + a_{hive} + b * J_{hive} + \sum c_k * I[Treatment\text{-}sugar_{k, hive}] + \sum d_k * J_{hive} * I[Treatment\text{-}sugar_{k,hive}]$	$p = 0.87$; fail to reject the null; combined sugar effect model is sufficient

[a]LRT = Likelihood Ratio Test. Nested model comparisons were conducted using maximized log-likelihoods (ML) fitted mixed models. Summary of model statistics are presented in Table S2 and S3.

[b]Generation effects (F0, F2, F4) are presented as J, where J = 2 or 4. $I[Fj_{hive}]$ represent indicator variables for categorical generations (e.g. $I[F2_{hive}] = 1$ means that the sample was collected from the second generation after treatments started and from the specific 'hive'.)

Table S3. Summary of statistical models of different generation trend assumptions.

Categorical generation effect model	Value	Std.Error	DF	t-value	p-value
(Intercept)	-1.6968658	0.2661051	30	-6.38	4.89E-07
factor(Generation)1	0.7299132	0.3511761	30	2.08	4.63E-02
factor(Generation)2	1.6539405	0.3511761	30	4.71	5.28E-05
factor(treatment)2.IMI	0.01785783	0.3763295	15	0.05	9.63E-01
factor(treatment)3.CLO	0.04100932	0.3763295	15	0.11	9.15E-01
factor(Generation)1:factor(treatment)2.IMI	0.58093903	0.4966381	30	1.17	2.51E-01
factor(Generation)2:factor(treatment)2.IMI	0.64525665	0.4966381	30	1.30	2.04E-01
factor(Generation)1:factor(treatment)3.CLO	0.21503813	0.4966381	30	0.43	6.68E-01
factor(Generation)2:factor(treatment)3.CLO	0.26772914	0.4966381	30	0.54	5.94E-01
Linear generation effect model[a]	Value	Std.Error	DF	t-value	p-value
(Intercept)	-1.7292182	0.2410237	33	-7.17	3.19E-08
Generation	0.8269703	0.1684894	33	4.91	2.42E-05
factor(treatment)2.IMI	0.1039614	0.3408589	15	0.30	7.65E-01
factor(treatment)3.CLO	0.0680672	0.3408589	15	0.20	8.44E-01
Generation:factor(treatment)2.IMI	0.3226283	0.2382800	33	1.35	1.85E-01
Generation:factor(treatment)3.CLO	0.1338646	0.2382800	33	0.56	5.78E-01
Quadratic generation effect model	Value	Std.Error	DF	t-value	p-value
(Intercept)	-1.7345863	0.2494462	32	-6.95	7.09E-08
Generation	0.85917898	0.3825424	32	2.25	3.17E-02
Generation_sq	-0.0161044	0.1710781	32	-0.09	9.26E-01
factor(treatment)2.IMI	0.1039614	0.3434282	15	0.30	7.66E-01
factor(treatment)3.CLO	0.06806717	0.3434282	15	0.20	8.46E-01
Generation:factor(treatment)2.IMI	0.32262833	0.241941	32	1.33	1.92E-01
Generation:factor(treatment)3.CLO	0.13386457	0.241941	32	0.55	5.84E-01

[a]Final selected model.

Table S4. Summary of statistical models of different sucrose/HFCS assumptions.

Combined sucrose/HFCS effect[a]	Value	Std.Error	DF	t-value	p-value
(Intercept)	-1.72921819	0.2410237	33	-7.17	3.19E-08
Generation	0.41348513	0.0842447	33	4.91	2.42E-05
factor(treatment)2.IMI	0.1039614	0.3408589	15	0.30	7.65E-01
factor(treatment)3.CLO	0.06806717	0.3408589	15	0.20	8.44E-01
Generation:factor(treatment)2.IMI	0.16131416	0.11914	33	1.35	1.85E-01
Generation:factor(treatment)3.CLO	0.06693228	0.11914	33	0.56	5.78E-01
Separate sucrose/HFCS effect	Value	Std.Error	DF	t-value	p-value
(Intercept)	-1.691426461	0.3590051	30	-4.71	5.26E-05
Generation	0.465253028	0.1234967	30	3.77	7.21E-04
factor(Pesticide)2	0.217809046	0.5077099	12	0.43	6.76E-01
factor(Pesticide)3	-0.003663355	0.5077099	12	-0.01	9.94E-01
factor(Pesticide)4	-0.075583459	0.5077099	12	-0.15	8.84E-01
factor(Pesticide)5	-0.085469702	0.5077099	12	-0.17	8.69E-01
factor(Pesticide)6	0.06421424	0.5077099	12	0.13	9.01E-01
Generation:factor(Pesticide)2	0.092893004	0.1746507	30	0.53	5.99E-01
Generation:factor(Pesticide)3	0.064943859	0.1746507	30	0.37	7.13E-01
Generation:factor(Pesticide)4	-0.103535803	0.1746507	30	-0.59	5.58E-01
Generation:factor(Pesticide)5	0.126199519	0.1746507	30	0.72	4.76E-01
Generation:factor(Pesticide)6	-0.034615093	0.1746507	30	-0.20	8.44E-01

[a]Final selected model. Note that this is the same selected model in Table S2.

CHAPTER 3

Trans-generational Effects of Sub-lethal Neonicotinoids Exposure in Honeybees (Apis mellifera): A Metabolome-wide Association Study (MWAS)

Chi-Hsuan Chang[1],

Bernardo Lemos[1],

David MacIntosh[1],

Chensheng Lu[1, †]

[1]Department of Environmental Health, Harvard T.H. Chan School of Public Health, Boston, Massachusetts

Abstract

The causation of honeybee colony collapse disorder (CCD) is a long-time mystery ad has been linked to multiple factors, including insecticide exposure, particularly neonicotinoids. Previous hypothesis and findings of neonicotinoids' influence on honeybees were to do with diminishing ATP generation in mitochondria for highly demanding foraging or thermoregulation activities. Previously, we found that increasing relative mitochondrial DNA copy number (RmtDNAcn) in bees that brood later by the aging queens and that cumulative imidacloprid and clothianidin exposure led to additional increase in RmtDNAcn over time. In this chapter, we conducted metabolomics analyses with a selection of pathways associated with energy metabolism to further understand the metabolic mechanism of sublethal cumulative neonicotinoids exposure. We found that both biological aging- (due to queens' aging) and neonicotinoids- induced change in abundance of several metabolites indirectly or directly related to energy metabolism. Biological aging was significantly associated with change in reducing abundance in several precursors of glutathione metabolism that could be associated with oxidative stress. Neonicotinoids exposure were associated with reducing abundance of intermediates in TCA cycle or increasing NAD+ abundance and increasing RmtDNAcn ratio contributed to further disturbance in metabolite abundance in control and treated bees. Although none of the change in metabolite abundance due to neonicotinoids treatments remained significant after we adjust for multiplicity, we believe this exploratory result served as a start to encourage more research on neonicotinoids' impact on the relative abundance of metabolites in the glutathione and energy metabolism (TCA cycle and OXPHOS).

Introduction

Neonicotinoids are the most widely used insecticides globally with the registration in more than 100 countries for more than 120 different crops.[1, 7, 8] Although their primary use in agriculture is in the seed treatments for crops such as corn, oilseed rape, and sunflower, neonicotinoids are also commonly used in nursery and veterinary medicine. Because all neonicotinoids are highly water soluble, they are systemic insecticides and persistent in the environment where neonicotinoids are found in soil and groundwater with the biological half-lives ranging from 100 to 1000 days.[63] In recent years, neonicotinoids have been receiving great attention worldwide because of the implication in the causation to the massive and sudden decline in global honeybee (*Apis mellifera*) population over the winter, a phenomenon referred as colony collapse disorder (CCD).[48, 64] In combination of their property as systemic insecticides, lengthy biological half-lives in the environment, and increasing global usage, the concern of neonicotinoids exposures and their toxic effects not only to pollinators, such as honeybees, but also human is warranted.

Neonicotinoids were found to be associated with adverse effects in honeybees at the sub-lethal levels, including impairing reproductive and behavioral abilities[39], decrease in brood size[41, 42, 65], affecting foraging activities and syrup consumption, [8, 41, 42, 65, 66] and the occurrence of CCD.[48] In terms of neonicotinoids association with CCD, one main hypothesis is the link to the lack of sufficient ATP generation for bees' high energy-demanding activities.[9-11] To maintain the thermal homeostasis in a colony during winter, bees cluster tightly and shiver inside their hive and this shivering mechanism is in fact very energy demanding. [11] Since CCD usually occurs during winter season, the sudden and massive disappearance of adult bees from their hives resulted from insufficient ATP production due to mitochondrial dysfunction is biologically probable.[44]

In Chapter 2, we found chronic sub-lethal neonicotinoids exposure could result in additional increase in mitochondrial DNA copy number (mtDNAcn) in worker bees, a biological measurement that often leads to impairments in energy metabolism. In order to understand the metabolic mechanism of this process, we conducted metabolomics analyses with a selection of pathways associated with energy metabolism. We hypothesized that metabolite abundance could be modified across different honeybee brood generations from the same queens due to biological aging (earlier aging compared to the observed age due to later-brood by aging queens), chronic sub-lethal neonicotinoids exposure, along with the increase in mtDNAcn associated with both aging and treatment effects. We evaluated the hypothesis by detecting change in metabolite abundance closely related to the energy metabolism using KEGG PATHWAY Database and aimed to identify key metabolites with meaningful change that are related to both biological aging- and neonicotinoids treatment.

Materials and Methods

Specimen Collection and Mitochondrial DNA copy number (mtDNAcn) Measurement. Detailed specimen collection scheme has been published earlier.[48] In brief, we set up 6 honeybee hives at each of the 3 independent apiaries, or a total of 18 hives. At each apiary, hives were fed with 0.5 gallon of either sucrose (table sugar; N = 3) or high-fructose corn syrup (HFCS; N = 3). In each of the two sugar feeding groups, hives were given a weekly dose of either 258 µg of imidacloprid (IMI), 258 µg of clothianidin (CLO), or no pesticide (control) for 13 consecutive weeks (from July 2nd to September 17th, 2012). Assuming each healthy hive contained 50,000 bees during the dosing weeks when bees are active in brood rearing and foraging, the weekly dose of 258 µg in 0.5 gallon of sugar water per hive is equivalent to 0.74 ng/bee/day. Adult worker bees per hive were collected by intercepting at the entrance of their hives returned from foraging. We collected samples from three brood generations of each hive (from the same queens) on July 2nd (F0, the baseline/pre-treatment generation), August 20th (F2, the during-treatment generation), and October 15th (F4, the post-treatment generation) in 2012. After interception, bees were transferred to a 50-mL centrifuge tube immediately after capture, placed in a cooler with dry ice during transportation, and then stored in a -80°C freezer in the lab until mtDNAcn and metabolomics analyses.

We quantified mtDNAcn in the middle section, or thoracic muscle, of an adult foraging honeybee using the DNeasy Blood & Tissue Kit (Qiagen) in triplicates per hive per brood generation, as previously described in Chapter 2. We selected Cyt *b* (11004bp-12155bp) and *18s rRNA* to represent mtDNA and the nuclear DNA, respectively. The primers used for Cyt b and*18s rRNA* genes for q-PCR were: *Cyt b* F-5'AGC AGC TGC ATT TAT AGG ATA TG 3'; *Cyt b* R-5' AGA TTA GTA ATA ACT GTT GCA CCT C 3'; *18s rRNA* F- 5'GTG GGC CGA TAC GTT TAC TT 3'; *18s rRNA* R-5' CCG AGG TCC TAT TCC ATT ATT CC 3'. We normalized

mtDNAcn by the copy number of a selected nuclear DNA (nDNAcn) as the internal reference gene to calculate ΔCt for each sample, known as log2-transformed relative mtDNAcn (RmtDNAcn), using the following equation:

$$\Delta Ct = Ct_{(Cyt.\ b)} - Ct_{(18s\ rRNA)}$$

(Equation 12)

where Ct is the threshold cycle number at the determined level of log-based fluorescence and therefore inverse proportional to the log-based initial copy number of the target gene. At the final step, we took the average of ΔCt (the hive-level ΔCt, n = 3 brood generations x 18 hives = 54) for the samples collected from the same hive at the same time to link with the hive-level metabolite abundance, which will be described below.

Metabolic Profiling. A total of 325 metabolites were analyzed in each of the 54 samples at Metabolon Inc.(Morrisville NC) in which Metabolon has been participating in numerous metabolomic analyses.[67, 68] In brief, samples were prepared using the automated MicroLab STAR® system (Hamilton Company, Salt Lake City, UT, USA). After the preparation process, sample extracts were frozen and dried under vacuum before analyzed either by GC/MS (Thermo-Finnigan Trace DSQ fast-scanning single quadrupole mass spectrometer using electron impact ionization) or by LC/MS/MS (Waters ACQUITY UPLC and a Thermo-Finnigan LTQ mass spectrometer using electrospray ionization (ESI) source and linear ion-trap (LIT) mass analyzer) platform. Metabolites were identified either by comparing biochemicals to the purified standards in the metabolic library or by their recurrent chromatographic and mass spectral nature.

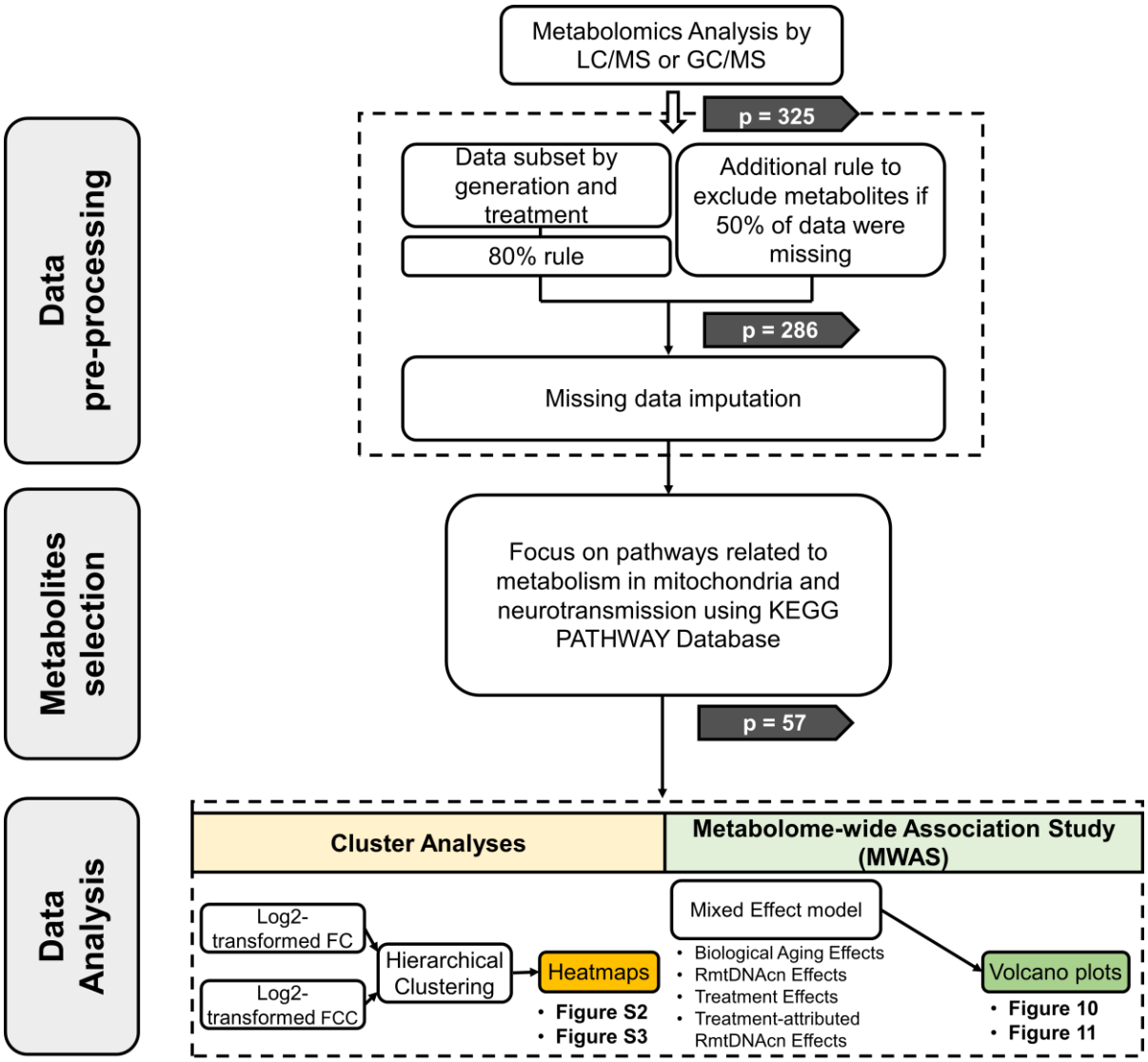

Figure 8. Data Processing and Analyses Flowchart.

Data processing.

1. ***Missing data exclusion.*** To ensure the robustness of statistical analyses on metabolomics data and to avoid the potential over-imputation of missing data, it is a common practice to remove metabolites containing high proportion of missing data.[69] We excluded metabolites with more than 20% of features missing within each generation and treatment group (the 80% rule applied to the subset datasets[70]). In addition, we excluded metabolites with more than 50% of missing values (the 50% rule applied to the whole dataset). After this QC step, 286 metabolites were left in the combined dataset (with 6% missing values remained) for the metabolomics analyses. The 39 excluded metabolites were summarized in **Table S5**.
2. ***Missing data imputation.*** Raw metabolite abundance data were normalized to Bradford protein concentration and then rescaled to set the median as one per metabolite. Samples with missing values for the 286 metabolites were imputed with the minimum value of the scaled abundance of such metabolite.

Metabolic pathway selection. We used 'pathview' in R package to map our metabolites with their involved pathways of honeybee's metabolism using Kyoto Encyclopedia of Genes and Genomes (KEGG) PATHWAY Database. Since we hypothesized chronic sub-lethal neonicotinoids exposure would lead to change in RmtDNAcn, mitochondrial malfunction, and subsequently change in metabolite abundance, we selected the following pathways (KEGG Pathway ID), which are also shown in **Figure 9**:

1. **Citrate cycle (TCA cycle, ame00020) and oxidative phosphorylation (OXPHOS, ame00190)** pathways are energy metabolic pathways that directly take place in mitochondria.
2. **Glutathione metabolism (ame00480)** pathways are part of the Phase II detoxification, which is important for detoxifying xenobiotics, such as neonicotinoids.[67] Two relative abundance

metabolites, glutathione (GSH) and oxidized-glutathione (GSSG), are related to reactive oxygen species (ROS) generation.[67, 71]

3. **Glycolysis/Glycogenesis (ame00010), Nicotinate/Nicotinamide (ame00760), Pentose Phosphate (ame00030), Purine metabolism (ame00230), and Pyruvate metabolism (ame00620)** pathways are included due to their indirect but close link to metabolites involved in the energy metabolism (citrate cycle and oxidative phosphorylation).
4. **Neuroactive ligand-receptor interaction metabolism (ame04080)** pathway is included because of the mode of action of neonicotinoids that is nicotinic acetylcholine receptor (nAChR) agonism.

Among those 286 metabolites, we were able to map 57 metabolites that specifically match with the study interest, as described in 2.1 – 2.4. Detail information for these metabolites is summarized in **Table S6**.

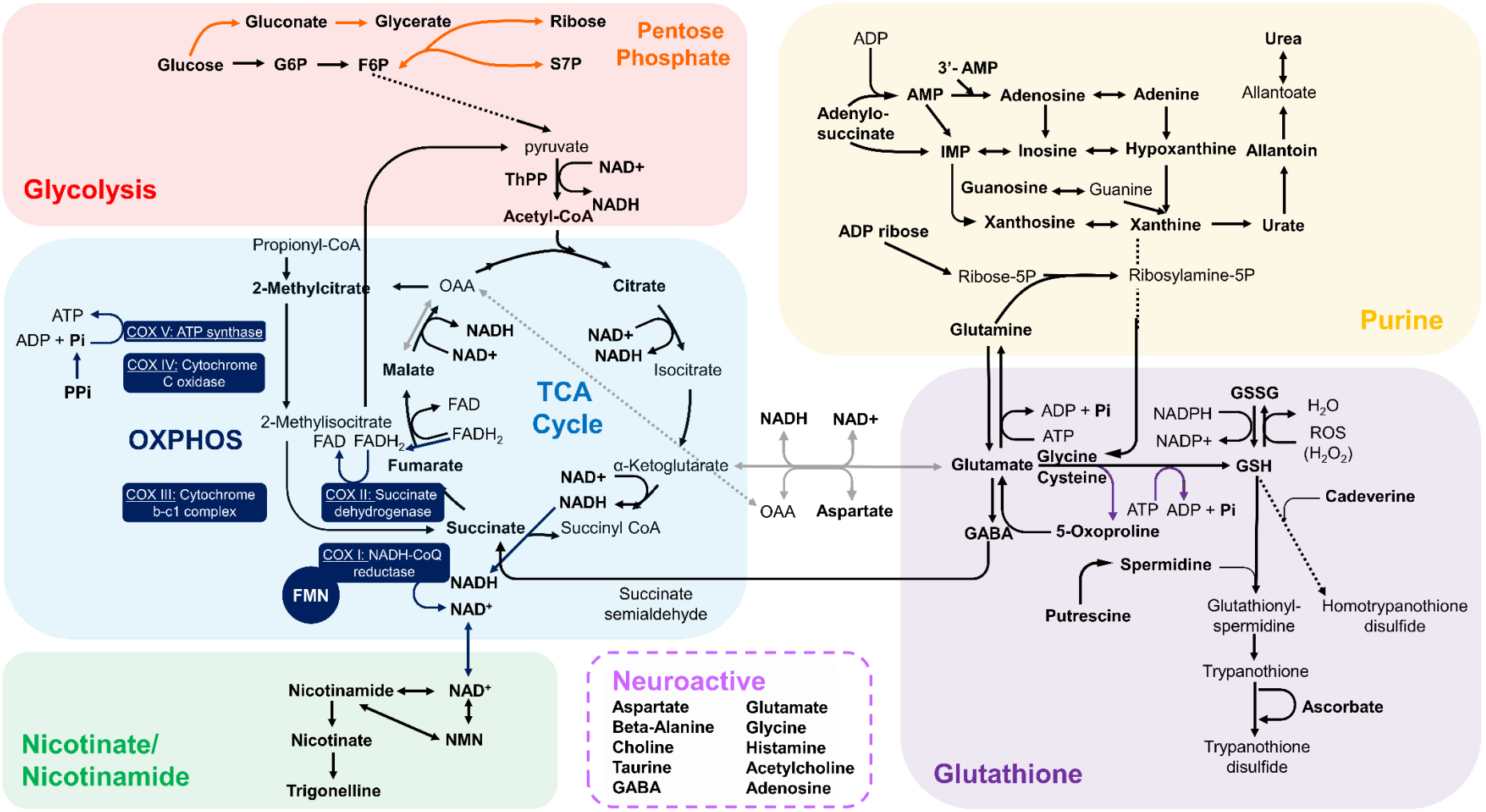

Figure 9. Schematic overview of the selected metabolites and pathways. Metabolites involved in multiple metabolic pathways were colored in gray.

Statistical modeling for metabolome-wide association (MWA). We used the following mixed effect model (Equation 13) with random hive intercept and fixed effects (treatments, brood generations, log2 RmtDNAcn ratio, and their two-/three-way interactions) to study the association between sub-lethal neonicotinoids treatments and change in the abundance of those 57 metabolites through increasing relative mitochondrial DNA copy number (RmtDNAcn). P-values (two-sided) for these covariates were reported ($\alpha = 0.05$) for determination of significant changing metabolite abundance ratio due to the covariates. We also used false discovery rate (FDR, q-values) to adjust the results from multiple testing, in which q-values < 0.05 were presented. The model could be grouped into four parts;

$$\begin{aligned}
&\mathrm{Log2}(FC_{FJ\ vs.\ F0}) \sim a_{hive} \\
&+ Ctrl_{F2\ vs.\ F0} + Ctrl_{F4\ vs.\ F2} \\
&+ Ctrl_{F2\ vs.\ F0} * [-\Delta\Delta C_{T,\ F2\ vs.\ F0}] \\
&+ Ctrl_{F4\ vs.\ F2} * [-\Delta\Delta C_{T,\ F4\ vs.\ F2}] \\
&+ \Delta IMI_{F2\ vs.\ F0} + \Delta CLO_{F2\ vs.\ F0} \\
&+ \Delta IMI_{F4\ vs.\ F2} + \Delta CLO_{F4\ vs.\ F2} \\
&+ \Delta IMI_{F2\ vs.\ F0} * [-\Delta\Delta C_{T,\ F2\ vs.\ F0}] \\
&+ \Delta CLO_{F2\ vs.\ F0} * [-\Delta\Delta C_{T,\ F2\ vs.\ F0}] \\
&+ \Delta IMI_{F4\ vs\ F2} * [-\Delta\Delta C_{T,\ F4\ vs.\ F2}] \\
&+ \Delta CLO_{F4\ vs.\ F2} * [-\Delta\Delta C_{T,\ F4\ vs.\ F2}]
\end{aligned}$$

(A) Biological aging effect on metabolite abundance ratio

(B) Metabolite abundance ratio changes with increasing RmtDNAcn ratio

(C) Treatment effect on metabolite abundance ratio

(D) Metabolite abundance ratio changes with neonicotinoids-attributed increasing RmtDNAcn ratio

(Equation 13)

where:

- FC is the abundance ratio of later-brood (F2 and F4) generations versus the baseline (F0) generation;
- a_{hive} represents random hive effect on log2 abundance ratio at F2;

- $Ctrl_{F2\ vs.\ F0}$, $\Delta IMI_{F2\ vs.\ F0}$ and $\Delta CLO_{F2\ vs.\ F0}$ represent the abundance ratio in relate to biological aging and neonic-attributed change in log2 abundance ratio at F2 compare to F0; biological aging was defined as the effects seen in later-brood adult bees brood by the aging queens, which had the same age of days on average while were in fact aging in a faster speed biologically.
- $\Delta IMI_{F4\ vs.\ F2}$ and $\Delta CLO_{F4\ vs.\ F2}$ show the change in abundance ratio due to cumulative neonic-treatments from F2 to F4, comparing to non-neonic treatment ($Ctrl_{F4\ vs.\ F2}$);
- $-\Delta\Delta C_T$ is the log2 RmtDNAcn ratio between two generations, which is the $-(\Delta Ct_{Fj} - \Delta Ct_{F0})$. $Ctrl_{Fj\ vs.\ Fk}$*$[-\Delta\Delta C_{T,\ Fj\ vs.\ Fk}]$ shows the change in log2 abundance ratio in relate to every 2-fold increase in RmtDNAcn ratio between j and k generations adjusting for the effect of treatments. As a result, we defined this effect as the biological association between change in RmtDNAcn and change in metabolite abundance;
- $\Delta neonic_{Fj\ vs.\ Fk}$*$[-\Delta\Delta C_{T,\ Fj\ vs.\ Fk}]$ represents the neonic-attributed change in the above described association between j and k generations.

Results and Discussion

Table 9 shows the total number of metabolites with significant changes in abundance ratios associated with the biological aging effect, the effect of increasing RmtDNAcn ratio, treatment effect, or the effect from neonic-attributed change in RmtDNAcn ratio. In general, we found several metabolites their abundances are significantly perturbed for biological aging, and most of them associated with reduction of abundance especially among the F4 generation. Fewer metabolites were seen to significantly associate with additional change in their abundance due to neonicotinoids treatments or increasing RmtDNAcn ratio.

Table 9. Numbers of metabolites with significant changes (red for increase and green for decrease) in abundance ratios (out of the 57 selected metabolites).

Total number of biochemicals regarding effects in	**Biological Aging Effect**	**Effect of Increasing RmtDNAcn Ratio**	**Treatment Effect**		**Effect from Neonic-Attributed Change in RmtDNAcn Ratio**	
			IMI	**CLO**	**IMI**	**CLO**
• **with p < 0.05**						
Biochemicals (↑|↓) at F2	**0|3**	**3|1**	**0|4**	**2|0**	**2|1**	**0|0**
Biochemicals (↑|↓) at F4	**2|14**	**0|2**	**2|0**	**3|0**	**0|0**	**0|2**
• **with 0.05 < p < 0.1**						
Biochemicals (↑|↓) at F2	**2|2**	**0|3**	**0|1**	**1|1**	**0|1**	**1|3**
Biochemicals (↑|↓) at F4	**0|6**	**3|0**	**3|1**	**2|1**	**3|1**	**0|3**
• **with q < 0.05**						
Biochemicals (↑|↓) at F2	**0|0**	**0|0**	**0|0**	**0|0**	**0|0**	**0|0**
Biochemicals (↑|↓) at F4	**2|9**	**0|0**	**0|0**	**0|0**	**0|0**	**0|0**
• **with 0.05 < q < 0.1**						
Biochemicals (↑|↓) at F2	**0|0**	**0|0**	**0|0**	**0|0**	**0|0**	**0|0**
Biochemicals (↑|↓) at F4	**0|0**	**0|0**	**0|0**	**0|0**	**0|0**	**0|0**

Figure 10 shows the changes in metabolite abundance ratios across F0, F2 and F4 brood generations (vertical alignment, results from Part (A) of equation 13), as well as between neonicotinoids-treated and control groups (horizontal alignment, results from Part (C) of equation 13). **Figure 11** distinguishes the additional changes in metabolic abundance ratios resulting from biological aging- (vertical alignment, results from Part (B) of equation 13) and neonicotinoids treatment- induced (vertical alignment, results from Part (D) of equation 13) increase in RmtDNAcn ratios. In both figures, we used the heatmaps to show the average abundance ratios of different treatment/generation groups under the circumstances when any of the tested change in equation 13 was significant ($p < 0.05$, without adjustment of multiplicity). We highlighted metabolites with significance by their abundance ratios and p-values in **Figures 10B** and **11B**, and cross-compared these findings with **Figures 10A** and **11A**. Specifically, the blue-boxed areas of the volcano plots in **Figures 10B** and **11B** show the changes of metabolite abundance due to biological aging effects and due to increasing RmtDNAcn ratios that we observed in the control group, respectively. Likewise, the yellow-boxed areas in **Figures 10B** and **Figure 11B** show the change of metabolite abundance ratio due to treatment effects and due to neonicotinoids-attributed increase in RmtDNAcn ratio, respectively. For the purpose of streamlining the results, we summarized the findings into the following four categories:

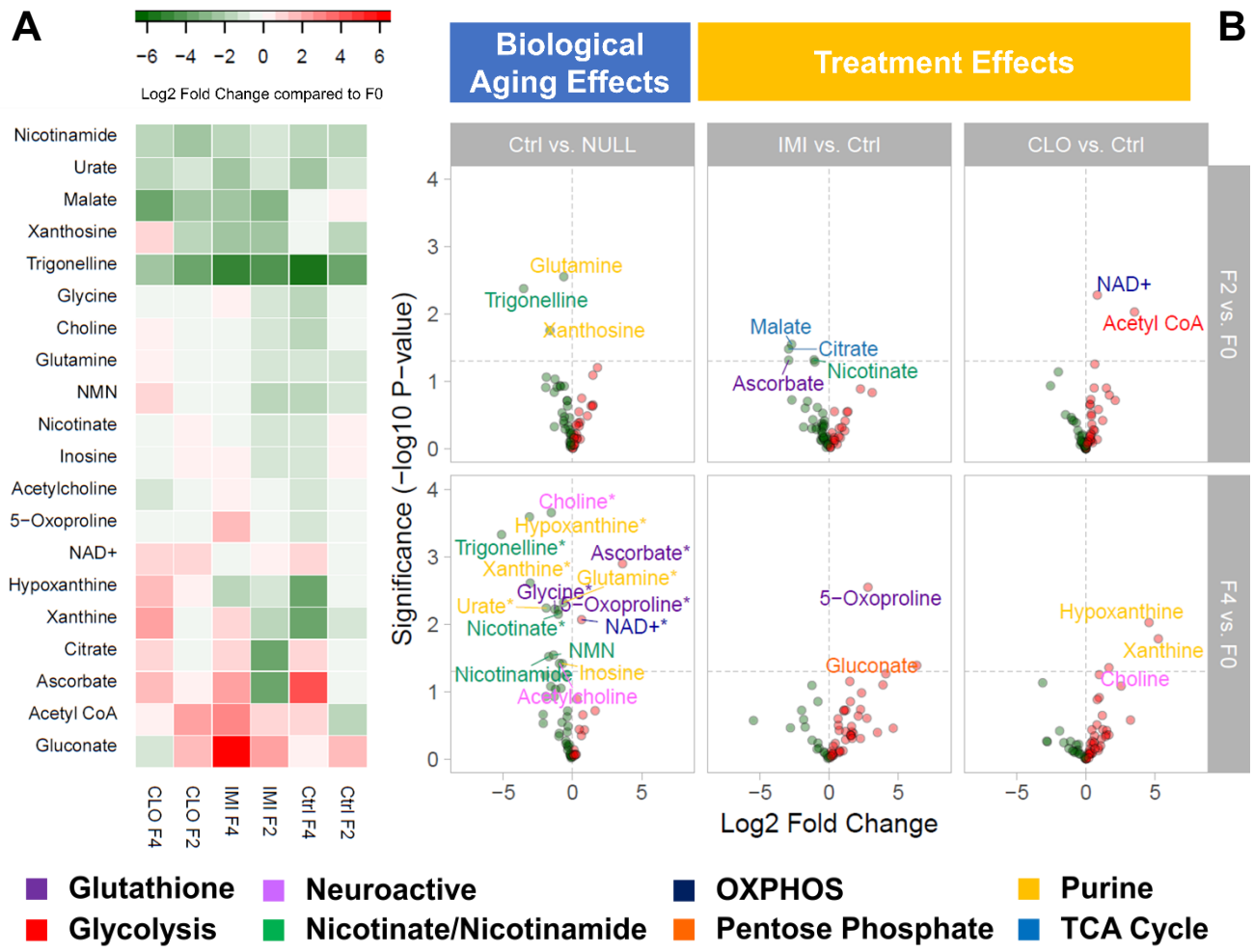

Figure 10. (A) Heatmap of average log2 fold change (FC) of abundance between later-brood generations (F2 or F4) vs. baseline generation (F0) for metabolites with significant abundance changes. Averages were calculated by Equation 13 given no change in RmtDNAcn ratio. Hierarchical clusters of metabolites were based on Euclidean distance of the log2 FC values, where metabolites aligned closer were more correlated. **(B)** Volcano plots showing the log2 fold change of abundance in later-brood generations (F2 or F4) versus F0 for 57 metabolites given no change in RmtDNAcn ratio. Differences in log2 fold change between treatments (Ctrl vs. NULL, IMI vs. Ctrl and CLO vs. Ctrl) were tested using Equation 13 and metabolites with significant abundance changes were labeled here if $p < 0.05$ without multiplicity adjustment. Metabolites remain significant after FDR adjustment for multiplicity ($q < 0.05$) were marked with (*).

1. Biological aging effects on metabolite abundance ratios. As shown in **Figure 10B** (and in **Figure S2** in the supplemental materials), we found significant change ($p<0.05$) of abundance ratios due to biological aging for glutathione, nicotinate/nicotinamide, neuroactive, and purine metabolisms. In general, those changes were in the decreasing trend of abundance levels. Several of them, including the reduction in trigonelline and glutamine, remained statistically significant after adjustment of multiplicity using FDR method ($q<0.05$) in the F4 generation. Although none of those metabolites directly take part in the TCA cycle, we observed significant increase in NAD+ abundance, which is an important intermediate in both oxidative phosphorylation and nicotinate/nicotinamide metabolisms in the F4 generation ($p<0.05$ and $q < 0.05$).

2. Neonicotinoids-attributed change in metabolite abundance ratios. As shown in **Figure 10B** (and in **Figure S3** in the supplemental materials), we found significant ($p < 0.05$) IMI-attributed reduction in abundance levels of citrate and malate, which are intermediates of the TCA cycle, in the F2 generation that were directly exposing to imidacloprid. Although we didn't observe similar reduction of CLO-attributed abundance levels in these intermediates in the F2 generation, we observed significant increase in NAD+ abundance among them along with significant increase in Acetyl CoA abundance (the metabolite linking glycolysis metabolism and the TCA cycle).

3. Effect of RmtDNAcn on metabolite abundance ratios. As shown in **Figure 11B**, we found significantly ($p < 0.05$) lower abundance ratios of malate and higher abundance ratios of acetyl CoA that were associated with increasing RmtDNAcn ratios in the control group. Both directions were the same as those we observed in the treatment effects of IMI and CLO, as shown in **Figure 11B**. Xanthosine and guanosine in purine metabolism were statistically ($p < 0.05$) lower with increasing RmtDNAcn ratios, which appears to be similar to the observation of reduction in most metabolites in the purine metabolism due to biological aging.

4. Neonicotinoids-attributed change in RmtDNAcn ratio on metabolite abundance ratios. As shown in **Figure 11B**, we found significant ($p < 0.05$) differences in abundance ratios of malate, ascorbate, acetyl CoA, and 5-oxoproline in both F2 and F4 generations that are associated with IMI-attributed increasing RmtDNAcn ratio. On the other hand, significant abundance changes due to CLO-attributed increasing RmtDNAcn ratio were only observed for xanthine and hypoxanthine in the F4 generation.

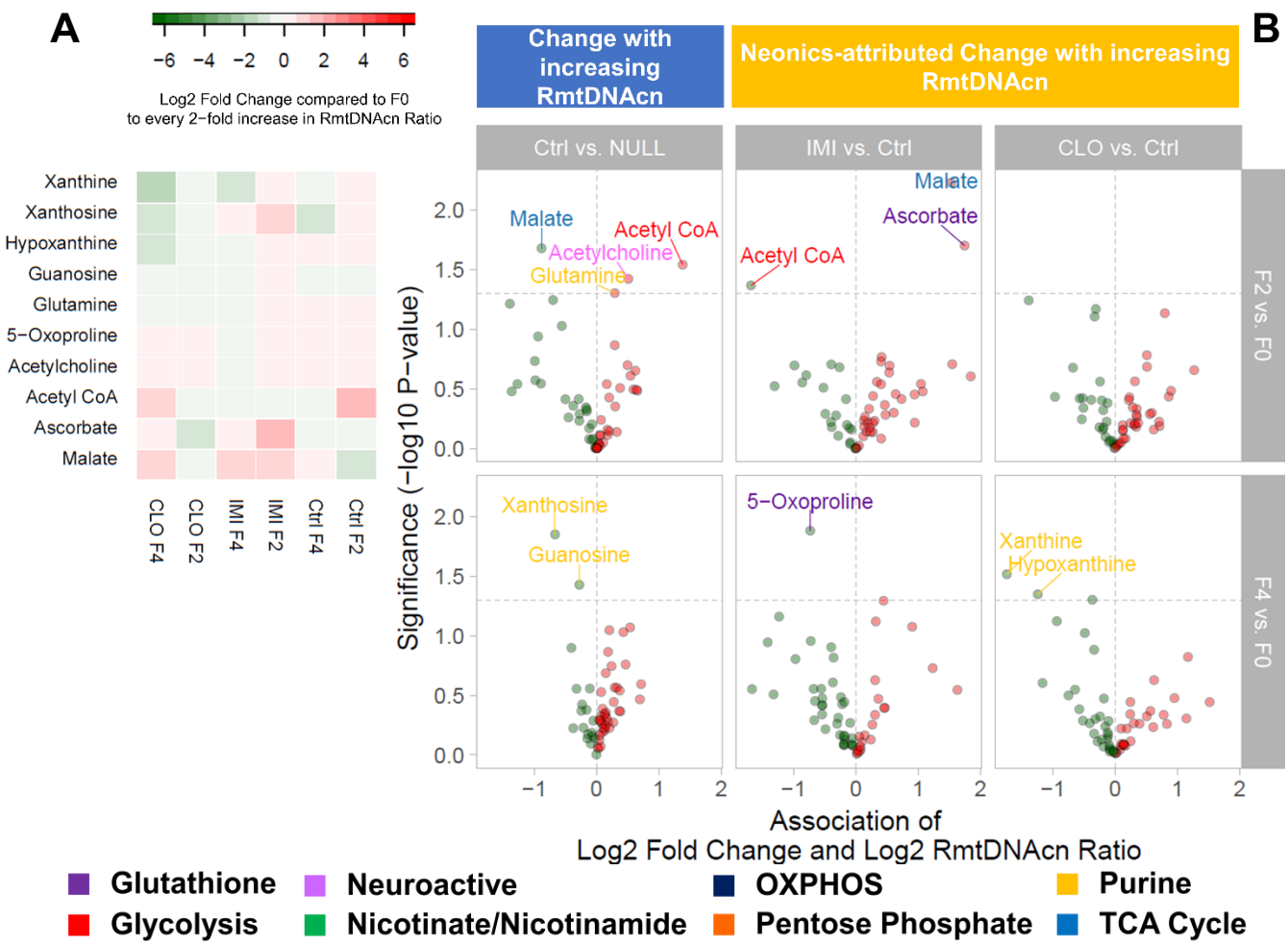

Figure 11. (A) Heatmap of average log2 fold change (FC) of abundance associated with every 2-fold increase in RmtDNAcn ratio between later-brood generations (F2 or F4) vs. baseline generation (F0) for metabolites with significant abundance changes. Averages were calculated by Equation 13 given no change in RmtDNAcn ratio. Hierarchical clusters of metabolites were based on Euclidean distance of the log2 FC values, where metabolites aligned closer were more correlated. **(B)** Volcano plots showing effect of RmtDNAcn ratio on metabolite abundance ratio (Ctrl vs. NULL; highlighted with blue box) and neonicotinoids-attributed (IMI vs. Ctrl and CLO vs. Ctrl; highlighted with yellow box) change in log2 fold change of abundance associated with increasing RmtDNAcn ratio in later-brood generations (F2 or F4) versus F0 for 57 metabolites. These effects were tested using Equation 13 and metabolites with significant abundance changes were labeled here if $p < 0.05$ without multiplicity adjustment. Metabolites remain significant after FDR adjustment for multiplicity ($q < 0.05$) were marked with (*).

In our best knowledge, this is the first study that aims to explore the trans-generational effects in organisms as the result of chemical exposure to environmentally relevant levels over multiple generations. Such trans-generational effects were subsequently validated in a metabolome-wide association study (MWAS) in which perturbation of metabolic pathways relevant to the biological changes as observed in the trans-generational effects were identified. The use of honeybee specimens collected from the field ecological study in which honeybees that are exposed to neonicotinoids in a sub-lethal dosing regime is ideal for the purpose of this chapter. This is because none of the honeybee hives that are set up for the ecological study showed any apparent toxicological effects during the 13-week of neonicotinoids administration, but later exhibited the symptoms of colony collapse disorder (CCD) in the brood generations that are absent from neonicotinoids exposure.[48]

We conducted MWAS using the mixed-effects model for the 57 pre-selected metabolites of interests as it allows us to discover how sub-lethal neonicotinoids exposure could influence the micro levels of biomarkers (the abundance of individual metabolites) and their associated metabolic pathways.[72] As a result, we were able to reference the discovery of abundance changes in metabolites in literature for the explanation of the results from the honeybee study in a biologically feasible manner. Although the results from the MWAS models have demonstrated the perturbation of metabolic pathways that are more related to the aging effects in the F2 and F4 generations, these changes in abundance levels could also be reflective of energy-related metabolisms, such as TCA cycle or OXPHOS. Minor changes in several metabolites associated with TCA cycle or OXPHOS were also observed in the generation at the presence of either IMI or CLO exposure, which might be supportive of our hypothesis that neonicotinoids could perturb

pathways that are relevant to energy metabolism, and therefore added on to the effects of biological aging.

The significant reduction of glutamine abundance ($p < 0.05$ and $q < 0.05$) in both F2 and F4 generations seen in **Figure 11A** and **Table 9** is consistent to the effect of aging, as reported by previous studies. Being the most abundant non-essential amino acid[73], the reduction in glutamine signals that less glutamine was available for the catabolic states, which is generally associated with aging due to protein wasting and with higher risk of morbidity and mortality.[71, 74] Moreover, glutamine plays an important role in the glutathione metabolism, which regulates the redox potential.[71] Glutamine can be synthesized from glutamate by glutamine synthase with consumption of ATP and ammonia (NH_3). Reversely, glutamine can be converted to glutamate by glutaminase. Glutamate, along with cysteine and glycine[71], are the precursors of glutathione (the reduced form: GSH; the oxidized form: GSSG). Since it is generally agreed that aging is associated with accumulation of oxidative damage, GSH and GSSG levels (or in together, tGSH) are also crucial markers of aging. It is also true that increasing levels of tGSH is a sign of detoxification[67] and protection mechanism of cells from moderate but not yet imbalanced level of oxidative stress while decreasing level of GSH and GSSG could be a sign of excessive oxidative stress.[75] Although age-dependent change in abundance of GSH or tGSH could vary by tissues and animals, studies have shown that decreasing level of GSH and tGSH are generally associated with aging.[75] In this chapter, we found lower abundance levels of glutamate (not statistically significant), glycine (statistically significant at F4, $p < 0.05$ and $q < 0.05$), and cysteine (not statistically significant) in bees collected from F2 and F4 generations, which is associated with the generation effects in **Figure 11B**. Although we didn't find significant change in GSH nor GSSG comparing to the F0 generation

associated with biological aging, we found changing levels of both metabolites due to neonicotinoids treatments and change in RmtDNAcn in which will be discussed in later sections.

Glutamine and glutamate are also the precursors of neurotransmitters, γ-Aminobutyric acid (GABA), and reduction of GABA and glutamate levels could be a sign of aging in adult honeybees resulted from neuro-degeneration because both precursors of neurotransmitters would reach the maximum abundance level in bees at age of 10 days and declining since then.[76] Although we did not find significant difference in the abundance of GABA in all treatment groups, GABA abundance levels eventually decreased in F4 generation of the control group, which coincides with findings of previous literature about aging related to neuro-degeneration. In addition to glutamate and GABA, decreasing level of acetylcholine (ACh) is also aging-related in adult bees[76], and we found a significant reduction of ACh abundance in the F4 generation compared to the F0 generation. Besides the association with aging, glutamine, GABA, glycine, and ACh are also important neurotransmitters in which changes in their abundances across generations could indicate perturbation in neurological metabolic pathways.[77] For instance, GABA and glycine are the inhibitory neurotransmitters in the central nervous system (CNS), and significant reduction in these inhibitors could result in continuously less synaptic inhibition.[51]

In addition to GABA's involvement in neurotransmission, it is also an important precursor of the energy metabolism as shown in **Figure 10**. GABA is abundant in all neuropils of honeybee brain[78], and it's predominately synthesized from glucose through GABA shunt in which α-ketoglutarate goes through transamination in the TCA cycle to form glutamate.[51, 79] GABA could be converted to succinate and then metabolized in the TCA cycle by enzymes, such as aminotransferase and succinic semialdehyde dehydrogenase, in order to mediate cellular ATP synthesis.[51] Based on the outcomes from the MWAS, we observed a reduction, although non-

significant reduction of succinate abundance in both F2 and F4 generations along with the increase in ascorbate and NAD+ abundance levels in the F4 generation compared with the F0 generation (**Figure 11B**). These findings could be the signs of defense over oxidative stress. Increased ascorbate (also known as the antioxidant, vitamin C) abundance levels could also be an indication of the antioxidant defense system in which the antioxidant would increase to defend the production of ROS (similar to the glutathione metabolism).[80, 81] On the other hand, NAD+ and its redox mechanism play a very important role in energy metabolism in mitochondria.[82, 83] NAD+ accepts H+ to form NADH, which maintains the process of TCA cycle to fuel OXPHOS. Decreasing NAD+ is commonly seen in animals during aging or when they are on high-fat diets,[84] while increasing NAD+ is associated with aging-related metabolic complications and protection mechanism against dietary in mammals.[83] The associations between aging and reduction in the activity of citrate synthase (CS: for citrate synthesis), α-ketoglutarate dehydrogenase (KGDH: for succinyl CoA synthesis), and malate dehydrogenase (MDH: OAA synthesis) found in yeast experiments could provide some plausible explanations to our results.[85, 86] When the queen bee in any given experimental hive continues to age, worker bees collected from F2 and F4 generations should biologically reflect the aging status of the queen bee. The reduction of CS, KGDH, and MDH activities should lead to less load into the TCA cycle, and subsequently led to lower abundance of Acetyl CoA and NADH in F2 generation while these continuing reductions in those enzyme activities could ultimately lead to the accumulation of Acetyl CoA and NAD+. Hence, we saw higher abundance level of NAD+ in F4 generation compared to the baseline, according to the MWAS results. These findings support the hypothesis that in addition to normal aging as associated with the queen, bees rearing from the later-brood generations could suffer from

additional aging, which likely involved the biological changes of mitochondria, as indicated by the perturbation of energy metabolism.

Beyond the implication on aging, another objective of this chapter was to understand whether IMI or CLO treatment would lead to perturbation of different metabolic pathways or accelerate the biological aging effects. The attribution of IMI exposure to the perturbation of the TCA cycle by significantly reducing the abundances of citrate and malate ($p<0.05$, while not $q<0.05$) and succinate (while $p > 0.05$) further provided the evidence of acceleration of aging in worker bees. We also observed that IMI-attributed effects on glutathione metabolism, which could also further accelerate the normal biological aging process in the F2 and F4 generations. Additional lower levels of glutamine, glutamate, cysteine and glycine during IMI exposure, although non-significant, were observed that should have led to lower level of GSH accordingly if the glutathione mechanism functioned properly as usual. Therefore, the observation of higher abundance of GSH but lower GSSG abundance during IMI exposure could be a sign of accumulation of GSH rather than more GSH synthesis. As articulated earlier, increasing biosynthesis of GSH is usually a protection mechanism against oxidative stress.[75] The finding of significant ($p<0.05$) increasing abundance of 5-oxoproline and gluconate in IMI-treated bees were also important signs of oxidative stress in the F4 generation.[68] Accumulation of 5-oxoproline could be due to the activation of ATP-depleting futile 5-oxoproline cycle due to simultaneous decline in GSH and cysteine.[87] Decrease in GSH induces the activity of γ-glutamyl cysteine synthase (utilization of ATP) to formulate γ -glutamyl phosphate while lack of cysteine to form γ-glutamyl cysteine.[87] The perturbation of energy metabolism was also captured by the increasing levels of intermediates in glycolysis/gluconeogenesis in IMI-treated bees, resulting in higher levels of glucose, G6P, F6P, and Acetyl CoA in the F4 generation because they are metabolic precursors of TCA cycle.

Comparing to IMI, CLO treatment didn't reduce the abundance of TCA intermediates as much as by IMI. According to MWAS results, CLO exposure only reduced malate abundance. Interestingly, abundance of NAD+ increased then decreased during and post neonicotinoids treatments, respectively. Those changes, when evaluated with the reduction in abundance of TCA intermediates, were likely the sign that the flow of TCA cycle became more active while the cycle was in fact less efficient in actual production. Similar to those seen in the control group, CLO didn't significantly lead to the changes in GSH and GSSG abundance levels in F2 and F4 generations. However, CLO treatment led to slight increase in glutamine and glutamate abundance levels. As both changing directions of GSH and GSSG could potentially due to increasing levels of ROS at different intensity, and the effects were not significantly different from that of the control group, we could not conclude that neonicotinoids exposure would lead to excessive oxidative stress but to present our exploratory findings as a guide for future study of neonicotinoids effects.

Another important finding of this chapter was to evaluate whether the aging- and neonicotinoids-induced changes in RmtDNAcn could explain any change in metabolite abundance levels. Although MWAS were not able to detect any significant ($q<0.05$) changes of metabolite abundance associated with increasing RmtDNAcn after adjusting for multiplicity, we found several metabolites that are significant ($p<0.05$) and meaningful to the study objectives before FDR adjustment. For instance, reducing malate abundance and increasing acetyl CoA abundance along with increasing RmtDNAcn in F2 and F4 generations, which was the same changing direction as the effects of neonicotinoids-treatment described earlier. However, there were other abundance change associated with increasing RmtDNAcn that were in fact different from what we observed in age- or neonicotinoids-related effects in F2 and F4 generations. As the change in metabolite abundance levels could vary due to a lot of factors as well as sensitive to sampling time

points, we claimed that the significant changes in abundance should be seen as signs of perturbation of metabolisms captured by the increase in RmtDNAcn while more evidence are in needs for further interpretation of associations between increase in RmtDNAcn and aging or neonicotinoids treatments.

Despite of the above new findings, we noted several limitations. The most profound limitation has to do with the numbers of beehives we have set up for this experiment to achieve meaningful statistical power with these many metabolites and covariates of interest. With the consideration of lacking statistical power to detect effects when adjusting for multiple testing, we chose to report effects that were significantly different when evaluating with p-values or q-values for every metabolite. In addition, the aims to evaluate the changes of metabolite abundance levels due to biological aging, neonic treatments, and their influence through the pathway of changing RmtDNAcn have left us with too many covariates in the model. This could also compromise the power to detect changes for main effects when the true metabolic mechanisms are not associated with the hypothetical influence from other pathways. For example, when the change in abundance of a metabolite mainly due to biological aging but not neonic treatment, then our model would lead to a loss of power in detecting the biological aging effect by incorporating too many other covariates. However, with 57 metabolites to be analyzed simultaneously, we could not fit 57 models with different assumptions on the hypothetical mechanisms. In addition to the sample size issue, the field experimental design also left with several uncertainties in interpreting our results. As we collected foraging bees when they came back to hives, we could not strictly control their ages and foraging activities in which could influence their metabolite abundance at either direction or the abundance variability between bees.

Supplemental Materials

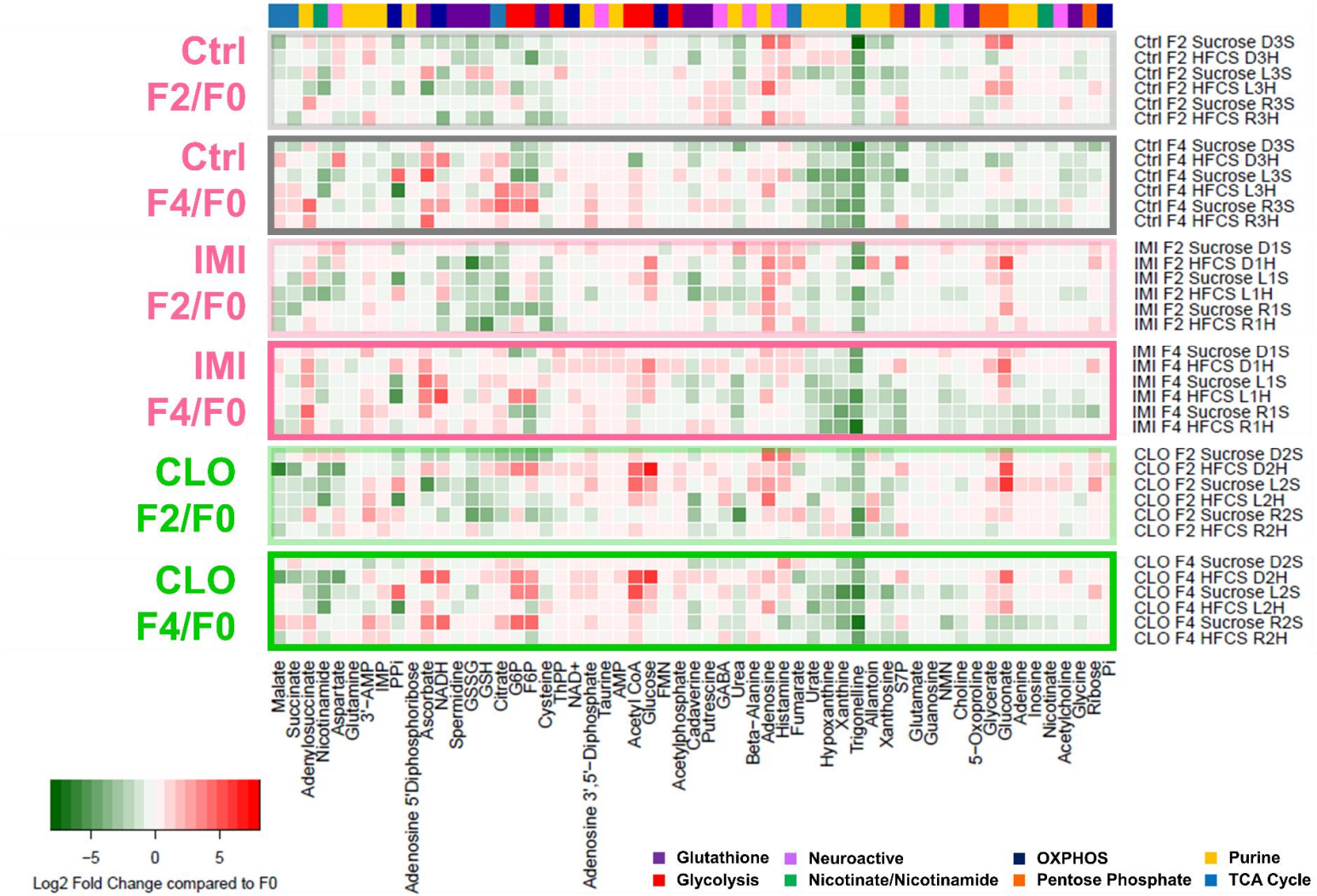

Figure S2. Heatmap of log2 transformed abundance ratios of later-brood generation (F2 and F4) vs. baseline generation (F0) for the 57 selected metabolites.

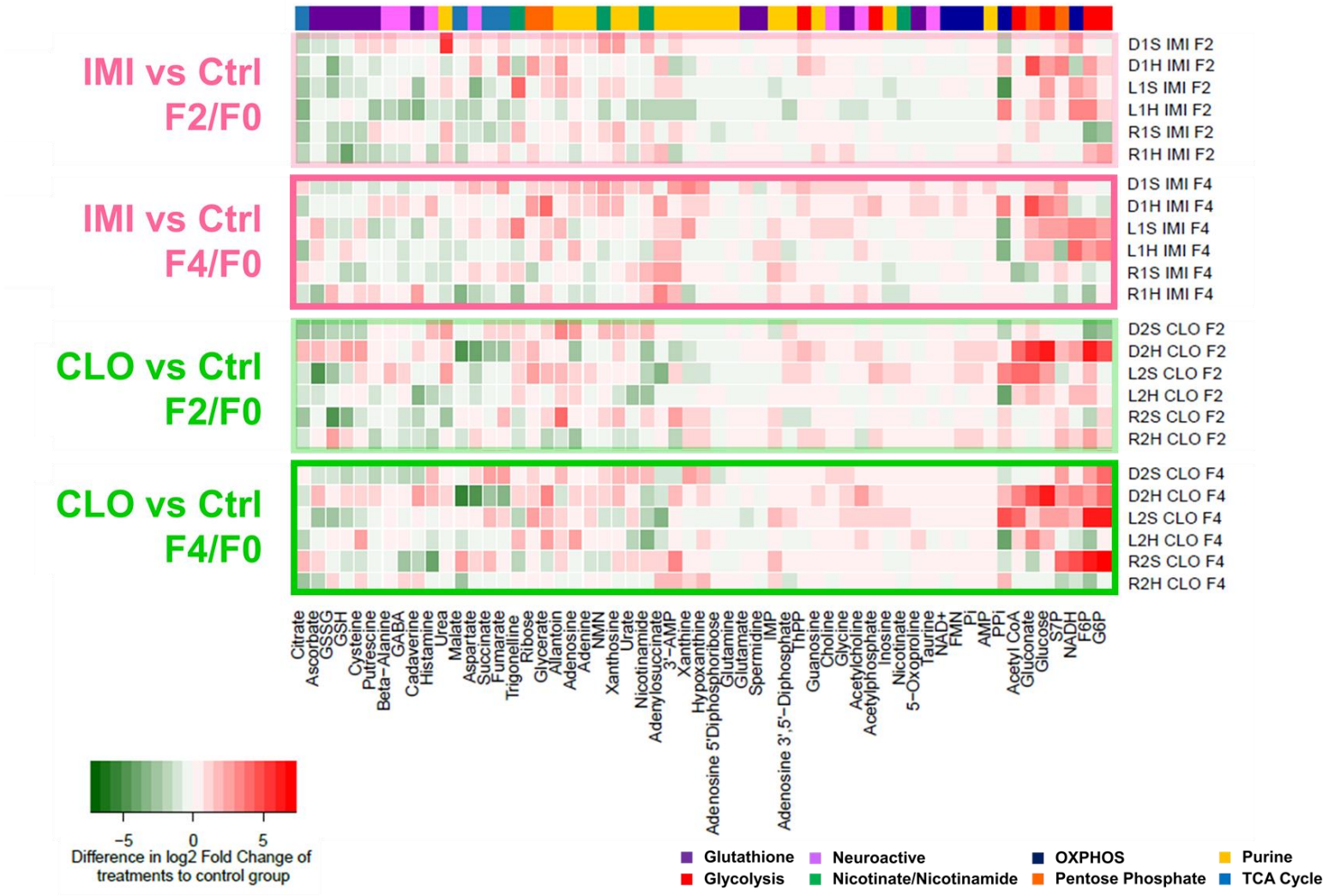

Figure S3. Heatmap of Difference in log2 fold change of abundance between later-brood generation (F2 and F4) vs. baseline generation (F0) for the 57 selected metabolites. Difference of the log2 abundance fold change were calculated by comparing that of individual neonicotinoids treated hives to the average levels (conditioning on generation and sugar syrup) of control hives.

Table S5. Summary of excluded metabolites due to severe missing measurements.

Metabolite	Pathway	Sub-pathway
2-aminopentanoate	Amino acid	Lysine metabolism
2-linoleoylglycerophosphoinositol*	Lipid	Lysolipid
2-methylcitrate	Energy	Krebs cycle
2-oleoylglycerophosphoinositol*	Lipid	Lysolipid
2-oleoylglycerophosphoserine*	Lipid	Lysolipid
3-hydroxydecanoate	Lipid	Fatty acid, monohydroxy
3-hydroxyoctanoate	Lipid	Fatty acid, monohydroxy
4-hydroxycinnamate	Amino acid	Phenylalanine & tyrosine metabolism
8-hydroxyoctanoate	Lipid	Fatty acid, monohydroxy
ala-ala-ala	Peptide	Polypeptide
alpha-hydroxyisocaproate	Amino acid	Valine, leucine & isoleucine metabolism
anthranilate	Amino acid	Tryptophan metabolism
arabinose	Carbohydrate	Nucleotide sugars, pentose metabolism
biochanin A	Xenobiotics	Food component/Plant
chrysoeriol	Xenobiotics	Food component/Plant
cinnamate	Xenobiotics	Food component/Plant
coniferyl alcohol	Xenobiotics	Food component/Plant
coniferyl aldehyde	Xenobiotics	Food component/Plant
dihydromyricetin	Xenobiotics	Food component/Plant
ferulate	Xenobiotics	Food component/Plant
formononetin	Xenobiotics	Food component/Plant
glutamate, gamma-methyl ester	Amino acid	Glutamate metabolism
glycerophosphoethanolamine	Lipid	Glycerolipid metabolism
HEPES	Xenobiotics	Chemical
heptanoate (7:0)	Lipid	Medium chain fatty acid
isovalerate	Lipid	Fatty acid metabolism
kaempferol 3-O-beta-glucoside	Xenobiotics	Food component/Plant
leucylglutamate	Peptide	Dipeptide
lysylvaline	Peptide	Dipeptide
malitol	Xenobiotics	Sugar, sugar substitute, starch
muco-inositol	Lipid	Inositol metabolism
N-acetyltyrosine	Amino acid	Phenylalanine & tyrosine metabolism
N1-methylguanosine	Nucleotide	Purine metabolism, guanine containing
phenethylamine (isobar with 1-phenylethanamine)	Amino acid	Phenylalanine & tyrosine metabolism
phenylacetate	Amino acid	Phenylalanine & tyrosine metabolism
phenylacetylglycine	Amino acid	Phenylalanine & tyrosine metabolism
phenylalanylaspartate	Peptide	Dipeptide
pyroglutamylvaline	Peptide	Dipeptide
serylvaline	Peptide	Dipeptide

Table S6. 57 selected metabolites using KEGG PATHWAY Database.

KEGG Compound ID	Metabolite	KEGG Pathway ID	KEGG Pathway
C00003	NAD+	ame00760	Nicotinate and nicotinamide metabolism
		ame00190	Oxidative phosphorylation
C00004	NADH	ame00190	Oxidative phosphorylation
C00009	Pi	ame00190	Oxidative phosphorylation
C00013	PPi	ame00190	Oxidative phosphorylation
C00020	AMP	ame00230	Purine metabolism
C00024	AcetylCoA	ame00020	Citrate cycle (TCA cycle)
		ame00480	Glutathione metabolism
		ame00010	Glycolysis / Gluconeogenesis
		ame00620	Pyruvate metabolism
C00025	Glutamate	ame00480	Glutathione metabolism
		ame04080	Neuroactive ligand-receptor interaction
C00031	Glucose	ame00010	Glycolysis / Gluconeogenesis
		ame00030	Pentose phosphate pathway
C00037	Glycine	ame00480	Glutathione metabolism
		ame04080	Neuroactive ligand-receptor interaction
		ame00230	Purine metabolism
C00042	Succinate	ame00020	Citrate cycle (TCA cycle)
		ame00760	Nicotinate and nicotinamide metabolism
		ame00190	Oxidative phosphorylation
		ame00620	Pyruvate metabolism
C00049	Aspartate	ame04080	Neuroactive ligand-receptor interaction
		ame00760	Nicotinate and nicotinamide metabolism
C00051	GSH	ame00480	Glutathione metabolism
C00054	Adenosine3',5'-Diphosphate	ame00230	Purine metabolism
C00061	FMN	ame00190	Oxidative phosphorylation
C00064	Glutamine	ame00230	Purine metabolism
C00068	ThPP	ame00020	Citrate cycle (TCA cycle)
		ame00010	Glycolysis / Gluconeogenesis
		ame00620	Pyruvate metabolism
C00072	Ascorbate	ame00480	Glutathione metabolism
C00086	Urea	ame00230	Purine metabolism
C00097	Cysteine	ame00480	Glutathione metabolism
C00099	Beta-Alanine	ame04080	Neuroactive ligand-receptor interaction
C00114	Choline	ame00031	Neuroactive ligand-receptor interaction
C00121	Ribose	ame00030	Pentose phosphate pathway
C00122	Fumarate	ame00020	Citrate cycle (TCA cycle)
		ame00760	Nicotinate and nicotinamide metabolism
		ame00190	Oxidative phosphorylation
		ame00620	Pyruvate metabolism
C00127	GSSG	ame00480	Glutathione metabolism
C00130	IMP	ame00230	Purine metabolism
C00134	Putrescine	ame00480	Glutathione metabolism
C00147	Adenine	ame00230	Purine metabolism
C00149	Malate	ame00020	Citrate cycle (TCA cycle)
		ame00620	Pyruvate metabolism
C00153	Nicotinamide	ame00760	Nicotinate and nicotinamide metabolism
C00158	Citrate	ame00020	Citrate cycle (TCA cycle)
C00212	Adenosine	ame04080	Neuroactive ligand-receptor interaction
		ame00230	Purine metabolism
C00227	Acetylphosphate	ame00620	Pyruvate metabolism
C00245	Taurine	ame04080	Neuroactive ligand-receptor interaction
C00253	Nicotinate	ame00760	Nicotinate and nicotinamide metabolism

(Continued)			
C00257	Gluconate	ame00030	Pentose phosphate pathway
C00258	Glycerate	ame00030	Pentose phosphate pathway
C00262	Hypoxanthine	ame00230	Purine metabolism
C00294	Inosine	ame00230	Purine metabolism
C00301	Adenosine5'Diphosphoribose	ame00230	Purine metabolism
C00315	Spermidine	ame00480	Glutathione metabolism
C00334	GABA	ame04080	Neuroactive ligand-receptor interaction
		ame00760	Nicotinate and nicotinamide metabolism
C00366	Urate	ame00230	Purine metabolism
C00385	Xanthine	ame00230	Purine metabolism
C00387	Guanosine	ame00230	Purine metabolism
C00388	Histamine	ame04080	Neuroactive ligand-receptor interaction
C00455	NMN	ame00760	Nicotinate and nicotinamide metabolism
C00668	G6P	ame00010	Glycolysis / Gluconeogenesis
		ame00030	Pentose phosphate pathway
C01004	Trigonelline	ame00760	Nicotinate and nicotinamide metabolism
C01367	3'-AMP	ame00230	Purine metabolism
C01672	Cadaverine	ame00480	Glutathione metabolism
C01762	Xanthosine	ame00230	Purine metabolism
C01879	5-Oxoproline	ame00480	Glutathione metabolism
C01996	Acetylcholine	ame04080	Neuroactive ligand-receptor interaction
C02350	Allantoin	ame00230	Purine metabolism
C03794	Adenylosuccinate	ame00230	Purine metabolism
C05345	F6P	ame00010	Glycolysis / Gluconeogenesis
		ame00030	Pentose phosphate pathway
C05382	S7P	ame00030	Pentose phosphate pathway

CONCLUSION

With our exploration of exposure, novel biomarker, and intermediate outcomes of neonicotinoids exposure in human and honeybee health, we came to the following conclusions in this dissertation.

Firstly, the results from Chapter 1 imply that the current dietary intakes of total neonic at the population level do not impose a safety concern under the current cRfD established for imidacloprid. The model simulation coupled with the uses of UI and RPF that we demonstrated in this chapter is merely the first step toward the development of a more sensitive and robust dietary exposure assessment for total neonic intakes. We recommend that future research should focus on: (1) collecting more and better-quality residue data as an intervention to the elevated LOD issue seen with the USDA/PDP dataset; and (2) better understanding of biologically relevant toxicological thresholds of neonics in mammals in order to reduce the uncertainty in the cRfD establishment. Since neonics have been, and most likely will continue to be the most widely used insecticides worldwide in the future given its increasing rate of usage[88, 89], it is logical to expect the ubiquity of neonic residues in foods that individuals consume daily. Therefore, it is important to carry out routine dietary intake assessment for total neonic at the population level.

Secondly, Chapter 2 elucidated the possible mechanism of increasing RmtDNAcn resulting from sub-lethal exposure of neonics by quantifying mtDNAcn in honeybees' thoracic muscle over subsequent brood generations of honeybee. In addition to normal aging occurred in queen bees, results from this chapter have demonstrated cumulative RmtDNAcn in foraging bees over subsequent brood generations even at the absence of neonics exposure. We found higher levels of RmtDNAcn in adult bees from later brood generations associated with sub-lethal neonics exposure,

and the RmtDNAcn were cumulative and likely inheritable from the aging queen bees. Although there were no apparent adverse health effects at individual bees, or the whole hive, during neonic administration and prior to the arrival of winter, the persistent and cumulative increase in RmtDNAcn in winter bees might negatively impact their hives' survival over the winter due to insufficient energy production. Those results shall contribute to the explanation of potential mechanism of CCD. It is therefore imperative to focus on validating our finding in the future research and to fill the gap of neonics induced mitochondrial dysfunctions and inefficient hive thermoregulation, which could ultimately lead to the explanation of the onset of CCD.

Lastly, Chapter 3 illustrated the application of MWAS to identify metabolic pathways of biological aging and mechanisms of neonicotinoids exposure in adult honeybees. Our results demonstrated several possible metabolic pathways for accelerating biological aging of the adult bees in later brood generations with the change in metabolite abundance levels. We also provided evidences that neonicotinoids exposure was associated with less efficient TCA cycles that might also be likely the sign of aging. Although we did not find significant changes of metabolite abundance that is due to the effects of increasing RmtDNAcn ratio in later-brood generations, neonicotinoids treatments, or increasing RmtDNAcn ratio due to neonicotinoids treatments over time, we suggest more research should be conducted focusing on the metabolic pathways in the glutathione and energy metabolism (TCA cycle and OXPHOS).

BIBLIOGRAPHY

1. Simon-Delso, N.; Amaral-Rogers, V.; Belzunces, L. P.; Bonmatin, J. M.; Chagnon, M.; Downs, C.; Furlan, L.; Gibbons, D. W.; Giorio, C.; Girolami, V.; Goulson, D.; Kreutzweiser, D. P.; Krupke, C. H.; Liess, M.; Long, E.; McField, M.; Mineau, P.; Mitchell, E. A.; Morrissey, C. A.; Noome, D. A.; Pisa, L.; Settele, J.; Stark, J. D.; Tapparo, A.; Van Dyck, H.; Van Praagh, J.; Van der Sluijs, J. P.; Whitehorn, P. R.; Wiemers, M., Systemic insecticides (neonicotinoids and fipronil): trends, uses, mode of action and metabolites. *Environmental science and pollution research international* **2015,** *22*, (1), 5-34.

2. Casida, J. E.; Durkin, K. A., Neuroactive insecticides: targets, selectivity, resistance, and secondary effects. *Annual review of entomology* **2013,** *58*, 99-117.

3. Jeschke, P.; Nauen, R.; Schindler, M.; Elbert, A., Overview of the status and global strategy for neonicotinoids. *Journal of agricultural and food chemistry* **2011,** *59*, (7), 2897-908.

4. Douglas, M. R.; Tooker, J. F., Large-scale deployment of seed treatments has driven rapid increase in use of neonicotinoid insecticides and preemptive pest management in US field crops. *Environmental science & technology* **2015,** *49*, (8), 5088-97.

5. Tomizawa, M.; Casida, J. E., Neonicotinoid insecticide toxicology: mechanisms of selective action. *Annual review of pharmacology and toxicology* **2005,** *45*, 247-68.

6. Lu, C.; Warchol, K. M.; Callahan, R. A., In situ replication of honeybee colony collapse disorder *Bull Insectol* **2012,** *65*, (1), 99-106.

7. Woodcock, B. A.; Bullock, J. M.; Shore, R. F.; Heard, M. S.; Pereira, M. G.; Redhead, J.; Ridding, L.; Dean, H.; Sleep, D.; Henrys, P.; Peyton, J.; Hulmes, S.; Hulmes, L.; Sarospataki, M.; Saure, C.; Edwards, M.; Genersch, E.; Knabe, S.; Pywell, R. F., Country-specific effects of neonicotinoid pesticides on honey bees and wild bees. *Science* **2017,** *356*, (6345), 1393-1395.

8. Gill, R. J.; Ramos-Rodriguez, O.; Raine, N. E., Combined pesticide exposure severely affects individual- and colony-level traits in bees. *Nature* **2012,** *491*, (7422), 105-8.

9. Nicodemo, D.; Maioli, M. A.; Medeiros, H. C.; Guelfi, M.; Balieira, K. V.; De Jong, D.; Mingatto, F. E., Fipronil and imidacloprid reduce honeybee mitochondrial activity. *Environ Toxicol Chem* **2014,** *33*, (9), 2070-5.

10. Moffat, C.; Pacheco, J. G.; Sharp, S.; Samson, A. J.; Bollan, K. A.; Huang, J.; Buckland, S. T.; Connolly, C. N., Chronic exposure to neonicotinoids increases neuronal vulnerability to mitochondrial dysfunction in the bumblebee (Bombus terrestris). *FASEB J* **2015,** *29*, (5), 2112-9.

11. LaLone, C. A.; Villeneuve, D. L.; Wu-Smart, J.; Milsk, R. Y.; Sappington, K.; Garber, K. V.; Housenger, J.; Ankley, G. T., Weight of evidence evaluation of a network of adverse outcome pathways linking activation of the nicotinic acetylcholine receptor in honey bees to colony death. *Sci Total Environ* **2017,** *584-585*, 751-775.

12. Gu, F.; Chauhan, V.; Kaur, K.; Brown, W. T.; LaFauci, G.; Wegiel, J.; Chauhan, A., Alterations in mitochondrial DNA copy number and the activities of electron transport chain complexes and pyruvate dehydrogenase in the frontal cortex from subjects with autism. *Transl Psychiatry* **2013,** *3*, e299.

13. Georghiou, G. P.; Mellon, R. B., Pesticide resistance in time and space. In *Pest resistance to pesticides*, Springer: 1983; pp 1-46

14. Cimino, A. M.; Boyles, A. L.; Thayer, K. A.; Perry, M. J., Effects of Neonicotinoid Pesticide Exposure on Human Health: A Systematic Review. *Environ Health Perspect* **2017,** *125*, (2), 155-162.

15. Development of a Relative Potency Factor (RPF) Approach for Polycyclic Aromatic Hydrocarbon (PAH) Mixtures. In Agency, U. S. E. P., Ed. Washington, DC., 2010.

16. Recommended Toxicity Equivalence Factors (TEFs) for Human Health Risk Assessments of 2,3,7,8-Tetrachlorodibenzo-p-dioxin and Dioxin-Like Compounds. Risk Assessment Forum. In Agency, U. S. E. P., Ed. Environmental Protection Agency: Washington, DC, 2010.

17. Conservancy, A. B., Neonicotinoid Insecticides Harmful to Birds and Bees Found in Congressional Caffeteria Food. **2015**.

18. U.S. Department of Agriculture (USDA), A. R. S., Pesticide Data Program. Ag Data Commons. http://dx.doi.org/10.15482/USDA.ADC/1287224. **2011**.

19. U.S. Department of Agriculture (USDA), A. R. S., Pesticide Data Program. Ag Data Commons. http://dx.doi.org/10.15482/USDA.ADC/1287224. **2012**.

20. U.S. Department of Agriculture (USDA), A. R. S., Pesticide Data Program. Ag Data Commons. http://dx.doi.org/10.15482/USDA.ADC/1287224. **2013**.

21. U.S. Department of Agriculture (USDA), A. R. S., Pesticide Data Program. Ag Data Commons. http://dx.doi.org/10.15482/USDA.ADC/1287224. **2014**.

22. MacIntosh, D. L.; Spengler, J. D.; Ozkaynak, H.; Tsai, L. H.; Ryan, P. B., Dietary exposures to selected metals and pesticides. *Environ Health Persp* **1996,** *104*, (2), 202-209.

23. Lu, C. A.; Chang, C.-H.; Tao, L.; Chen, M., Distributions of neonicotinoid insecticides in the Commonwealth of Massachusetts: a temporal and spatial variation analysis for pollen and honey samples. *Environmental Chemistry* **2015,** *13*, (1), 4-11.

24. Tooze, J. A.; Kipnis, V.; Buckman, D. W.; Carroll, R. J.; Freedman, L. S.; Guenther, P. M.; Krebs-Smith, S. M.; Subar, A. F.; Dodd, K. W., A mixed-effects model approach for estimating the distribution of usual intake of nutrients: the NCI method. *Statistics in medicine* **2010,** *29*, (27), 2857-68.

25. (NCI), N. C. I., Usual dietary intakes: the NCI method. Available: https://epi.grants.cancer.gov/diet/usualintakes/method.html [accessed October 2016]. **2010**.

26. U.S. Environmental Protection Agency (EPA), Acetamiprid; Pesticide Tolerances. Fed Reg 77: 43524-43529. 2012.

27. U.S. Environmental Protection Agency (EPA), Clothianidin; Pesticide Tolerances. Fed Reg 68: 32390-32400. 2005.

28. U.S. Environmental Protection Agency (EPA), Dinotefuran; Pesticide Tolerance. Fed Reg 70: 14535-14546. 2005.

29. U.S. Environmental Protection Agency (EPA), Imidacloprid; Pesticide Tolerances for Emergency Exemptions. Fed Reg 70: 3634-3642. 2005.

30. U.S. Environmental Protection Agency (EPA), Thiacloprid; Pesticide Tolerance. Fed Reg 68: 55503-55513. 2003.

31. U.S. Environmental Protection Agency (EPA), Thiamethoxam; Pesticide Tolerance. Fed Reg 65: 80343-80353. 2000.

32. Dodd, K. W.; Guenther, P. M.; Freedman, L. S.; Subar, A. F.; Kipnis, V.; Midthune, D.; Tooze, J. A.; Krebs-Smith, S. M., Statistical methods for estimating usual intake of nutrients and

foods: a review of the theory. *Journal of the American Dietetic Association* **2006,** *106*, (10), 1640-50.

33. Shim, J. S.; Oh, K.; Kim, H. C., Dietary assessment methods in epidemiologic studies. *Epidemiol Health* **2014,** *36*, e2014009.

34. Dietary Assessment Primer, 24-hour Dietary Recall (24HR) At a Glance. National Institutes of Health, National Cancer Institute. (https://dietassessmentprimer.cancer.gov/) [Accessed on: November 28, 2017].

35. Barton, H. A.; Flemming, C. D.; Lipscomb, J. C., Evaluating human variability in chemical risk assessment: hazard identification and dose-response assessment for noncancer oral toxicity of trichloroethylene. *Toxicology* **1996,** *111*, (1-3), 271-87.

36. Dourson, M. L.; Stara, J. F., Regulatory history and experimental support of uncertainty (safety) factors. *Regul Toxicol Pharmacol* **1983,** *3*, (3), 224-38.

37. Renwick, A. G.; Lazarus, N. R., Human variability and noncancer risk assessment--an analysis of the default uncertainty factor. *Regul Toxicol Pharmacol* **1998,** *27*, (1 Pt 1), 3-20.

38. Chen, M.; Tao, L.; McLean, J.; Lu, C., Quantitative analysis of neonicotinoid insecticide residues in foods: implication for dietary exposures. *Journal of agricultural and food chemistry* **2014,** *62*, (26), 6082-90.

39. Blacquiere, T.; Smagghe, G.; van Gestel, C. A.; Mommaerts, V., Neonicotinoids in bees: a review on concentrations, side-effects and risk assessment. *Ecotoxicology* **2012,** *21*, (4), 973-92.

40. Decourtye, A.; Devillers, J.; Cluzeau, S.; Charreton, M.; Pham-Delègue, M.-H., Effects of imidacloprid and deltamethrin on associative learning in honeybees under semi-field and laboratory conditions. *Ecotoxicology and environmental safety* **2004,** *57*, (3), 410-419.

41. Decourtye, A.; Armengaud, C.; Renou, M.; Devillers, J.; Cluzeau, S.; Gauthier, M.; Pham-Delègue, M.-H., Imidacloprid impairs memory and brain metabolism in the honeybee (Apis mellifera L.). *Pesticide biochemistry and physiology* **2004,** *78*, (2), 83-92.

42. Ramirez-Romero, R.; Chaufaux, J.; Pham-Delègue, M.-H., Effects of Cry1Ab protoxin, deltamethrin and imidacloprid on the foraging activity and the learning performances of the honeybee Apis mellifera, a comparative approach. *Apidologie* **2005,** *36*, (4), 601-611.

43. Yang, E. C.; Chuang, Y. C.; Chen, Y. L.; Chang, L. H., Abnormal foraging behavior induced by sublethal dosage of imidacloprid in the honey bee (Hymenoptera: Apidae). *J Econ Entomol* **2008,** *101*, (6), 1743-8.

44. Vanengelsdorp, D.; Evans, J. D.; Saegerman, C.; Mullin, C.; Haubruge, E.; Nguyen, B. K.; Frazier, M.; Frazier, J.; Cox-Foster, D.; Chen, Y.; Underwood, R.; Tarpy, D. R.; Pettis, J. S., Colony collapse disorder: a descriptive study. *PLoS One* **2009,** *4*, (8), e6481.

45. Hou, L.; Zhu, Z. Z.; Zhang, X.; Nordio, F.; Bonzini, M.; Schwartz, J.; Hoxha, M.; Dioni, L.; Marinelli, B.; Pegoraro, V.; Apostoli, P.; Bertazzi, P. A.; Baccarelli, A., Airborne particulate matter and mitochondrial damage: a cross-sectional study. *Environmental health : a global access science source* **2010,** *9*, 48.

46. Lee, H. C.; Wei, Y. H., Mitochondrial role in life and death of the cell. *Journal of biomedical science* **2000,** *7*, (1), 2-15.

47. Meyer, J. N.; Leung, M. C.; Rooney, J. P.; Sendoel, A.; Hengartner, M. O.; Kisby, G. E.; Bess, A. S., Mitochondria as a target of environmental toxicants. *Toxicological sciences : an official journal of the Society of Toxicology* **2013,** *134*, (1), 1-17.

48. Lu, C.; Warchol, K. M.; Callahan, R. A., Sub-lethal exposure to neonicotinoids impaired honey bees winterization before proceeding to colony collapse disorder. *Bulletin of Insectology* **2014,** *67*, (1), 125-130.

49. Amdam, G. V.; Omholt, S. W., The regulatory anatomy of honeybee lifespan. *Journal of theoretical biology* **2002,** *216*, (2), 209-28.

50. Omholt, S. W.; Amdam, G. V., Epigenetic regulation of aging in honeybee workers. *Science of aging knowledge environment : SAGE KE* **2004,** *2004*, (26), pe28.

51. Abou-Shaara, H., The foraging behaviour of honey bees, Apis mellifera: a review. *Veterinarni Medicina* **2014,** *59*, (1).

52. Williams, D. B.; Sutherland, L. N.; Bomhof, M. R.; Basaraba, S. A.; Thrush, A. B.; Dyck, D. J.; Field, C. J.; Wright, D. C., Muscle-specific differences in the response of mitochondrial proteins to beta-GPA feeding: an evaluation of potential mechanisms. *American journal of physiology. Endocrinology and metabolism* **2009,** *296*, (6), E1400-8.

53. Pavanello, S.; Dioni, L.; Hoxha, M.; Fedeli, U.; Mielzynska-Svach, D.; Baccarelli, A. A., Mitochondrial DNA copy number and exposure to polycyclic aromatic hydrocarbons. *Cancer epidemiology, biomarkers & prevention : a publication of the American Association for Cancer Research, cosponsored by the American Society of Preventive Oncology* **2013,** *22*, (10), 1722-9.

54. Barrett, M. J.; Alones, V.; Wang, K. X.; Phan, L.; Swerdlow, R. H., Mitochondria-derived oxidative stress induces a heat shock protein response. *Journal of neuroscience research* **2004,** *78*, (3), 420-9.

55. Tuppen, H. A.; Blakely, E. L.; Turnbull, D. M.; Taylor, R. W., Mitochondrial DNA mutations and human disease. *Biochimica et biophysica acta* **2010,** *1797*, (2), 113-28.

56. Trifunovic, A., Mitochondrial DNA and ageing. *Biochimica et biophysica acta* **2006,** *1757*, (5-6), 611-7.

57. Yakes, F. M.; Van Houten, B., Mitochondrial DNA damage is more extensive and persists longer than nuclear DNA damage in human cells following oxidative stress. *Proceedings of the National Academy of Sciences of the United States of America* **1997,** *94*, (2), 514-9.

58. Bai, R. K.; Perng, C. L.; Hsu, C. H.; Wong, L. J., Quantitative PCR analysis of mitochondrial DNA content in patients with mitochondrial disease. *Ann N Y Acad Sci* **2004,** *1011*, 304-9.

59. Pirini, F.; Guida, E.; Lawson, F.; Mancinelli, A.; Guerrero-Preston, R., Nuclear and mitochondrial DNA alterations in newborns with prenatal exposure to cigarette smoke. *Int J Environ Res Public Health* **2015,** *12*, (2), 1135-55.

60. Wong, L. J., Diagnostic challenges of mitochondrial DNA disorders. *Mitochondrion* **2007,** *7*, (1-2), 45-52.

61. Cline, S. D.; Lodeiro, M. F.; Marnett, L. J.; Cameron, C. E.; Arnold, J. J., Arrest of human mitochondrial RNA polymerase transcription by the biological aldehyde adduct of DNA, M1dG. *Nucleic acids research* **2010,** *38*, (21), 7546-57.

62. Brooks, P. J., The 8,5'-cyclopurine-2'-deoxynucleosides: candidate neurodegenerative DNA lesions in xeroderma pigmentosum, and unique probes of transcription and nucleotide excision repair. *DNA repair* **2008,** *7*, (7), 1168-79.

63. Bonmatin, J. M.; Giorio, C.; Girolami, V.; Goulson, D.; Kreutzweiser, D. P.; Krupke, C.; Liess, M.; Long, E.; Marzaro, M.; Mitchell, E. A.; Noome, D. A.; Simon-Delso, N.; Tapparo, A., Environmental fate and exposure; neonicotinoids and fipronil. *Environmental science and pollution research international* **2015,** *22*, (1), 35-67.

64. Lu, C. A.; Chang, C.-H.; Tao, L.; Chen, M., Distributions of neonicotinoid insecticides in the Commonwealth of Massachusetts: a temporal and spatial variation analysis for pollen and honey samples. *Environmental Chemistry 13*, (1), 4-11.

65. Decourtye, A.; Devillers, J.; Cluzeau, S.; Charreton, M.; Pham-Delegue, M. H., Effects of imidacloprid and deltamethrin on associative learning in honeybees under semi-field and laboratory conditions. *Ecotoxicol Environ Saf* **2004,** *57*, (3), 410-9.

66. Yang, E.; Chuang, Y.; Chen, Y.; Chang, L., Abnormal foraging behavior induced by sublethal dosage of imidacloprid in the honey bee (Hymenoptera: Apidae). *Journal of economic entomology* **2008,** *101*, (6), 1743-1748.

67. du Rand, E. E.; Smit, S.; Beukes, M.; Apostolides, Z.; Pirk, C. W.; Nicolson, S. W., Detoxification mechanisms of honey bees (Apis mellifera) resulting in tolerance of dietary nicotine. *Sci Rep* **2015,** *5*, 11779.

68. D'Alessandro, A.; Hansen, K. C.; Silliman, C. C.; Moore, E. E.; Kelher, M.; Banerjee, A., Metabolomics of AS-5 RBC supernatants following routine storage. *Vox Sang* **2015,** *108*, (2), 131-40.

69. Armitage, E. G.; Godzien, J.; Alonso-Herranz, V.; Lopez-Gonzalvez, A.; Barbas, C., Missing value imputation strategies for metabolomics data. *Electrophoresis* **2015,** *36*, (24), 3050-60.

70. Bijlsma, S.; Bobeldijk, I.; Verheij, E. R.; Ramaker, R.; Kochhar, S.; Macdonald, I. A.; van Ommen, B.; Smilde, A. K., Large-scale human metabolomics studies: a strategy for data (pre-) processing and validation. *Anal Chem* **2006,** *78*, (2), 567-74.

71. Meynial-Denis, D., Glutamine metabolism in advanced age. *Nutr Rev* **2016,** *74*, (4), 225-36.

72. Nicholson, J. K.; Holmes, E.; Elliott, P., The Metabolome-Wide Association Study: A New Look at Human Disease Risk Factors. *Journal of Proteome Research* **2008,** *7*, (9), 3637-3638.

73. Sadowska-Bartosz, I.; Bartosz, G., Effect of antioxidants supplementation on aging and longevity. *Biomed Res Int* **2014,** *2014*, 404680.

74. Boelens, P. G.; Nijveldt, R. J.; Houdijk, A. P.; Meijer, S.; van Leeuwen, P. A., Glutamine alimentation in catabolic state. *J Nutr* **2001,** *131*, (9 Suppl), 2569S-77S; discussion 2590S.

75. Maher, P., The effects of stress and aging on glutathione metabolism. *Ageing Res Rev* **2005,** *4*, (2), 288-314.

76. Fuchs, E.; Dustmann, J.; Stadler, H.; Schürmann, F., Neuroactive compounds in the brain of the honeybee during imaginal life. *Comparative Biochemistry and Physiology Part C: Comparative Pharmacology* **1989,** *92*, (2), 337-342.

77. Purves, D.; Augustine, G.J.; Fitzpatrick, D., et al., editors. Neuroscience. 2nd edition. Sunderland (MA): Sinauer Associates; 2001. GABA and Glycine. Available from: https://www.ncbi.nlm.nih.gov/books/NBK11084/.

78. Galizia, C. G.; Eisenhardt, D.; Giurfa, M., *Honeybee neurobiology and behavior: a tribute to Randolf Menzel*. Springer Science & Business Media: 2011.

79. Olsen, R.W.; DeLorey, T.M.. GABA Synthesis, Uptake and Release. In: Siegel GJ, Agranoff BW, Albers RW, et al., editors. Basic Neurochemistry: Molecular, Cellular and Medical Aspects. 6th edition. Philadelphia: Lippincott-Raven; 1999. Available from: https://www.ncbi.nlm.nih.gov/books/NBK27979/.

80. Lamb, R. E.; Goldstein, B. J., Modulating an oxidative-inflammatory cascade: potential new treatment strategy for improving glucose metabolism, insulin resistance, and vascular function. *Int J Clin Pract* **2008,** *62*, (7), 1087-95.

81. Birben, E.; Sahiner, U. M.; Sackesen, C.; Erzurum, S.; Kalayci, O., Oxidative stress and antioxidant defense. *World Allergy Organ J* **2012,** *5*, (1), 9-19.

82. Song, S. B.; Jang, S. Y.; Kang, H. T.; Wei, B.; Jeoun, U. W.; Yoon, G. S.; Hwang, E. S., Modulation of Mitochondrial Membrane Potential and ROS Generation by Nicotinamide in a Manner Independent of SIRT1 and Mitophagy. *Mol Cells* **2017,** *40*, (7), 503-514.

83. Canto, C.; Menzies, K. J.; Auwerx, J., NAD(+) Metabolism and the Control of Energy Homeostasis: A Balancing Act between Mitochondria and the Nucleus. *Cell Metab* **2015,** *22*, (1), 31-53.

84. Verdin, E., NAD(+) in aging, metabolism, and neurodegeneration. *Science* **2015,** *350*, (6265), 1208-13.

85. Breitenbach, M.; Rinnerthaler, M.; Hartl, J.; Stincone, A.; Vowinckel, J.; Breitenbach-Koller, H.; Ralser, M., Mitochondria in ageing: there is metabolism beyond the ROS. *FEMS Yeast Res* **2014,** *14*, (1), 198-212.

86. Samokhvalov, V.; Ignatov, V.; Kondrashova, M., Inhibition of Krebs cycle and activation of glyoxylate cycle in the course of chronological aging of Saccharomyces cerevisiae. Compensatory role of succinate oxidation. *Biochimie* **2004,** *86*, (1), 39-46.

87. Emmett, M., Acetaminophen toxicity and 5-oxoproline (pyroglutamic acid): a tale of two cycles, one an ATP-depleting futile cycle and the other a useful cycle. *Clin J Am Soc Nephrol* **2014,** *9*, (1), 191-200.

88. Jeschke, P.; Nauen, R., Neonicotinoids-from zero to hero in insecticide chemistry. *Pest Manag Sci* **2008,** *64*, (11), 1084-98.

89. Seltenrich, N., Catching Up with Popular Pesticides: More Human Health Studies Are Needed on Neonicotinoids. *Environ Health Perspect* **2017,** *125*, (2), A41-A42.